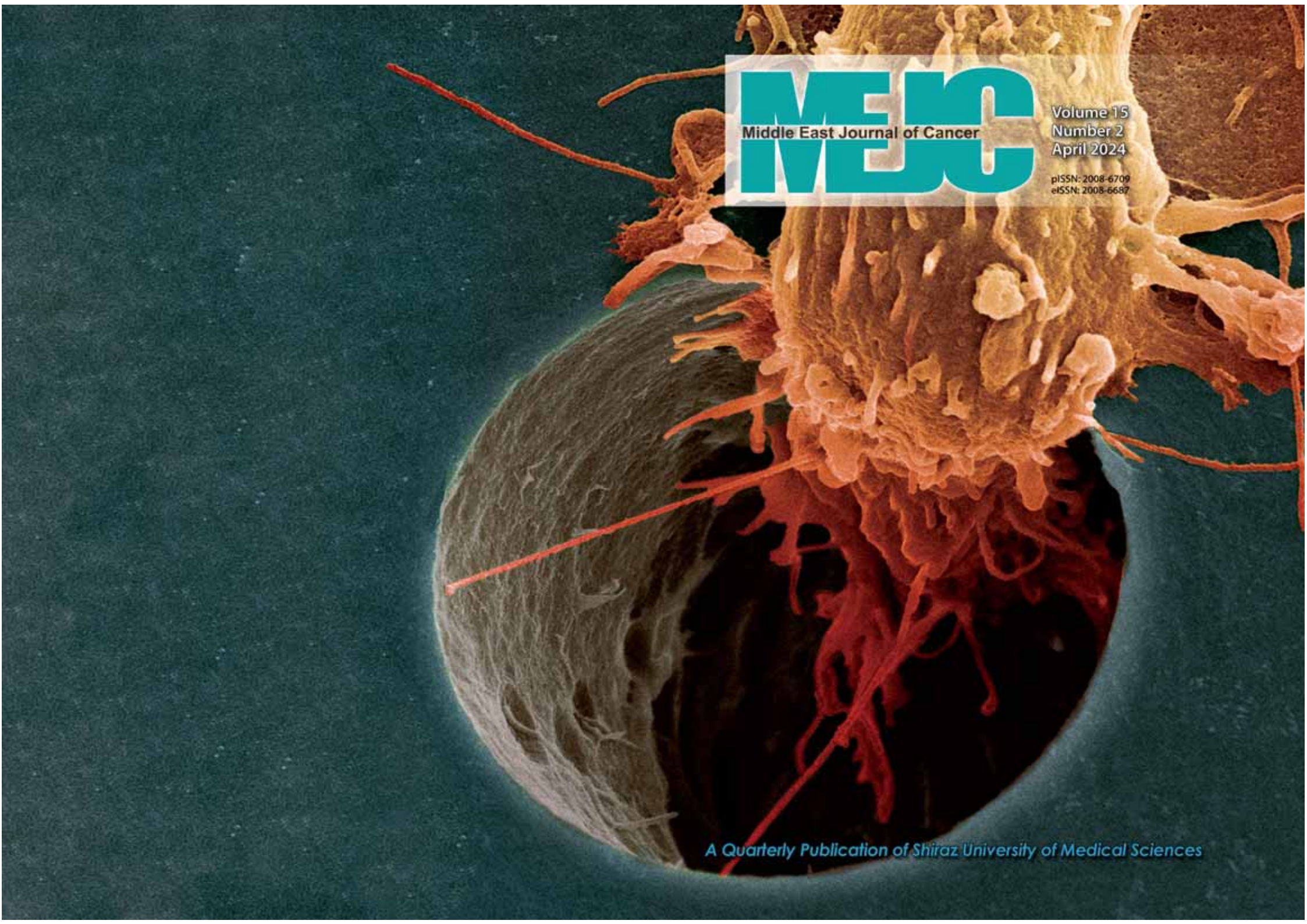
MEJC
Middle East Journal of Cancer
Volume 15
Number 2
April 2024
pISSN: 2008-6709
eISSN: 2008-6687
A Quarterly Publication of Shiraz University of Medical Sciences

Middle East Journal of Cancer

Online Submission
http://mejc.sums.ac.ir

Middle East Journal of Cancer

MEJC was developed to provide a forum for communicating original and novel research findings within the following fields:

- ☐ Cancer biology/genetics
- ☐ Cancer immunology
- ☐ Cancer epidemiology
- ☐ Cancer prevention
- ☐ Cancer imaging and non-surgical interventions
- ☐ Cancer diagnosis
- ☐ Cancer treatment
- ☐ Cancer rehabilitation
- ☐ Cancer palliative care

MEJC welcomes manuscript submissions for the following sections:

- ☐ Editorials
- ☐ Reviews
- ☐ Original Articles
- ☐ Brief Communications
- ☐ Case Reports
- ☐ What is your Diagnosis?
- ☐ Images in Clinical Oncology
- ☐ Middle East Special Reports
- ☐ Tumor Board Corner
- ☐ Letters to the Editor

Online Submission System

We recommend that you submit your manuscripts via our online submission system at: http://mejcsubmission.sums.ac.ir
Also you can easily click on the "Online Submission" link when you log onto our website.
The system is designed so that you can easily submit your manuscripts, track them through the review process, view reviewers' comments and revise your manuscripts. If you have any difficulties please send an email which contains your information to middle.east.journal@gmail.com or mejc@sums.ac.ir.
If you have a strong background in the field of cancer research and are also interested in reviewing manuscripts please let us know by sending us an email to middle.east.journal@gmail.com or mejc@sums.ac.ir specifying your field of interest.

Instructions for Authors

Aim and Scope:

Middle East Journal of Cancer (MEJC) is an international peer-reviewed journal which aims to publish high-quality basic science and clinical research in the field of cancer. This journal also reflects the current status of research as well as diagnostic and treatment practices in the field of cancer in the Middle East, where cancer is becoming a growing health problem.

Submission Process:

Manuscripts can be submitted preferably through the on-line submission system: (http://mejcsubmission.sums.ac.ir) or by email: mejc@sums.ac.ir or middle.east.journal@gmail.com

Peer Review Process:

The articles are primarily evaluated by our internal screeners and statisticians who check the articles for any methodological flaw, format, and their compliance with journal's instructions. Then a submission code will be allocated and all the future contacts should cite this code. The articles will then be reviewed by at least three external peer reviewers. Their comments will be passed to the authors, and the authors' responses to the comments and revisions in the manuscript will then be evaluated by the Editor and a final reviewer who can be a member of the Editorial Board. After final deliberation, the Editor will inform the authour(s) if the manuscript is accepted for publication.

Cover Letter:

Please confirm that you will not submit your article to another journal until the reviewing process is completed. Also please indicate whether the author(s) have published or submitted any related papers from the same study.

Assignment of Copyright and Authorship Responsibilities:

Your article will not be published unless a Copyright Assignment Form has been signed and received by MEJC (Available from http://MEJC.sums.ac.ir/forms/Copyright.pdf).

You should indicate when you submit a manuscript that "This article is an original work, has not been published before and is not being considered for publication elsewhere in its final form either in printed or electronic form".

Language and Style:

Contributions should be in American English. The text must be clear and concise, conforming to accepted standards of English style and usage. Non-native English speakers may be advised to seek professional help with the language.

Types of contribution:

Editorials, reviews, original articles, brief communications, case reports, what is your diagonsis?, images in clinical oncology, Middle East special reports, tumor board corner and letters to the editor.

Preparation of Manuscripts:

Manuscripts must be written in English. Authors whose native language is not English are recommended to seek the advice of a native English speaker, if possible, before submitting their manuscripts.

Manuscripts should be prepared with wide margins and double spacing throughout, including the abstract, footnotes and references. Every page of the manuscript, including the title page, references, tables, etc., should be numbered. However, in the text no reference should be made to page numbers; if necessary, one may refer to sections. Try to avoid the excessive use of italics and boldface.

Manuscripts should be organized in the following order:

- Title page
- Body of text (divided by subheadings)
- Acknowledgements
- References

SI units should be used, i.e., those based on meters, kilograms, seconds, etc.

Title page:

The title page should provide the following information:

- Title (should be clear, descriptive and not too long)
- Name(s) of author(s); please indicate who is the Corresponding author
- Full affiliation(s)
- Complete address of Corresponding author, including telephone and fax numbers and email address
- Keywords.

Abstract:

The Abstract should be structured for original articles into the sections Background/Objective, Methods, Results and Conclusion, and should not exceed 300 words.

Abstracts for the other types of contributions should be non-structured and provide the essential information.

Abstracts for review articles should consist of a concise summary of the salient points. No abbreviations should be used in the abstract.

Keywords:

Keywords are used for indexing purposes; each article should provide three to five keywords selected from the Medical Index Subject Headings (MeSH).

Introduction:

The Introduction should provide a context or background and specify the purpose or research objective of the study.

Materials and Methods:

Must clearly indicate the steps you applied to conduct your study. Be sure that it includes only information that was available at the time the study was planned or the protocol for the study was written. It should be detailed (including controls, inclusion and exclusion criteria, etc.) and may be separated into subsections. Repeating the details of standard techniques is best avoided.

The software used for statistical analysis should be mentioned, and the actual statistical tests should be described.

All studies using human or animal subjects should include an explicit statement in the Materials and Methods section identifying the review and approval committee for each study. Editors reserve the right to reject papers if there are doubts whether appropriate procedures have been used.

Results:

The Results should be presented in a chronological sequence in the text, tables, and figures. Organize the results according to their importance. Only results from the study reported in the manuscript should be included.

Tables:

Number as Table 1, Table 2, etc., and refer to all of them in the text.

Each table should be provided on a separate page. Tables should not be included in the text.

Each table should have a brief and self-explanatory title.

Any explanations essential to the understanding of the table should be given in footnotes at the bottom of the table.

Figures:

Number figures as Fig. 1, Fig. 2, etc. and refer to all of them in the text.

Each figure should be provided on a separate page. Figures should not be included in the text. They should be saved as single JPEG files at 300 dpi resolution or greater.

Each figure should have a self-explanatory caption. The captions to all figures should be typed on a separate page of the manuscript. Photographs are only acceptable if they have good contrast and brightness.

Discussion:

The Discussion should emphasize the new and important aspects of the study and the conclusions that follow from them. Possible mechanisms or explanations for these findings should be explored. The limitations of the study and the implications of the findings for future research or clinical practice should be explored.

Supplementary Materials such as movie clips, questionnaires, etc. may be published the online version of the journal.

Acknowledgments:

Any technical help, general, financial, and material support or contributions that need acknowledging but do not justify authorship can be cited at the end of the text as Acknowledgments.

References:

For citations in the text, numbers should be in superscript format. All publications cited in the text should be presented in a list of references in numerical order of appearance in the text of the manuscript. Using old references is discouraged. If there are more than 6 authors in any of the references, please add et al. after writing the name of the first 6 authors.

References should be listed in the following style:

1. Handjani F, Delir S, Sodaifi M, Kumar PV. Lupus vulgaris following bacilli calmette-guerin vaccination. *Br J Dermatol* 2001;144(2):444-5.
2. Lippman, ME. Breast Cancer. In: Braunwald, E: Fauci, A: Kasper, DL: et al., editors. Harrison's principles of internal medicine, 15th ed. New York: McGraw-Hill, 2001:571-8.

For further information please contact the Editorial Office:

Tel: +98-711-2303715, Fax: +98-711-2303715
Email: mejc@sums.ac.ir or middle.east.journal@gmail.com
Website: http://mejc.sums.ac.ir

Middle East Journal of Cancer

Middle East Journal of Cancer
Volume 15, Number 2, April 2024
ISSN: print 2008-6709, online 2008-6687
The Official Publication of Shiraz University of Medical Sciences

Indexed in Web of Scince: Emerging Sources Citation Index (ESCI), Scopus, ISC, EBSCO, Chemical Abstracts Service (CAS), DOAJ, Index Copernicus, Index Medicus for WHO Eastern Mediterranean Region (IMEMR), Open J-Gate, SID, CINAHL, Magiran, Free Medical Journals, Iran Medex, EMBASE/Excerpta Medica and approved by the Commission for Accreditation and Improvement of Iranian Medical Journals.

Editorial Office
Middle East Journal of Cancer
Office Address: Shiraz University of Medical Sciences, School of Medicine,
Medical Library, 8th floor, Shiraz, Iran.
Tel/Fax: +98-71-32303715
Email: mejc@sums.ac.ir & middle.east.journal@gmail.com
Website: http://mejc.sums.ac.ir

Middle East Journal of Cancer
Volume 15, Number 2, April 2024
ISSN: print 2008-6709, online 2008-6687

Table of Contents

Call for Papers

Please visit us at:
http://mejc.sums.ac.ir
for further information

Middle East Journal of Cancer

MEJC

Editorial
Middle East Journal of Cancer; April 2024; 15(2): 87-88

Molecular Characterization and Metastatic Gene Signatures Based on Targeted Cancer Treatment Modalities

Sami El Khatib♦, PhD

Department of Biomedical Sciences, School of Arts and Sciences, Lebanese International University, Khiyara-West Bekaa, Lebanon

Please cite this article as: El Khatib S. Molecular characterization and metastatic gene signatures based on targeted cancer treatment modalities. Middle East J Cancer. 2024;15(2):87-8. doi: 10.30476/mejc.2023.97702.1875.

Despite being the hallmark of the illness and being responsible for up to 90% of cancer-related deaths, metastasis is the part of cancer pathophysiology that is least understood.[1] Cancer cells can infiltrate, settle, and colonize through their interaction with the tumor microenvironment (TME), which facilitates their passage through stromal barriers. The initial tumor persists and extravasates into the parenchyma of distant tissues throughout the vascular walls after intravasation into the surrounding tissues via the lymphatic and blood system's microvasculature. This invasiveness encourages the formation of micro-metastatic colonies by cancer cells in the parenchyma, which eventually grow to produce overt, clinically apparent metastatic lesions (colonization).[2] Additionally, several clones with inherent cellular plasticity may have variable degrees of metastatic potential within a population of cancer cells. The TME, which consists of immune cells, fibroblasts, endothelial cells, pericytes, bulk tumors, and tumor stromal cells, can affect cancer development by generating cytokines that encourage or inhibit cancer growth and invasion.[3] Stephen Paget's "seed and soil theory" for cancer spread postulates that the TME may operate as a determining factor, analogous to Darwin's "natural selection," to distinguish clones that can spread from the central location to distant regions.[4] Scientists must thoroughly understand the fundamental concepts underlying the metastatic process to find open therapeutic windows for efficient medicines. Such efforts will help scientists understand the metastatic process better and develop practical and pioneering approaches to hinder the progression of cancer metastasis in the future.[5]

Alternatively, the complexity and consistency of the complex clinical and genetic data have raised serious concerns. How should essential genes be found to enhance antimetastatic therapeutic options and stop or delay tumor metastatic spread? How can metastases be detected during treatment with high specificity and sensitivity? Finding out these genes' molecular functional properties and modes of action is the first step in developing a precise therapeutic benefit for cancer patients. Another crucial issue is how the

♦Corresponding Author:
Sami El Khatib, PhD
Department of Biomedical Sciences, Lebanese International University, Khiyara-West Bekaa, Lebanon
Email: sami.khatib@liu.edu.lb

Received: January 08, 2023; Accepted: October 22, 2023

current treatment affects every gene and pathway linked to metastasis. Despite essential developments and an advanced understanding of the biology of tumor metastasis, the treatment plan for many contemporary patients is insufficient because of lethal metastases. Importantly, improved tumor models and modern technologies have made it possible to establish unique gene signatures that predict the spread of metastatic disease to particular body sites. The goal of future treatment studies based on genetic markers should be to quickly identify cancer patients who are most prone to experience distant metastases. By identifying those patients who will benefit from therapeutic targeting of genes and pathways related to metastatic disease while avoiding unnecessary treatment, it will be possible to develop more cost-effective metastatic therapies that will reduce morbidity and mortality caused by this systemic disease.

Previous studies on metastasis have demonstrated that cancer stem cells (CSCs) are crucial for tumor development, immune evasion, co-selection of metastatic microenvironments, and recurrence in distant organs.[6] To improve metastasis prevention and therapy, it is crucial to have a mechanistic understanding of how molecular factors influence CSC features. Even though the current research indicates that CSC plays a substantial role in metastatic colonization, effective therapeutic targeting of these cells may still be necessary to get a better understanding of metastasis and design more effective treatments.[7]

A substantial research focus suggests that extracellular vesicles produced by CSC may contribute to metastasis, stemness, and changes in the tumor immunological environment.[8] To target CSCs with precision medicine and better prognosis and hinder cancer spread, it is essential to comprehend the cell communication pathways in the TME. The metabolic regulatory interaction between CSC and TME in the maintenance of metastasis in distant organs is another fascinating element of metastasis research that should attract further interest. There is still much to learn about how metabolic plasticity and TME affect CSC, which calls for more study that might result in the discovery of novel therapeutic targets.[9,10]

References

1. Gupta GP, Massagué J. Cancer metastasis: building a framework. *Cell.* 2006;127(4):679-95. doi: 10.1016/j.cell.2006.11.001.
2. Lawson DA, Kessenbrock K, Davis RT, Pervolarakis N, Werb Z. Tumour heterogeneity and metastasis at single-cell resolution. *Nat Cell Biol.* 2018;20(12):1349-60. doi: 10.1038/s41556-018-0236-7.
3. Quail DF, Joyce JA. Microenvironmental regulation of tumor progression and metastasis. *Nat Med.* 2013;19(11):1423-37. doi: 10.1038/nm.3394.
4. Paget S. The distribution of secondary growths in cancer of the breast. *Cancer Metastasis Rev.* 1989; 8(2):98-101.
5. Albini A, Mirisola V, Pfeffer U. Metastasis signatures: genes regulating tumor-microenvironment interactions predict metastatic behavior. *Cancer Metastasis Rev.* 2008;27(1):75-83. doi: 10.1007/s10555-007-9111-x.
6. Li F, Tiede B, Massagué J, Kang Y. Beyond tumorigenesis: cancer stem cells in metastasis. *Cell Res.* 2007;17(1):3-14. doi: 10.1038/sj.cr.7310118.
7. Wu M, Zhang X, Zhang W, Chiou YS, Qian W, Liu X, et al. Cancer stem cell regulated phenotypic plasticity protects metastasized cancer cells from ferroptosis. *Nat Commun.* 2022;13(1):1371. doi: 10.1038/s41467-022-29018-9.
8. Wang Z, Zöller M. Exosomes, metastases, and the miracle of cancer stem cell markers. *Cancer Metastasis Rev.* 2019;38(1-2):259-95. doi: 10.1007/s10555-019-09793-6.
9. Sancho P, Barneda D, Heeschen C. Hallmarks of cancer stem cell metabolism. *Br J Cancer.* 2016; 114(12):1305-12. doi: 10.1038/bjc.2016.152.
10. Tyagi A, Wu SY, Sharma S, Wu K, Zhao D, Deshpande R, et al. Exosomal miR-4466 from nicotine-activated neutrophils promotes tumor cell stemness and metabolism in lung cancer metastasis. *Oncogene.* 2022;41(22):3079-92. doi: 10.1038/s41388-022-02322-w.

Original Article
Middle East Journal of Cancer; April 2024; 15(2): 89-97

Prevalence and Prognostic Impact of MYC, BCL2, and BCL6 Rearrangements in Large B Cell Lymphoma Patients: A Multicenter Historical Cohort Study from Iran

Fatemeh Radmanesh*, MD, Ahmad Monabati, MD, Maedeh Motavas*, MD, Alireza Rezvani***, MD, Mehdi Montazer**♦, MD**

*Department of Pathology, Shiraz University of Medical Sciences, Shiraz, Iran
**Department of Molecular Pathology and Cytogenetics, Shiraz University of Medical Sciences, Shiraz, Iran
***Hematology Research Center, Shiraz University of Medical Sciences, Shiraz, Iran

Please cite this article as: Radmanesh F, Monabati A, Motavas M, Rezvani A, Montazer M. Prevalence and prognostic impact of MYC, BCL2, and BCL6 rearrangements in large B cell lymphoma patients: a multicenter historical cohort study from Iran. Middle East J Cancer. 2024;15(2):89-97. doi:10.30476/mejc.2023.98321.1891.

Abstract

Background: Diffuse large B cell lymphoma (DLBCL) is the most prevalent subtype of non-Hodgkin's lymphoma, characterized by remarkable molecular heterogeneity. This study evaluates the prevalence of MYC, BCL2, and BCL6 gene rearrangements among Iranian DLBCL patients.

Method: This historical cohort study encompassed 152 patients drawn from six reference hospitals who participated in the research. Interphase dual-color break-apart fluorescence in situ hybridization (FISH) was applied to formalin-fixed paraffin-embedded DLBCL specimens categorized as "not otherwise specified" alongside 20 normal controls. Survival data was analyzed using the Kaplan-Meier method and the Log-Rank test.

Results: Among the patients, 7 (4.8%), 4 (2.9%), and 15 (10.2%) exhibited MYC, BCL2, and BCL6 rearrangements, respectively. Additionally, 1.5% of the patients demonstrated double-hit (DH) characteristics with both MYC and BCL2 rearrangements, while no triple rearrangements were observed. The presence of rearrangements appeared to be independent of clinicopathological variables. Patients with rearrangements experienced reduced survival durations, with reductions of 26.6, 31.2, 9.1, and 34.2 months for MYC, BCL2, BCL6-rearranged, and DH tumors, respectively ($P > 0.05$). Adverse prognosis was associated with age, activated B-cell-like phenotype, disease stage, B symptoms, lactate dehydrogenase levels, and risk grouping according to the National Comprehensive Cancer Network (NCCN) International Prognostic Index.

Conclusion: DLBCL cases featuring MYC, BCL2, and/or BCL6 translocations are relatively rare. Patients harboring these rearrangements tend to exhibit aggressive disease progression with shortened overall survival. However, these differences did not reach statistical significance, necessitating further research to validate the incorporation of such tests into the routine workup of DLBCL patients.

♦Corresponding Author:
Mehdi Montazer, MD
Department of Molecular Pathology and Cytogenetics, Shiraz University of Medical Sciences, Shiraz, Iran
Tel: 071-32301784
Email: mehdi.montazer@gmail.com

Keywords: Diffuse large B cell lymphoma, Gene rearrangement, MYC, BCL2, BCL6

Received: March 29, 2023; Accepted: November 25, 2023

Introduction

Lymphomas are a heterogeneous group of hematological malignancies classified into two major categories: Hodgkin's lymphoma (HL) and non-Hodgkin's lymphoma (NHL). The most common subtype of NHL is diffuse large B-cell lymphoma (DLBCL), which accounts for approximately 40 and 20% of lymphoma cases in adults and children, respectively.[1-3]

Most DLBCLs are diagnosed based on histopathologic examination and immunophenotyping by immunohistochemistry (IHC). What is more, as the World Health Organization (WHO) advocates, are IHC-based algorithms that further categorize DLBCLs into germinal center B-cell-like (GCB) and activated B-cell-like (ABC) groups based on their presumed cell of origin.[1, 3-4]

The 2017 update of the WHO classification of lymphoid neoplasms introduced a new entity, "high-grade B-cell lymphoma (HGBL), with MYC and BCL2 and/or BCL6 translocations" which encompasses those lymphomas that harbor either two or three of MYC, BCL2, or BCL6 gene rearrangements designated as double-hit (DHL) and triple-hit (THL) lymphomas, respectively. These types of lymphomas show resistance to standard treatments and are thus associated with an unfavorable clinical course.[5-7] Of note, MYC/BCL6-rearranged tumors bear high heterogeneity and distinct gene expression and mutational profiles from MYC/BCL2-rearranged lymphomas. That is why the upcoming 5th edition of the WHO classification of hematolymphoid tumors, which was released online in August 2022, classifies cases with dual MYC and BCL6 aberrations as a subtype of DLBCL or HGBL, not otherwise specified (NOS), and the International Consensus Classification (ICC) separates it into a provisional entity, "HGBL with MYC and BCL6 rearrangements.[8-10]

About 5%-25% of DLBCLs show MYC rearrangements.[5] MYC is an oncogene located on 8q24, which encodes a transcription factor involved in several biological processes mainly related to cell cycle regulation.[1, 3] Likewise, BCL2, located on 18q21, also acts in cell cycle control and is a well-known antiapoptotic protein. BCL2 was initially identified in the more indolent follicular lymphoma and is expressed by more than 50% of DLBCLs.[1, 3] Importantly, the rearrangements in MYC and BCL2 genes are gain-of-function aberrations that lead to overexpression of their corresponding proteins, which consequently cause cell proliferation and the intensification of the survival advantage of tumor cells to emerge. On the other hand, BCL6, located on 3q27, is a negative regulator of transcription, and its rearrangements mainly result in loss of function and subsequent upregulation of transcription, cell proliferation, and dysregulation of apoptosis.[1, 3, 11]

This study evaluated the prevalence of MYC, BCL2, and BCL6 rearrangements in DLBCL patients by fluorescence in situ hybridization (FISH) and their association with other prognostic factors and overall survival (OS).

To the best of knowledge, this is the first study of its kind from Iran.

Materials and Methods

Patient selection

This retrospective cohort study was conducted on 152 patients at six reference hospitals affiliated with the Shiraz University of Medical Sciences, all of whom had received a pathological diagnosis of DLBCL, NOS between 2008 and 2016.

Clinical data, encompassing age, gender, primary site of involvement, presence of B symptoms, nodal and/or extra-nodal involvement, lactic dehydrogenase (LDH) levels, Ann Arbor staging, Eastern Cooperative Oncology Group (ECOG) performance status, International Prognostic Index (IPI) score, and National Comprehensive Cancer Network-IPI (NCCN-IPI) risk categorization, were meticulously extracted through a comprehensive review of medical records. The classification of cell origin, whether Germinal Center (GC)-like or Activated B-cell (ABC)-like, had been determined using the HANS algorithm and was documented in the pathology reports.

All patients had undergone immunochemotherapy, precisely the R-CHOP regimen consisting of rituximab, cyclophosphamide, doxorubicin

hydrochloride, vincristine, and prednisolone.

After treatment, patients were diligently monitored through telephone contacts. The median follow-up duration was 43.5 months, ranging from 1 to 106 months. As of the latest follow-up assessment, 62 (40.8%) patients had deceased, while the remaining 90 (59.2%) were alive. This study received approval from the Shiraz University of Medical Sciences and its affiliated ethics committee (Approval No: 14070). Given the study's retrospective nature, the informed consent requirement was waived.

Interphase FISH

Tissue microarrays (TMA) were constructed employing cores from two representative tumor areas. The 1.0 mm diameter cores were spaced every 0.2 mm on each slide, with 30 patients on each TMA block.

FISH was performed on formalin-fixed paraffin-embedded tissue specimens using dual-color break-apart probes for MYC, BCL2, and BCL6 (The ZytoLight SPECT, ZytoVision GmbH, Bremerhaven, Germany).

In brief, 4-µm thick sections on positively charged slides were deparaffinized in a 70°C oven and two subsequent containers of xylene (each for 10 min) and rehydrated in consecutive baths of graded ethanol (100%, 100%, 90%, and 70% each for 5 min). Pretreatment and proteolysis were carried out by boiling the slides in pre-warmed Heat Pretreatment Solution Citric at 98°C for 15 min, followed by incubation with Pepsin Solution at 37°C for 10 min. After dehydration with graded ethanol (70%, 90%, and 100% each for 1 min), 10 µl of the probe was applied, and denaturation was performed at 75°C for 10 min. Next, the slides were transferred to a humidity chamber (Thermobrite System, Abbott, Illinois, USA) and hybridized overnight at 37°C. The following day, after washing extra probes in saline-sodium citrate (SSC) buffer and hydration in graded alcohol (70%, 90%, and 100% ethanol each for 1 min), 30 µl of DAPI/Antifade-Solution was administered onto the slides and the sections were incubated in the dark until evaluation.

Nikon E600 fluorescent microscope and Genesis software were employed to evaluate the signals and take representative images. In each case, 200 interphase nuclei were searched for break-apart signals. Standard controls, including ten reactive lymph nodes and ten tonsilar tissues, were all negative. Therefore, the technical cut-off was calculated as 3% by applying the inverse beta distribution (betainv) method. The clinical cut-off was set at 10% based on the previous reports.[12, 13]

Statistical analysis

The statistical analysis was carried out utilizing IBM SPSS Statistics 20.0 software. Chi-square, T-tests, and Mann-Whitney U tests were employed to facilitate comparisons. Survival data analysis was executed through the Kaplan-Meier method, complemented by the Log-Rank test. Survival curves were generated using GraphPad Prism 5.04 for Windows (GraphPad Software, San Diego, California, USA, www.graphpad.com). A significance level 0.05 was adopted as the threshold throughout the statistical analyses.

Results

The clinical information of the patients is summarized in table 1. The mean (±SD) age was 54 years (±16.2), ranging from 13 to 90 years. Cervical lymph nodes were the predominant site of involvement, accounting for 57% of patients with nodal disease. Axillary, inguinal, and mediastinal regions were affected in 16%, 13%, and 7% of cases, respectively. Extra-nodal disease was present in 48 (31.6%) patients, distributed as follows: 37% in the gastrointestinal tract, 35% in the head and neck area, 23% in skin and soft tissue, and 5% in the retroperitoneum and spleen.

7 (4.8%), 4 (2.9%), and 15 (10.2%) patients exhibited MYC, BCL2, and BCL6 rearrangements, respectively. Characteristic FISH findings for negative (no rearrangement) and positive (rearranged gene) results are depicted in figure 1. The mean (±SD) percentage of interphases harboring a break-apart signal was 38 (±18.2) for MYC, 30 (±14.1) for BCL2, and 36 (±21.5) for BCL6-rearranged DLBCLs, with ranges of 20-70, 20-50, and 15-80, respectively.

2 (1.5%) patients harbored DHL

rearrangements involving MYC and BCL2. Both DHL patients were male, presented with extra-nodal disease affecting the scalp and tonsils, had no B symptoms, normal LDH levels, low-stage disease (Stage I or II), and a ki67 proliferation index of 70%. However, one DHL patient was 81 years old with a GC-like tumor and a high intermediate IPI score, succumbing after 11 months, while the other DHL patient had an ABC-like lymphoma, a low IPI score, and remained alive for 50 months of follow-up. Notably, the percentage of positive cells for MYC/BCL2 was 40%/30% and 20%/50% for the former and latter patients, respectively.

No significant association was found between rearrangement status and age, sex, presence of B symptoms, IPI score, NCCN-IPI score, ECOG performance status, stage, and ki67 proliferation index (Table 1).

The mean OS time was 39.15 months, and it did not differ statistically between patients with rearrangements and those without any aberrations (Log-Rank test, $P > 0.05$). However, patients harboring rearrangements experienced markedly worse survival times (Table 2), with reductions of 26.6, 31.2, 9.1, and 34.2 months for CMYC, BCL2, BCL6-rearranged, and DHL tumors, respectively. Figure 2 illustrates the survival curves based on clinical, laboratory, and molecular parameters.

ABC-like and high-stage (Ann Arbor stage III/IV) DLBCLs exhibited worse outcomes, with approximately 19 months shorter OS times, though this did not reach statistical significance. Survival analysis based on ECOG performance status was inconclusive, as all cases with ECOG scores less than 5 were still alive.

Older age (>60 years) (OS, 95% confidence interval (CI): 50.0, 36.1-61.0 vs. 71.6, 62.2-80.9, $P = 0.034$), presence of B symptoms (OS, 95% CI: 43.7, 31.3-56.1 vs. 77.4, 67.3-87.4, $P < 0.001$), higher LDH levels (OS, 95% CI: 34.1, 23.3-44.8 vs. 79.2, 69.3-88.9, $P < 0.001$), and involvement of more than one extra-nodal site (OS, 95% CI: 46.2, 30.9-61.4 vs. 72.6, 62.9-82.3, $P = 0.022$) were significantly associated with an adverse prognosis.

Patients in low, low-intermediate, high-intermediate, and high NCCN-IPI risk groups demonstrated progressively worse outcomes (OS (95% CI): 63.3 (57.7-78.9), 54.8 (46.9-62.6), 28.9 (21.4-36.3), and 28.2 (18.5-37.8), respectively).

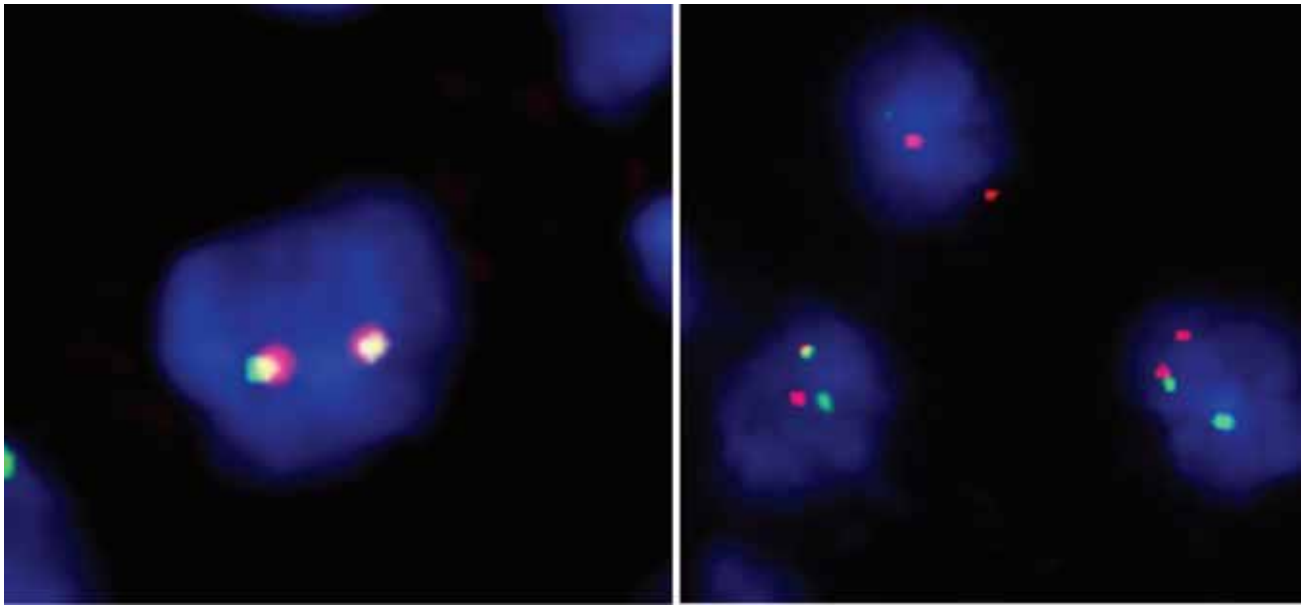

Figure 1. Fluorescent in situ hybridization utilizing a dual-color break-apart probe targeting the MYC gene is depicted. The red and green probes bind to the centromeric and telomeric segments of the MYC gene, respectively. Meanwhile, the background DNA within the nucleus is accentuated in blue using DAPI dye. Two fused red and green signals per nucleus denote the absence of the genetic rearrangement (left), whereas the presence of the rearrangement manifests as a configuration displaying one fused signal and two distinctly separated red and green signals (right).
DAPI: 4',6-diamidino-2-phenylindole

Table 1. Clinical features of the patients

	All patients (total: 152)		MYC rearranged (total: 7)		BCL2 rearranged (total: 4)		BCL6 rearranged (total:15)		Double-hit patients	
	N	%	N	%	N	%	N	%	N	%
Gender										
Male	85	55.9	5	71.4	2	50.0	11	73.3	2	100
Female	67	44.1	2	28.6	2	50.0	4	26.7	0	0
Nodal involvement										
Extranodal	55	36.4	4	57.1	4 ($P = 0.001$)	100.0	6	42.9	2	100
Nodal	96	63.6	3	42.9	0	0.0	8	57.1	0	0
B symptoms										
Absent	66	66.7	4	80.0	2	66.7	8	66.7	2	100
Present	33	33.3	1	20.0	1	33.3	4	33.3	0	0
LDH										
Normal	66	70.2	5	100.0	2	66.7	10	83.3	2	100
Elevated	28	29.8	0	0.0	1	33.3	2	16.7	0	0
Cell-of-origin based on HANS algorithm										
GC-like	43	31.2	3	42.9	2	50.0	7	50.0	1	50
ABC-like	95	68.8	4	57.1	2	50.0	7	50.0	1	50
Ann-Arbor staging										
1	81	53.3	4	57.1	2	50.0	4	26.7	1	50
II	39	25.7	2	28.6	2	50.0	8	53.3	1	50
III	20	13.2	1	14.3	0	0.0	3	20.0	0	0
IV	12	7.9	0	0.0	0	0.0	0 (P=0.040)	0.0	0	0
IPI Score										
Low	37	39.4	2	40.0	1	33.3	8	66.7	1	50
Low intermediate	13	13.8	0	0.0	0	0.0	1	8.3	0	0
High intermediate	21	22.3	3	60.0	2	66.7	1	8.3	1	50
High	23	24.5	0	0.0	0	0.0	2	16.7	0	0
ECOG performance score										
0	41	27.0	3	42.9	1	25.0	6	40.0	1	50
1	31	20.4	1	14.2	1	25.0	1	6.7	0	0
2	6	3.9	0	0.0	0	0.0	0	0.0	0	0
3	7	4.6	0	0.0	0	0.0	2	13.3	0	0
4	5	3.3	0	0.0	0	0.0	0	0.0	0	0
5	62	40.8	3	42.9	2	50.0	6	40.0	1	50
NCCN IPI										
Low	12	12.8	1	20.0	0	0.0	2	16.7	0	0
Low intermediate	32	34.0	1	20.0	1	33.3	7	58.3	1	50
High intermediate	26	27.7	2	40.0	1	33.3	1	8.3	0	0
High	24	25.5	1	20.0	1	33.3	2	16.7	1	50

ABC-like: Activated B cell-like; ECOG: Eastern Cooperative Oncology Group; GC-like: Germinal center-like; IPI: International Prognostic Index; LDH: Lactate dehydrogenase; N: Number; NCCN: National Comprehensive Cancer Network

The NCCN-IPI risk scoring combines the significant prognostic factors mentioned and logically correlates with OS ($P < 0.001$). A similar trend was observed for IPI (OS (95% CI): 29.0 (18.7-39.4), 26.4 (26.4-46.2), 27.5 (15.7-39.4), and 59.8 (52.9-66.7) in high, high-intermediate, low-intermediate, and low-risk groups, respectively; $P < 0.001$).

Discussion

In the present study, the investigation revolved around the rearrangements of MYC, BCL2, and BCL6 by FISH in Iranian DLBCL patients, evaluating their association with various clinico-pathologic characteristics, including OS. BCL6 emerged as the predominantly rearranged gene. Two double-hit patients were identified, with no triple-hit tumors observed. Additionally, it was found that, despite statistical non-significance,

these rearrangements adversely affected OS.

The prevalence of MYC, BCL2, and BCL6 rearrangements in the patient cohort was 4.8%, 2.9%, and 10.2%, respectively. These findings are comparable to those in a previous primary CNS DLBCLs (PCNSL) study, where the corresponding frequencies were 3.8%, 1.3%, and 12%, respectively.[13] They are also similar to the study conducted by Ting and colleagues.[14] However, others, particularly in recent years, generally have demonstrated higher positivity rates. The prevalence of MYC translocation has been reported as around 10% in the work of Cucco et al., up to 21.43% recorded by Ma et al., and regarding BCL2, Ma et al. and Abdul Salam et al. have described remarkably high frequencies of approximately 30%.[15-17] Similar high prevalences of 25%-40% are also on record for BCL6 rearrangements.[16-17]

The lower prevalence of MYC, BCL2, and BCL6 gene rearrangements in this series is likely attributed to the enrollment of patients with an expected better outcome, especially when considering the somewhat lower stage, lower LDH levels, and frequency of B symptoms compared to similar studies. Interestingly, Cucco et al. clearly state that their case selection was biased toward patients with a MYC translocation.[15] This underscores the potential consequences of clinical heterogeneity on the final results. Applying various FISH approaches (single versus multiple probes or break-apart versus fusion techniques) and distinct probe characteristics (such as length, location of binding, and type of dye) might be another reason for discrepant results. On the other hand, the

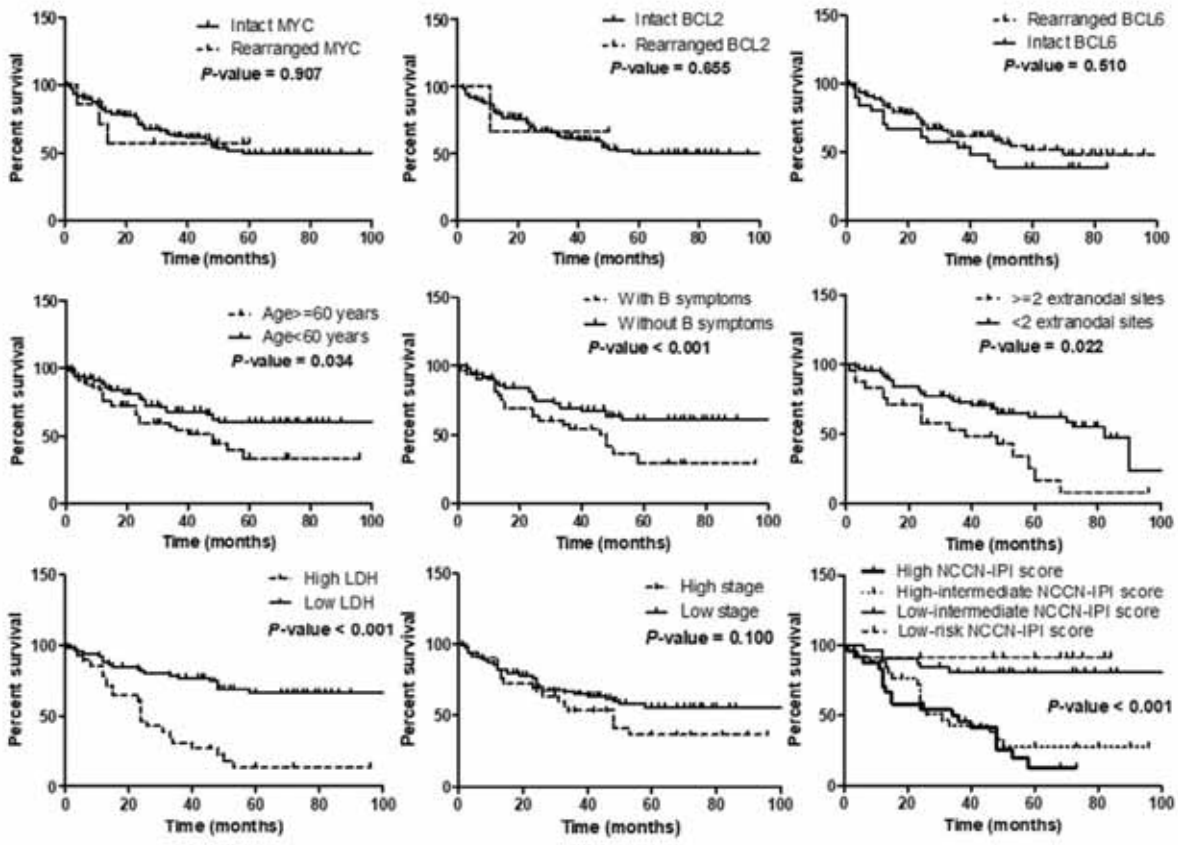

Figure 2. Kaplan-Meier curve analysis reveals that overall survival is not associated with MYC, BCL2, and BCL6 rearrangement status. Conversely, patients aged over 60 years, presenting B symptoms, elevated LDH levels, multiple extra-nodal site involvements, and a higher NCCN-IPI score exhibit a reduced overall survival. While an advanced stage demonstrates a connection to decreased survival time, this association does not attain statistical significance.

LDH: Lactate dehydrogenase; NCCN-IPI: National Comprehensive Cancer Network- International Prognostic Index

Table 2. Overall survival statistics based on MYC, BCL2, and BCL6 rearrangements status

Type of rearrangement	Mean OS (months)	Std. error	95% Confidence interval Lower	Upper	*P*-value (log-rank test)
C-MYC					
Rearranged (n=7)	38.4	9.47	19.9	57.0	0.907
Intact (n=140)	65.0	4.04	57.1	72.9	
BCL2					
Rearranged (n=4)	33.8	8.44	17.2	50.3	0.655
Intact (n=136)	65.0	4.08	57.0	73.0	
BCL6					
Rearranged (n=15)	54.0	6.87	40.5	67.5	0.510
Intact (n=128)	63.1	4.30	54.7	71.5	
Double-hit rearrangement					
Present (n=2)	30.5	13.79	3.5	57.5	0.785
Absent (n=133)	64.7	4.14	56.6	72.9	

n: Number; Std.: Standard; OS: Overall survival

differences in the prevalence of MYC, BCL2, and BCL6 gene aberrations may be a reflection of the striking molecular heterogeneity in DLBCL.[9, 18] Overall, a combination of case selection bias, technical aspects, and tumor heterogeneity contributes to the lower frequency of gene rearrangements in the cohort.

In the current study, DHLs (1.5% of all patients) had MYC and BCL2 rearrangements. According to multiple previous studies, coexisting rearrangements of MYC and BCL2 shape the most prevalent type of DHL.[11, 15-16] Similarly, in both the PCNSL series and the study by Ting et al., one patient (approximately 1.5%) had a DHL tumor.[13-14] DHLs are known to be associated with GCB-like status, and it has been postulated that they drive from BCL2-rearranged follicular lymphomas, which acquire a secondary MYC alteration, leading to aggressive behavior and poor response to standard treatments.[11, 15-16] Nevertheless, in this study, one DHL patient had GCB-like disease, and the other had ABC-like disease. Thus, the low DHL frequency prevented the discovery of such associations. The series did not include any triple rearrangement tumors, a rare finding in other studies. This study's results concerning double-hit and triple-hit tumors are relatively comparable to the available evidence.

In agreement with previous studies, it was also found that patients harboring any of these rearrangements are expected to experience a more aggressive clinical course and inferior outcome.[11, 14, 16, 19] However, the differences in OS failed to reach statistical significance, which may reflect the reasonably small sample size. Furthermore, it was demonstrated that both the IPI and the NCCN-IPI risk scores, along with their primary components, such as advanced age, the presence of B symptoms, elevated LDH levels, and involvement of multiple extra-nodal sites, all exert detrimental effects on the overall prognosis.[3, 16] Of note, The low IPI/NCCN-IPI score was associated with more than 30 months of longer outcomes compared to the high-risk IPI/NCCN-IPI group.

The present study is not without limitations. The retrospective nature makes it prone to the entry of possible errors in medical records into the study. Moreover, the relatively low sample size and the high censored rate (almost 60% alive subjects) lower the power of the statistical analysis, particularly the survival analysis, in finding significant differences. Furthermore, despite the present study not including comprehensive genetic profiling, the effects of the molecular heterogeneity of DLBCL in the study findings should not be overlooked.

Conclusion

DLBCL with MYC and BCL2 and/or BCL6 translocations is relatively uncommon. Despite these rearrangements, patients manifest an

aggressive form of the disease, resulting in diminished OS; however, these discrepancies lack statistical significance. Consequently, the current justification for incorporating these assessments into the routine evaluation of patients with DLBCL and NOS remains unsubstantiated. Further investigation is imperative to elucidate the clinical advantages of these tests, potentially by implementing more intensified treatment protocols tailored to tumors bearing such genetic rearrangements.

Acknowledgment

This research study constituted the graduate thesis of Dr. Fatemeh Radmanesh, undertaken to attain her pathology degree from Shiraz University of Medical Sciences, Shiraz, bearing registration number 14070.

Conflict of Interest

None declared

References

1. Gascoyne RD, Chen JKC, Campo E, Rosenwald A, Jaffe ES, Stein H, et al. Diffuse large B-cell lymphoma, NOS. In: Swerdlow SH, Campo E, Harris NL, Jaffe ES, Pileri SA, Stein H, Thiele J, editors. WHO Classification of Tumours of Haematopoietic and Lymphoid Tissues. Revised 4th ed. International Agency for Research on Cancer (IARC): Lyon, France; 2017.p.291-297.
2. Naeini YB, Wu A, O'Malley DP. Aggressive B-cell lymphomas: frequency, immunophenotype, and genetics in a reference laboratory population. *Ann Diagn Pathol.* 2016;25:7-14. doi: 10.1016/j.anndiagpath.2016.07.008.
3. Chan ACL, Chan JKC. Diffuse large B-cell lymphoma. In: Jaffe E, Arber DA, Campo E, Harris NL, Quintanilla-Fend L, editors. Hematopathology. 2nd ed. Elsevier: Philadelphia, US; 2017.p.415-444.
4. King JF, Lam JT. A practical approach to diagnosis of B-cell lymphomas with diffuse large cell morphology. *Arch Pathol Lab Med.* 2020;144(2):160-7. doi: 10.5858/arpa.2019-0182-RA.
5. Swerdlow SH, Campo E, Pileri SA, Harris NL, Stein H, Siebert R, et al. The 2016 revision of the World Health Organization classification of lymphoid neoplasms. *Blood.* 2016;127(20):2375-90. doi: 10.1182/blood-2016-01-643569.
6. Eldessouki T, Hanley K, Hamadeh F, Oshilaja OO, Sturgis CD. "Triple hit" lymphomas: A retrospective cytology case series of an uncommon high grade B-cell malignancy with C-MYC, BCL-2 and BCL-6 rearrangements. *Diagn Cytopathol.* 2018;46(9):807-11. doi: 10.1002/dc.24038.
7. Schiefer AI, Kornauth C, Simonitsch-Klupp I, Skrabs C, Masel EK, Streubel B, et al. Impact of single or combined genomic alterations of TP53, MYC, and BCL2 on survival of patients with diffuse large B-cell lymphomas: a retrospective cohort study. *Medicine.* 2015;94(52):e2388. doi: 10.1097/MD.0000000000002388.
8. Li W. The 5th Edition of the World Health Organization Classification of Hematolymphoid Tumors. In: Li W, editor. Leukemia [Internet]. Brisbane, Australia: Exon Publications; 2022. [cited 2023 June 5] Available from: https://www.ncbi.nlm.nih.gov/books/NBK586208/
9. Alaggio R, Amador C, Anagnostopoulos I, Attygalle AD, de Oliveira Araujo IB, Berti E, et al. The 5th edition of the World Health Organization Classification of haematolymphoid tumours: Lymphoid neoplasms. *leukemia*. 2022;36(7):1720-48. doi: 10.1038/s41375-022-01620-2.
10. Campo E, Jaffe ES, Cook JR, Quintanilla-Martinez L, Swerdlow SH, Anderson KC, et al. The International Consensus Classification of Mature Lymphoid Neoplasms: a report from the Clinical Advisory Committee. *Blood.* 2022;140(11):1229-53. doi: 10.1182/blood.2022015851.
11. Xia Y, Zhang X. The spectrum of MYC alterations in diffuse large B-cell lymphoma. *Acta Haematol.* 2020;19:1-9. doi:10.1159/000505892.
12. Yan LX, Liu YH, Luo DL, Zhang F, Cheng Y, Luo XL, et al. MYC expression in concert with BCL2 and BCL6 expression predicts outcome in Chinese patients with diffuse large B-cell lymphoma, not otherwise specified. *PLoS One.* 2014;9(8):e104068. doi: 10.1371/journal.pone.0104068.
13. Nosrati A, Monabati A, Sadeghipour A, Radmanesh F, Safaei A, Movahedinia S. MYC, BCL2, and BCL6 rearrangements in primary central nervous system lymphoma of large B cell type. *Ann Hematol.* 2019;98(1):169-73. doi: 10.1007/s00277-018-3498-z.
14. Ting CY, Chang KM, Kuan JW, Sathar J, Chew LP, Wong OLJ, et al. Clinical significance of BCL2, C-MYC, and BCL6 genetic abnormalities, epstein-barr virus infection, CD5 protein expression, germinal center B cell/non-germinal center B-cell subtypes, Co-expression of MYC/BCL2 Proteins and Co-expression of MYC/BCL2/BCL6 proteins in diffuse large B-cell lymphoma: a clinical and pathological correlation study of 120 patients. *Int J Med Sci.* 2019;16(4):556-66. doi: 10.7150/ijms.27610.
15. Cucco F, Barrans S, Sha C, Clipson A, Crouch S, Dobson R, et al. Distinct genetic changes reveal evolutionary history and heterogeneous molecular

grade of DLBCL with MYC/BCL2 double-hit. *Leukemia.* 2020;34(5):1329-41. doi: 10.1038/s41375-019-0691-6.
16. Ma Z, Niu J, Cao Y, Pang X, Cui W, Zhang W, et al. Clinical significance of 'double-hit' and 'double-expression' lymphomas. *J Clin Pathol.* 2020;73(3): 126-38. doi: 10.1136/jclinpath-2019-206199.
17. Salam DSDA, Thit EE, Teoh SH, Tan SY, Peh SC, Cheah SC. C-MYC, BCL2 and BCL6 translocation in B-cell non-Hodgkin lymphoma cases. *J Cancer.* 2020;11(1):190-8. doi: 10.7150/jca.36954.
18. Reddy A, Zhang J, Davis NS, Moffitt AB, Love CL, Waldrop A, et al. Genetic and functional drivers of diffuse large B cell lymphoma. *Cell.* 2017;171(2):481-94.e15. doi: 10.1016/j.cell.2017.09.027.
19. Gong J, Zhang Y, Zhang J, Zhang W, Li J, Ru K, et al. Clinical characteristics of high-grade B-cell lymphomas with rearrangement of MYC, bcl-6 and bcl-2. [In Chinese] *Zhonghua Bing Li Xue Za Zhi.* 2018;47(1):14-8. doi: 10.3760/cma.j.issn.0529-5807.2018.01.004.

Original Article
Middle East Journal of Cancer; April 2024; 15(2): 98-107

Metformin Enhances the Sensitivity of Glioblastoma Cancer Cells to Cisplatin through DNA Damage Assessment

Zaynab Saad Abdulghany♦, PhD

Department of Molecular Biology, Iraqi Center for Cancer and Medical Genetics Research, Mustansiriyah University, Baghdad, Iraq

Please cite this article as: Abdulghany ZS. Metformin enhances the sensitivity of glioblastoma cancer cells to cisplatin through DNA damage assessment. Middle East J Cancer. 2024;15(2):98-107. doi: 10.30476/mejc.2023.98580.1905.

Abstract

Background: Glioblastoma (GBM) stands out as the most prevalent primary brain tumor characterized by its high aggressiveness. Numerous therapeutic approaches have been employed, and the utility of combination therapies has been substantiated, particularly in GBM treatment. Cisplatin, an anticancer chemotherapeutic agent, is employed for the management of various malignancies, including GBM; however, it is associated with significant systemic toxicity. In the realm of combination therapy, metformin, a biguanide drug conventionally used as a first-line treatment for type 2 diabetes, has recently emerged as a valuable adjunct in the treatment of a diverse spectrum of tumors. This study aimed to elucidate the impact of metformin on sensitizing the human cerebral GBM cancer cell line (AMGM) to cisplatin chemotherapy by employing the comet assay as a means to assess DNA damage, thereby advocating the potential of metformin as an adjuvant for cisplatin-based therapy.

Method: In this experimental study, the AMGM cell line was cultured and subsequently treated with either single-agent cisplatin, metformin, or a combination of both drugs. Cell viability was assessed through growth inhibition calculations. The Chou–Talalay analysis was used to assess the cooperative effect of this drug combination. Furthermore, DNA fragmentation was quantified using the alkaline comet assay technique.

Results: The findings demonstrate that metformin significantly potentiates the therapeutic efficacy of cisplatin by synergistically inhibiting the growth of AMGM cells and reducing DNA damage.

Conclusion: These results underscore the potential utility of metformin as a valuable adjunct in enhancing the clinical effectiveness of chemotherapy regimens.

Keywords: Metformin, Cisplatin, Glioblastoma, Synergism effect, DNA fragmentation

♦Corresponding Author:
Zaynab Saad Abdulghany, PhD
Department of Molecular Biology, Iraqi Center for Cancer and Medical Genetics Research, Mustansiriyah University, Baghdad, Iraq
Email: zaynab.saad@iccmgr.org

Introduction

In Iraq, according to the annual Iraqi Cancer Registry 2022, the top 10 cancer incidences in both genders per 105 population in breast, lung, leukemia, non-Hodgkin lymphoma, thyroid, and brain with other central nervous system (CNS) were 22.2,

Received: April 11, 2023; Accepted: December 05, 2023

7.5, 6, 5.1 and 4.7 respectively.[1-2]

While in the statistics of the United States, malignant brain and other CNS tumors account for a small proportion, about 1% of all invasive cancer cases, but are the most commonly diagnosed solid tumor in children and adolescents and represent the leading cause of cancer death among males aged <40 years and females aged <20 years. In 2021, about 83,570 individuals were diagnosed with brain and other CNS tumors in the United States (24,530 malignant tumors and 59,040 non-malignant tumors), and 18,600 people died from the disease. Glioblastoma (GBM) is recorded to be less than one-third of all brain and other CNS tumors diagnosed in the United States; however, the majority of deaths are from its incidence.[3]

Cisplatin (cis-dichlorodiammineplatinum, CDDP) represents one alkylating agent as one of the well-known platinum-based chemotherapeutic drugs, induces DNA damage, interferes with its replication and transcription, and disrupts its structure. Cisplatin exhibits a high affinity towards sulfur donors such as cysteines and methionine, forming stable (Pt-S) bonds. It competes with the affinity towards the nitrogen atom in the backbone of DNA, thus contributing to resistance against the cytotoxic action of cisplatin.[4-5]

Although cisplatin shows a broad spectrum of anticancer activity, its utility is limited due to acquired drug resistance, side-effects, damage to non-targeted tissues, and long-term off-target effects, which represent one of the significant factors causing mortality in cancer survivors in a later stage of patients life.[6-7]

Several chemotherapeutic drugs used, like biguanides metformin, phenformin, and buformin, were initially derived from the herb Galega officinalis (French lilac) and were developed for the treatment of individuals with hyperglycemia and type 2 diabetes diseases; in addition, was evaluated as anticancer agent.[8-9]

Metformin (1,1-dimethyl biguanide hydrochloride) was associated with decreased cancer incidence and mortality in diabetic patients, and the insulin-lowering effects of metformin may be integral to its anticancer properties.[10-12]

In review,[13] they used metformin to enhance the activity of standard glioma therapies. In studies conducted by Adeberg et al. on a cohort of 276 patients with primary GBM, longer progression-free survival was demonstrated in diabetic patients treated with metformin.[12-14]

Another previous study on high-grade glioma

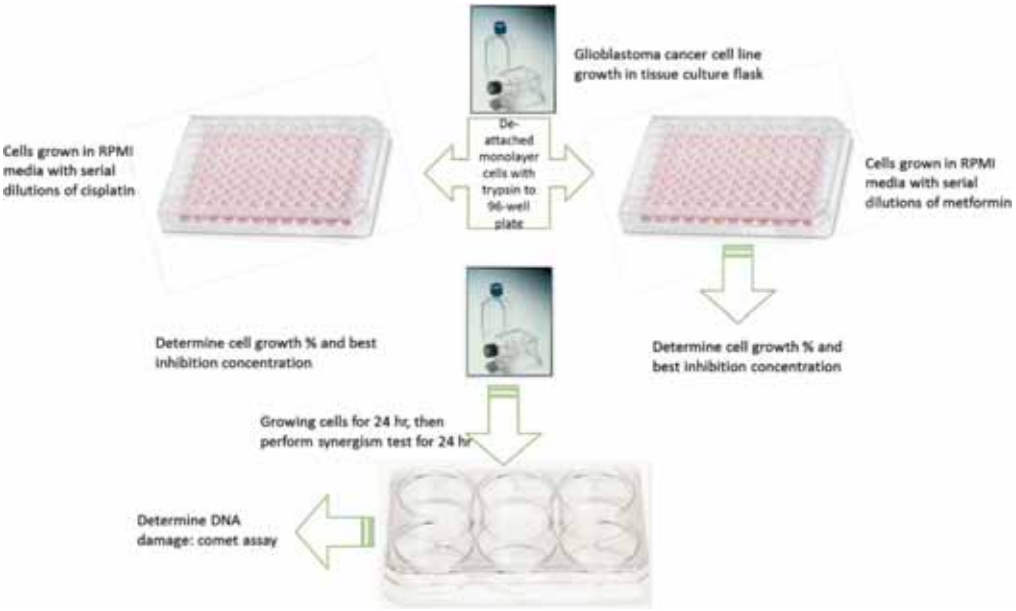

Figure 1. This figure illustrates the flowchart depicting the sequence of current consequence experiments. A Glioblastoma cancer cell line was cultured and tested for viability through a cytotoxicity assay and DNA damage assessment using a comet assay.

(HGG) patients included 1,093 patients with HGG; metformin was found to give a better overall and progression-free survival of patients with World Health Organisation (WHO) grade III, suggesting the mechanisms of isocitrate dehydrogenase (IDH) mutations which might sensitize to the metabolic drug metformin.[15]

In a recent study by Liu et al. published in October 2022 working on the association of high glucose levels in GBM patients, their findings were the lack of intrinsic differences among glioma patients, and the importance of decreasing glucose levels and glioma clinical trials could incorporate molecular subclasses by reproducible and widely adopted method such as DNA methylation. Suggested that the absence of methylation phenotype differences between tumors in different glucose levels leads to differences in how tumor cells utilize glucose.[16]

This study investigated metformin's potential effects in sensitizing the human cerebral glioblastoma-multiforme cancer cell line (AMGM) GBM cancer cell line to cisplatin chemotherapy using comet assay to determine DNA damage. The use of metformin as an adjuvant for cisplatin-based therapy was suggested.

Materials and Methods

This study represents an experimental study, and the flowchart experiments are displayed in figure 1. The study was approved according to the "Application for Biomedical Research Ethics Review" from the Research Ethics Committee of Mustansiriyah University (BCSMU code/2022).

Chemotherapeutic agent

Cisplatin (Celon laboratories, India), the anticancer drug, was gifted from the Radiation and Atomic Medicine Hospital (Baghdad, Iraq) with a concentration (50mg/50ml: IP). This drug was diluted with a medium without calf bovine serum just before use for in vitro studies.

Metformin, a drug used for diabetic patients, was purchased from Sigma Chemical Co. and dissolved in a culture medium without calf bovine serum before being used in vitro studies.

Cell line maintenance

Brain GBM cancer cell line (AMGM) was established by Al-Shammari et al.;[17] cells were maintained and cultured in RPMI-1640 medium supplemented with 10% FBS, 100 U/ml penicillin, and 100 µg/ml streptomycin at 37°C and 5% CO_2. The cells were a kind gift from the experimental therapy department, the Iraqi Center for Cancer Medical Genetics Research, and Mustansiriyah University.

Cytotoxicity assays

In order to assess the cytotoxic impact of metformin and cisplatin, the AMGM GBM cancer cell line was cultivated in two distinct 96-well plates until the formation of confluent monolayers. In the first plate, cells were subjected to metformin treatment alone, with serial dilutions ranging from 1000, 100, 80, 60, 40, 20, and 10 to 1 mg/ml, respectively. In the second plate, cells were exposed to the chemotherapeutic agent cisplatin, again with serial dilutions of 1000, 100, 10, 8, 6, 4, 2, and 1 mg/ml. Following a 24-hour incubation period, the manufacturer's protocol conducted a crystal violet assay utilizing a 96-well plate.

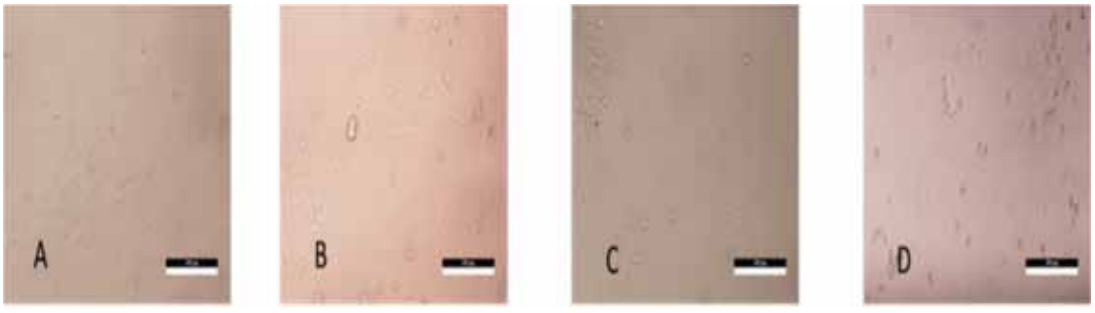

Figure 2. This figure depicts the growth of AMGM cells in identical exposure conditions: (a) control (untreated cells), (b) cisplatin alone, (c) metformin alone, and (d) a combination of both cisplatin and metformin.
AMGM: Human cerebral glioblastoma-multiforme cancer cell line

Subsequently, the culture media were aspirated, and the plates were washed with PBS before being stained with crystal violet for 20 minutes. Once the plates were thoroughly dried, absorbance measurements were obtained utilizing an ELISA reader spectrophotometer set at 570 nm (EnSpire Multiplate reader, Perkin Elmer, Boston, USA). Cell viability was represented as a percentage of viable cells relative to the untreated control cells. This assay was carried out in triplicate, and the inhibition rate of cell growth, expressed as the percentage of cytotoxicity, was calculated using the following equation:

Cell inhibition %= ((A-B))/A ×100%

, where A denotes the mean optical density of the untreated wells, and B signifies the optical density of the treated wells.

Combination assay according to Chou -Talalay (1984)

To evaluate the effect of the combination of metformin and cisplatin, the cells were cultured in 96-well plates until confluent monolayer formation. Cells were treated with a combination of the two (metformin + cisplatin) in serial dilutions for 24 hours. After an incubation duration, crystal violet stained the plates, and the absorbance was measured using an ELISA reader spectrophotometer at 570 nm (EnSpire Multiplate reader, Perkin Elmer, Boston, USA). To analyze the result of combination drugs, CompuSyn software (ComboSyn Inc., Paramus, NJ, USA) was utilized to compute the Chou–Talalay assay combination indices (CIs) and variable ratios of metformin and cisplatin. If a CI value less than 1 indicates synergism, greater than 1 indicates antagonism, and equal to 1 indicates additivity.[18]

Genotoxicity assay (comet assay)

For the detection of DNA fragmentation associated with apoptosis, the alkaline comet assay method pH=13, as described by Collins, was used:[19]

The AMGM cells were cultured in replicates of 6-well plates until a monolayer had formed. Once the monolayer had formed, the cells were incubated with cisplatin, metformin, and a combination of both. After a 24-hour incubation period, the cells were detached using a scraper, centrifuged, and the supernatant was removed. From the resulting precipitate, 10 µl was extracted and mixed with low-temperature melting agarose at a ratio of 1:10 (v/v). This mixture was then spread onto a previously prepared glass slide coated with agarose gel. Subsequently, the slides were immersed in pre-cooled lysis buffer (comprising 2.5 M NaCl, 100 mM EDTA, pH 10, 10 mM Tris base, and 1% Triton X-100) and kept at 4°C for 90 minutes. Following lysis and thorough rinsing, the slides were equilibrated in a TBE solution (composed of 40 mM Tris/boric acid and 2 mM EDTA, pH 8.3), electrophoresed at 1.0 V/cm^2 for 20 minutes, and then subjected

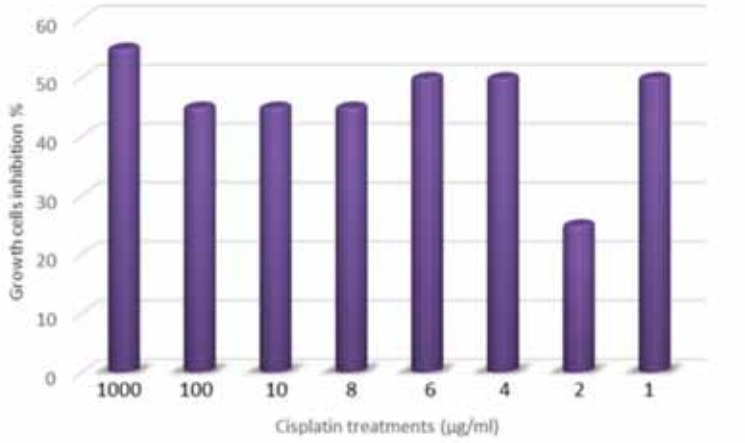

Figure 3. The cytotoxicity activity of cisplatin, at varying concentrations, is compared to untreated AMGM cells over 24 hours of incubation. The data represent the mean of three replicate experiments.
AMGM: Human cerebral glioblastoma-multiforme cancer cell line

to ethidium bromide staining for 5 minutes.

For comet pattern evaluation, 50 nuclei were counted from each slide. The scoring of apoptotic comets was conducted using the method devised by Collins. Images of the comets were captured under a fluorescence microscope (Leica) at ×100 magnification. For each sample, a minimum of 50 comets were analyzed, and the olive tail moment, calculated as [tail DNA (%) × (tail mean - head mean)], was quantified using the Comet Assay Software Project (CASP) Lab version 1.2.3b1, developed by the Free Software Foundation Inc. in Boston, MA, USA.

Statistical analysis

Each experiment was conducted thrice using independent cell passages. Statistical analysis was carried out using GraphPad Prism version 8.1.0. The data are represented as the mean ± standard deviation (SD). Differences between the means of treated and untreated samples were assessed through a one-way analysis of variance (one-way ANOVA). $P < 0.05$ was deemed statistically significant.

Results

Cytotoxicity of drugs on the human GBM AMGM cancer cell line

Assessing the antiproliferative activity of metformin and cisplatin on AMGM, various concentrations of both substances were employed to determine cell growth inhibition (GI) values. Depictions of cells before and after treatment can be seen in figure 2. Cytotoxicity results for cisplatin and metformin against the AMGM cell line are presented in figure 3 and 4 after a 24-hour incubation period, compared to untreated control cells.

Employing different dilutions of each substance to investigate their impact on GBM cancer cell line proliferation (AMGM), the optimal concentration that inhibited 50% of cancer cell growth after 24 hours of incubation with cisplatin was observed at a high concentration of 1000 mg/ml, while the lowest concentrations were 6 and 4 mg/ml, as shown in figure 3. Meanwhile, treatment with metformin during the same incubation period demonstrated that the highest concentration of 1000 mg/ml inhibited 60% of cancer cell growth, with the lowest concentration of 100 mg/ml inhibiting 55% of cell growth when compared with untreated AMGM cells, as depicted in figure 4.

Combination treatment of cisplatin and metformin on AMGM cell line growth

The combination treatment yielded a 50% GI, whereas cisplatin alone exhibited a 40.5% GI, and metformin treatment in isolation also demonstrated a 45.5% GI. No significant

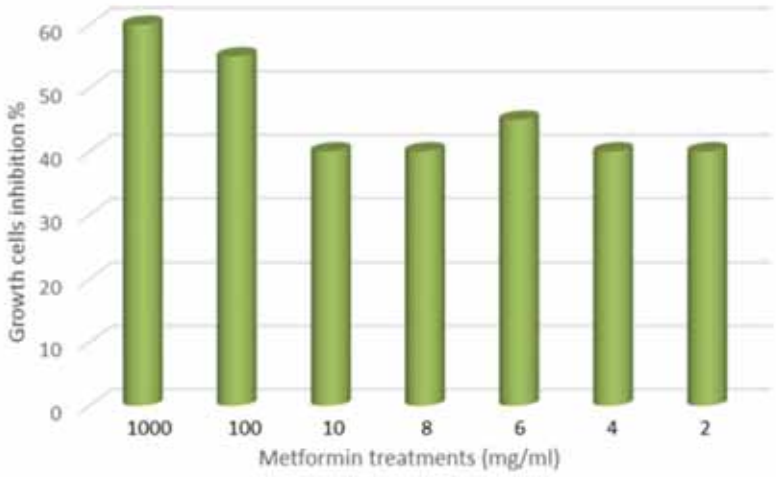

Figure 4. The cytotoxicity activity of metformin at different concentrations is compared to that of untreated AMGM cells during a 24-hour incubation period. The data represent the mean of three replicate experiments.
AMGM: Human cerebral glioblastoma-multiforme cancer cell line

differences were observed between the combination therapy and the individual treatments, as depicted in figure 5.

Chou-Talalay equations were employed to investigate potential interactions between cisplatin and the chemotherapeutic drug cisplatin. A CI less than 0.9 indicates a favorable interaction, a CI between 0.9 and 1.1 suggests an additive effect and a CI greater than 1.1 indicates an antagonistic interaction. Employing the dose-oriented isobologram technique, it was determined that the AMGM cell line demonstrated a favorable interaction between metformin and cisplatin at 50% GI doses, as illustrated in figure 6. This highlights the positive combined effects observed at points 2 (CI: 0.077), 3 (CI: 0.181), 4 (CI: 0.421), 5 (CI: 0.292), and 8 (CI: 0.069), respectively.

Induction of DNA damage by combination treatment of AMGM cancer cell line

The comet assay method assessed the DNA damage induced by metformin, cisplatin, and their combination on the AMGM cell line. The DNA tail moment and tail migration were analyzed as indicators of DNA damage. After a 24-hour incubation period, it was observed that metformin alone induced less DNA damage in AMGM cells, while cisplatin exhibited significantly higher toxicity to AMGM cells compared with untreated control cells. Figure 7 presents the combined effect of metformin, which minimized DNA damage on AMGM cells when used with cisplatin.

Discussion

In this study, the combination of two therapies used in the GBM cancer cell line, cisplatin and metformin, as well as determining the cytotoxic activity of combination therapies in inhibiting the growth of the GBM cell line, then determining the effect on DNA damage of this combination therapy on cancer cell line using the comet assay.

The treatment of cancer and GBM especially faces several main obstacles: blood-brain barriers, drug chemotherapy resistance, and cancer recurrence. Researchers and studies focused on developing better strategies to be adapted for increasing the efficacy of treating GBM patients.

The cytotoxicity of both treatments using different doses show inhibition to the GBM cell line at 50% after 24 hours of treatment; the combination therapy showed several synergism effects using different concentrations of metformin and cisplatin on the GBM cancer cell line. The comet assay DNA damage of the GBM cell line after being treated with combination therapy was higher than in treated cells with cisplatin alone. Hence, combination therapy using metformin and cisplatin against the GBM cell line was recommended according to the results of the current scenario.

In a study aimed at addressing resistance in two distinct glioma cancer cell lines, namely TMZ-resistant (T-98) and drug-sensitive (U-87) glioma cell lines, researchers investigated the efficacy of three novel drug combinations (TMZ with AC2, AC7, and AC26). The study findings showed a significant cooperative effect and high selectivity with minimal toxicity when using different doses. These promising results suggest the potential future use of these three novel drugs in treating drug-resistant glioma, offering hope for the management of GBM.[20]

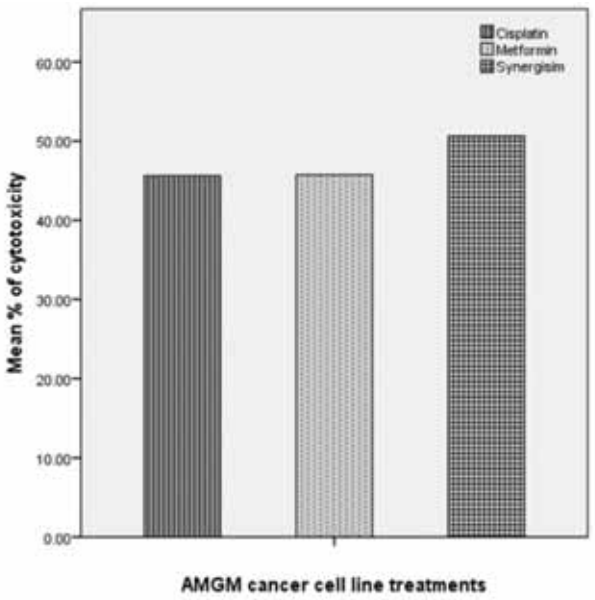

Figure 5. The mean cytotoxicity activity resulting from the combination of metformin and cisplatin is compared to untreated AMGM cells over 24 hours of incubation based on data from three replicate experiments.
AMGM: Human cerebral glioblastoma-multiforme cancer cell line

A preclinical phase II study proved that a dose of 2250 mg/day of metformin in combination with temozolomide in patients with newly diagnosed GBM appeared to be well tolerated with acceptable toxicity. Suggesting that cancer stem cells were resistant to existing radiotherapy or chemotherapy and targeting glioma-initiating cells using metformin as a novel therapeutic regimen that could improve the outcome of GBM.[21]

A recent study developed nanoparticles that efficiently co-load TMZ and CDDP and transport these across the blood-brain barriers to target glioma cells precisely. While using mice bearing U87MG or drug-resistant U251R GBM tumor and treated with this developed nanoparticle and TMZ+CDDP showed a potent anti-GBM effect, greatly extending survival time relative to mice receiving single-drug loaded nanoparticles or equivalent doses of free drugs without any side-effects in histological analyses or blood routine studies. Suggesting that this new nanoparticle formulation overcomes several obstacles that limit the efficacy of combined TMZ and CDDP drug therapy and could be a promising strategy for GBM combinatorial chemotherapy treatment.[22]

Another study suggested the efficiency of using metformin in treating SF268 glioma cancer cells, showing that metformin decreases the survival of glioma cells, inhibiting 2D cell motility and cell invasion and increasing cellular adhesion. Finally, this study recommended the anti-invasive anti-metastatic potential of metformin and its mechanism of action in GBM cells.[23]

Determination of response to chemotherapy is a significant requirement of personalized medicine single-cell gel electrophoresis, known as a comet assay, used to detect DNA damage in cells. The current study used comet assays to determine the response to chemotherapeutic drugs

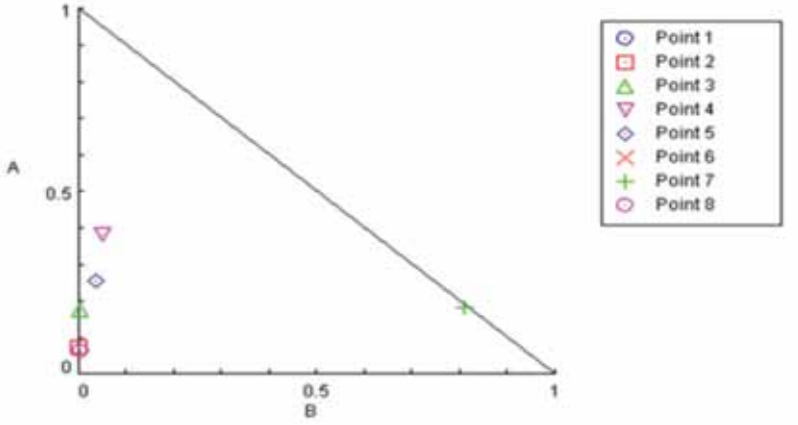

Points	Dose met	Dose Cis	Effect	CI	Interaction
1	1000.0	1000.0	0.55	2.58812	
2	100.0	100.0	0.6	0.07747	Synergism
3	80.0	10.0	0.55	0.18101	Synergism
4	60.0	8.0	0.5	0.43187	Synergism
5	40.0	6.0	0.5	0.29201	Synergism
6	20.0	4.0	0.4	8.19547	
7	10.0	2.0	0.45	0.99646	Synergism
8		1.0	0.5	0.06993	Synergism

Figure 6. Isobologram analysis reveals the synergistic effect of cisplatin and metformin after combination treatment on AMGM cells in vitro. The accompanying table presents each concentration's CI data, calculated using CompuSyn software.
CI: Combination indices; Cis: Cisplatin; met: Metformin; AMGM: GBM cancer cell line

widely used in the GBM cell line. The comet assay technique could allow authentic and quick results with the minor items and could be administrated to various drugs, human breast, and colon cancer cell lines treated with chemotherapies. The study results showed that drug activities varied even in the same cancer types, suggesting the heterogeneity of different cancer types.[24]

The limitation of using single chemotherapy in treating glioblastoma cells is that these chemotherapies do not kill all the cancer cells, and some cells survive, leading to the appearance of new cells resistant to the treatment and needing other therapies that sensitize the chemotherapy. The second limitation in the treatments could be the heterogeneity of glioblastoma cells. These could be overcome by combination therapy, drugs safe for normal cells, reduced cancer risk, and increased selectivity, specificity, and sensitivity of treatments.

Conclusion

The drug combinations involving cisplatin and metformin proposed in this study provide novel insights for treating drug-resistant GBM cell lines. As suggested in our study, the effective dosages of each combination have been determined through assessments of cytotoxic activity and DNA damage. The combination developed herein underscores the effectiveness of these dosage combinations in inhibiting glioma cell growth across a wide range of dosages, which would be impractical to screen experimentally. This

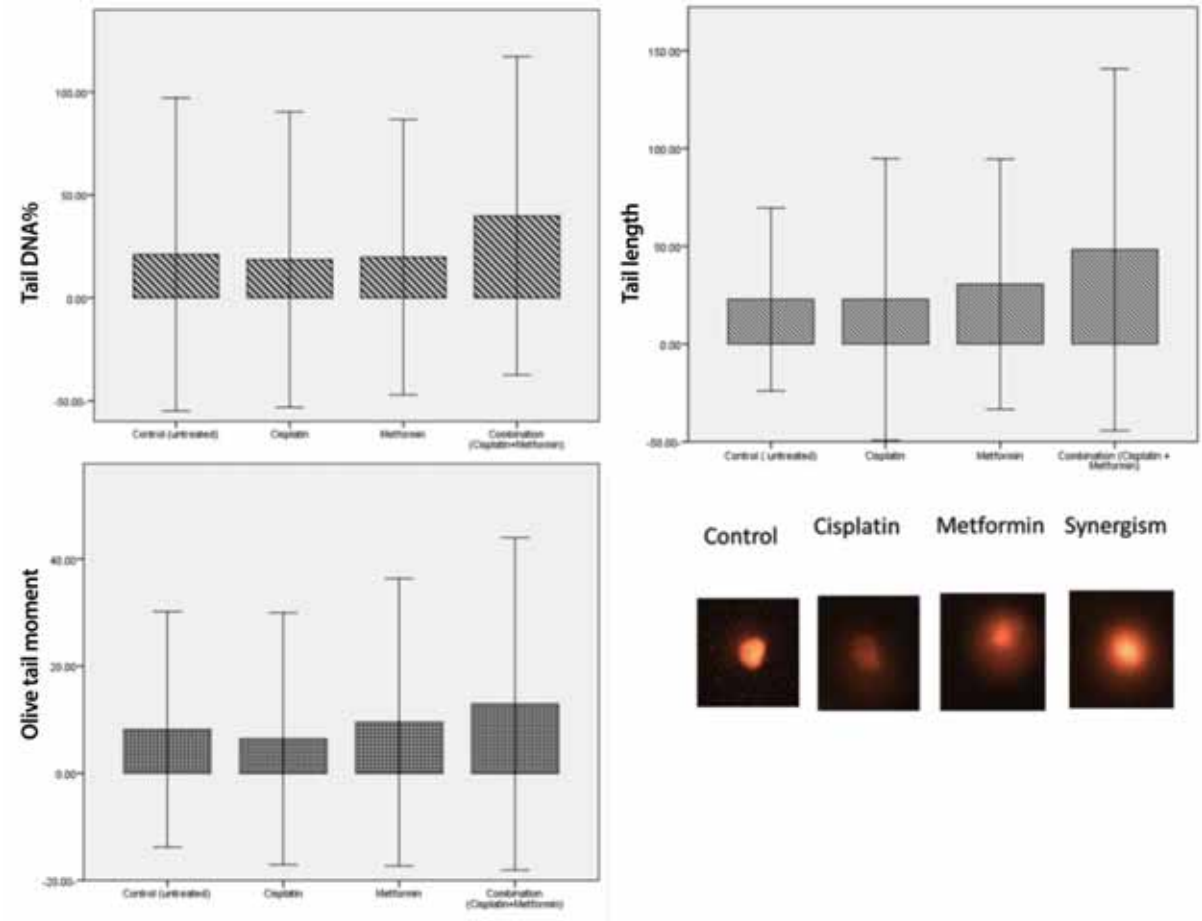

Figure 7. Alkaline comet assay results for the AMGM cancer cell line following treatments with metformin and cisplatin, either alone or in combination, after 24 hours of incubation. The represented results from the comet assay aim to detect DNA damage (original magnification, ×100). Olive tail moments were measured using CASP software, and values are presented as means ± SEM.
Con: Control; Met: Metformin; Cis: Cisplatin; SEM: Standard error of the mean; Synergism: Cisplatin combined with metformin; AMGM: Human cerebral glioblastoma multifrome cancer cell line; Correlation is significant at the 0.01 level (2-tailed). Cis/ con $P < 0.0001$**.

represents a crucial step in estimating the synergistic effects of the drug pairs.

This study elucidates the potential of metformin in conjunction with cisplatin for treating GBM cancer cell lines in an in vitro model. Furthermore, it employs the comet assay technique to demonstrate DNA damage, showcasing its reliability, speed, and value in assessing GBM treatment. Lastly, it suggests that metformin holds promise as a therapeutic candidate for GBM treatment. Further investigations are necessary to evaluate the efficiency of metformin in treating GBMs in vivo.

Acknowledgment

We are grateful to Assistant Professor, Dr. Amer Tawffeq for providing the chemotherapy drug and to Technician Teeba Hekmat for their invaluable assistance in conducting the comet assay technique.

Conflict of Interest

None declared.

References

1. Sung H, Ferlay J, Siegel RL, Laversanne M, Soerjomataram I, Jemal A, et al. Global cancer statistics 2020: GLOBOCAN estimates of incidence and mortality worldwide for 36 cancers in 185 countries. *CA Cancer J Clin.* 2021;71(3):209-49. doi: 10.3322/caac.21660.
2. Iraqi Cancer Board. Annual Report, Iraqi Cancer Registry 2021. Iraqi Cancer Board, Ministry of Health and Environment, Republic of Iraq; 2022. 306 p. Available from: https://moh.gov.iq/upload/1691449545.pdf
3. Siegel RL, Miller KD, Fuchs HE, Jemal A. Cancer statistics, 2021. *CA Cancer J Clin*. 2021;71(1):7-33. doi: 10.3322/caac.21654. Erratum in: *CA Cancer J Clin.* 2021;71(4):359.
4. Yimit A, Adebali O, Sancar A, Jiang Y. Differential damage and repair of DNA-adducts induced by anti-cancer drug cisplatin across mouse organs. *Nat Commun.* 2019;10(1):309. doi: 10.1038/s41467-019-08290-2.
5. Moretton A, Slyskova J, Simaan ME, Arasa-Verge EA, Meyenberg M, Cerrón-Infantes DA, et al. Clickable cisplatin derivatives as versatile tools to probe the DNA damage response to chemotherapy. *Front Oncol.* 2022;12:874201. doi: 10.3389/fonc.2022.874201.
6. Fung C, Dinh P Jr, Ardeshir-Rouhani-Fard S, Schaffer K, Fossa SD, Travis LB. Toxicities associated with cisplatin-based chemotherapy and radiotherapy in long-term testicular cancer survivors. *Adv Urol.* 2018;2018:8671832. doi: 10.1155/2018/8671832.
7. Chovanec M, Abu Zaid M, Hanna N, El-Kouri N, Einhorn LH, Albany C. Long-term toxicity of cisplatin in germ-cell tumor survivors. *Ann Oncol.* 2017;28(11):2670-9. doi: 10.1093/annonc/mdx360.
8. Bailey CJ, Day C. Metformin: its botanical background. *Practical Diabetes International.* 2004;21(3):115-7. doi:10.1002/pdi.606.
9. Dowling RJ, Goodwin PJ, Stambolic V. Understanding the benefit of metformin use in cancer treatment. *BMC Med.* 2011; 9: 33. doi:10.1186/1741-7015-9-33.
10. Buzzai M, Jones RG, Amaravadi RK, Lum JJ, DeBerardinis RJ, Zhao F, et al. Systemic treatment with the antidiabetic drug metformin selectively impairs p53-deficient tumor cell growth. *Cancer Res.* 2007;67(4):6745-52. doi: 10.1158/0008-5472.CAN-06-4447.
11. Ugwueze CV, Ogamba OJ, Young EE, Onyenekwe BM, Ezeokpo BC. Metformin: a possible option in cancer chemotherapy. *Anal Cell Pathol (Amst).* 2020;2020:7180923. doi: 10.1155/2020/7180923.
12. Saraei P, Asadi I, Kakar MA, Moradi-Kor N. The beneficial effects of metformin on cancer prevention and therapy: a comprehensive review of recent advances. *Cancer Manag Res.* 2019; 11:3295-313. doi: 10.2147/CMAR.S200059.
13. Mazurek M, Litak J, Kamieniak P, Kulesza B, Jonak K, Baj J, et al. Metformin as potential therapy for high-grade glioma. *Cancers (Basel)*. 2020;12(1):210. doi: 10.3390/cancers12010210
14. Ohno M, Kitanaka C, Miyakita Y, Tanaka S, Sonoda Y, Mishima K, et al. Metformin with temozolomide for newly diagnosed glioblastoma: results of phase I Study and a brief review of relevant studies. *Cancers (Basel)*. 2022;14:4222. doi: 10.3390/cancers14174222.
15. Seliger C, Luber C, Gerken M, Schaertl J, Proescholdt M, Riemenschneider MJ, et al. Use of metformin and survival of patients with high-grade glioma. *Int J Cancer.* 2019;144(2):273-80. doi: 10.1002/ijc.31783.
16. Liu EK, Vasudevaraja V, Sviderskiy VO, Feng Y, Tran I, Serrano J, et al. Association of hyperglycemia and molecular subclass on survival in IDH-wildtype glioblastoma. *Neurooncol Adv.* 2022;4(1):vdac163. doi: 10.1093/noajnl/vdac163.
17. Al-Shammari AM, Al-Juboory AA, Al-Mukhtar AA, Ali AM, Al-Hili ZA, Yaseen NY. Abstract 1221: Establishment and characterization of a chemoresistant glioblastoma cell line from an Iraqi patient. *Cancer Res.* 2014;74(19_Supplement): 1221. doi:10.1158/1538-7445.AM2014-1221.
18. Chou TC, Talalay P. Quantitative analysis of dose-effect relationships: the combined effects of multiple

drugs or enzyme inhibitors. Adv. *Enzyme Regul.* 1984;22:27-55. doi:10.1016/0065-2571(84)90007-4.
19. Collins AR. The comet assay for DNA damage and repair: principles, applications, and limitations. *Mol Biotechnol.* 2004;26(3):249-61. doi: 10.1385/MB:26:3:249.
20. Chakravarty M, Ganguli P, Murahari M, Sarkar RR, Peters GJ, Mayur YC. Study of combinatorial drug synergy of novel acridone derivatives with temozolomide using in-silico and in-vitro methods in the treatment of drug-resistant glioma. *Front Oncol.* 2021;11:625899. doi:10.3389/fonc.2021.625899.
21. Ohno M, Kitanaka C, Miyakita Y, Tanaka S, Sonoda Y, Mishima K, et al. Metformin with temozolomide for newly diagnosed glioblastoma: Results of phase I study and a brief review of relevant studies. *Cancers (Basel)*. 2022;14(17):4222. doi: 10.3390/cancers 14174222.
22. Zou Y, Wang Y, Xu S, Liu Y, Yin J, Lovejoy DB, et al. Brain co-delivery of temozolomide and cisplatin for combinatorial glioblastoma chemotherapy. *Adv Mater.* 2022;34(33):e2203958. doi: 10.1002/adma. 202203958.
23. Al Hassan M, Fakhoury I, El Masri Z, Ghazale N, Dennaoui R, El Atat O, et al. Metformin treatment inhibits motility and invasion of glioblastoma cancer cells. *Anal Cell Pathol (Amst)*. 2018;2018:5917470. doi: 10.1155/2018/5917470.
24. Apostolou P, Toloudi M, Kourtidou E, Mimikakou G, Vlachou I, Chatziioannou M, et al. Use of the comet assay technique for quick and reliable prediction of in vitro response to chemotherapeutics in breast and colon cancer. *J Biol Res (Thessalon)*. 2014;21(1):14. doi: 10.1186/2241-5793-21-14.

Original Article
Middle East Journal of Cancer; April 2024; 15(2):108-116

The Effect of 1% Pilocarpine Mouthwash on Salivary Flow Rate in Patients with Radiation-Induced Xerostomia: A Double-Blind Randomized Clinical Trial

Paria Motahari*, DDS, Farzaneh Pakdel*, DDS, Nastaran Hashemzadeh, PhD, Farid Heydari*, DDS, Reza Eghdam Zamiri***, MD, Katayoun Katebi*♦, DDS**

*Department of Oral and Maxillofacial Medicine, Tabriz University of Medical Sciences, Tabriz, Iran
**Pharmaceutical Analysis Research Center and Faculty of Pharmacy, Tabriz University of Medical Sciences, Tabriz, Iran
***Department of Radiation Oncology, Faculty of Medicine, Tabriz University of Medical Sciences, Tabriz, Iran

Please cite this article as: Motahari P, Pakdel F, Hashemzadeh N, Heydari F, Eghdam Zamiri R, Katebi K. The effect of 1% pilocarpine mouthwash on salivary flow rate in patients with radiation-induced xerostomia: a double-blind randomized clinical trial. Middle East J Cancer. 2024;15(2):108-16. doi:10.30476/mejc.2023.98297.1889.

♦Corresponding Author:
Katayoun Katebi, DDS
Department of Oral and Maxillofacial Medicine, Faculty of Dentistry, Tabriz University of Medical Sciences, Tabriz, Iran
Tel: +984133355965
Fax: +984133346977
Email: katebik@tbzmed.ac.ir
k_katebi@yahoo.co.uk

Abstract

Background: Radiation-induced hyposalivation is a common complication of radiotherapy for head and neck cancers. The most commonly prescribed medication for hyposalivation is pilocarpine. However, due to the numerous systemic side-effects associated with pilocarpine, there has been a proposal to use it as a mouthwash. This study aimed to evaluate the impact of 1% pilocarpine mouthwash on salivary flow in patients with radiation-induced xerostomia.

Method: This double-blind, randomized clinical trial involved 63 patients with radiation-induced xerostomia. The patients were randomly allocated into the pilocarpine hydrochloride 1% mouthwash group and the placebo one. Patients were instructed to use these mouthwashes four times a day, with 30 drops each time, for two minutes. Unstimulated saliva production in patients was measured using the spitting method at three stages: two weeks before the commencement of radiotherapy, two weeks after, and four weeks after the completion of radiotherapy. These measurements were then compared between the two groups. Statistical analysis included chi-square, independent t-test, and Analysis of Variance (ANOVA) with repeated measures and the Sidak post hoc test. Statistical analysis was conducted using SPSS 17, and a significance level of $P < 0.05$ was applied.

Results: A comparison of saliva secretion between the pilocarpine mouthwash group and the control group at various time points after radiotherapy revealed that saliva secretion in the control group significantly decreased compared with the pilocarpine mouthwash group ($P < 0.001$).

Conclusion: 1% pilocarpine mouthwash is recommended for managing radiation-induced xerostomia.

Keywords: Head and neck neoplasms, Salivation, Mouthwashes, Pilocarpine, Radiotherapy

Received: March 07, 2023; Accepted: November 13, 2023

Introduction

Radiation therapy is one of the most common treatment options for head and neck cancers and plays a vital role in the management of many cancers by increasing the patient's chances of survival. In addition, in some cases, it can result in a complete cure.[1] Head and neck radiotherapy, despite its apparent benefits, is associated with unavoidable side-effects such as hyposalivation, which in some patients can last for a lifetime. Unfortunately, in many patients, radiation-induced xerostomia caused by the damage to acinar cells of the salivary glands is inevitable.[1-4]

Decreased salivation can result in significant disorders, including severe pain, speech disorders, dysphagia, dental caries, especially cervical caries, mucosal infections such as candidiasis, atrophic papillary changes of the tongue, halitosis, nutritional and taste disorders.[5, 6] Furthermore, reduced salivation has considerable effects on the quality of life of these patients, as it can limit their social interactions and exacerbate depression.[7] Moreover, this state can cause or intensify mucositis, which may even limit the continuance of radiotherapy.[8] Various methods have been proposed to prevent radiation-induced

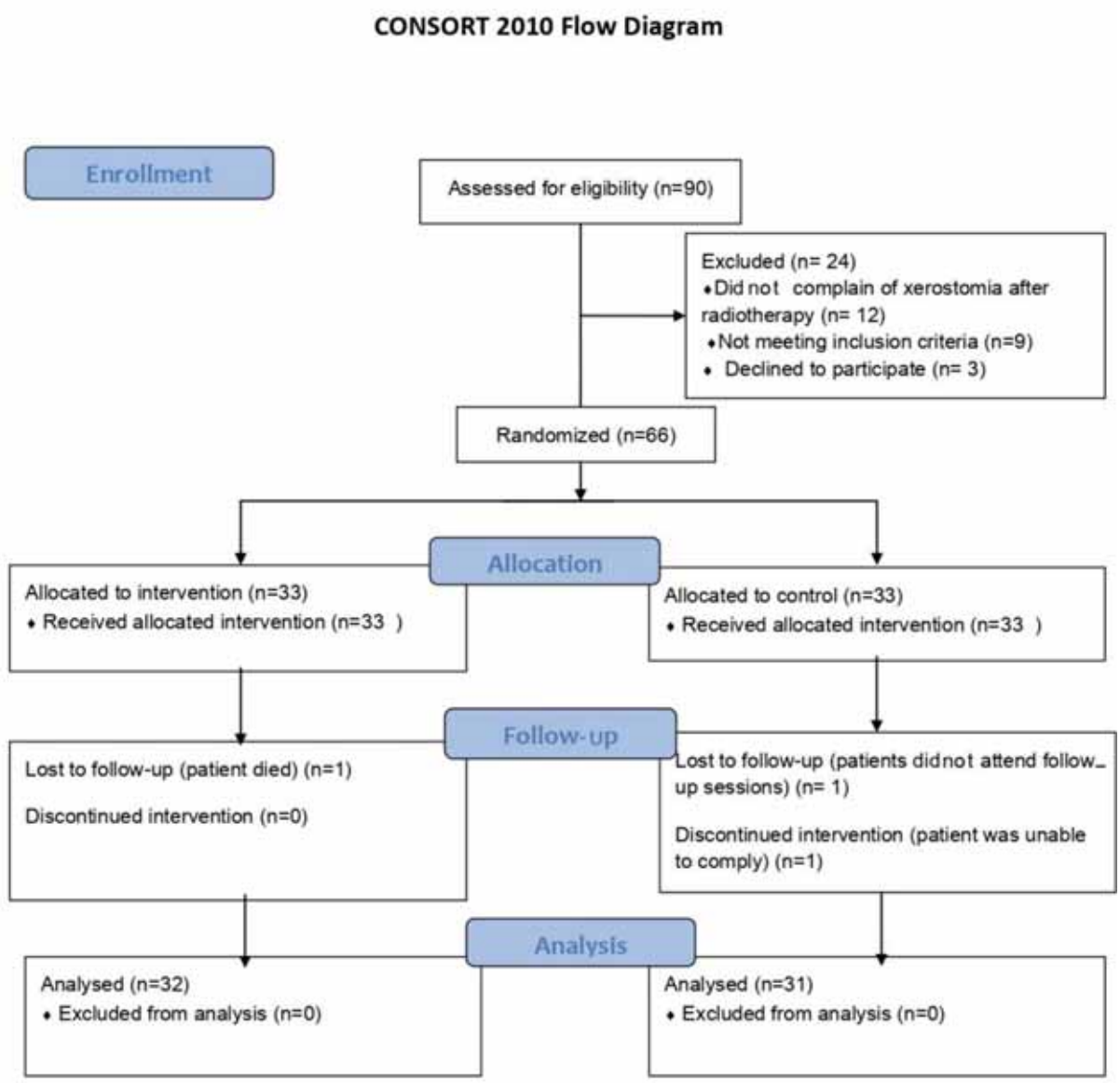

Figure 1. CONSORT 2010 flow diagram illustrates participant enrollment (in pilocarpine and placebo moutwash groups) follow-up procedures.

Table 1. Demographic characteristics and clinical features (cancer site and stage) of the study participants in pilocarpine and placebo mouthwash groups

Variable		Pilocarpine (n = 32) (frequency (percent))	Control (n = 31) (Frequency (percent))	*P*- value
Age (mean ± SD in years)		53.32 ± 6.08	51.48 ± 8.03	0.314[a]
Sex	Male	21 (65.7%)	19 (61.3%)	0.596[b]
	Female	11 (34.3%)	12 (38.7%)	
Cancer site				
	Larynx	10 (31.2%)	12 (38.7%)	0.826[c]
	Nasopharynx	4 (12.6%)	6 (19.4%)	
	Oral	9 (28.1%)	4 (12.9%)	
	Salivary gland	2 (6.2%)	1 (3.2%)	
	Nasal	6 (18.8%)	7 (22.6%)	
	Hypopharynx	1 (3.1%)	1 (3.2%)	
Cancer stage				
	I	3 (9.4%)	4 (12.9%)	0.786[c]
	II	10 (31.2%)	8 (25.8%)	
	III	15 (46.8%)	16 (51.6)	
	IV	4 (12.6%)	3 (9.7%)	

[a]*P*-value based on an independent t-test; [b]*P*-value based on chi-square; [c]*P*-value based on multinomial logistic regression

hyposalivation.[9] Frequent consumption of fluids and the use of sugar-free chewing gum, Bethanechol, and acupuncture are some of these approaches that can stimulate the remaining salivary capacity.[10] Systemic sialagogues can help to stimulate saliva as well.[11]

Pilocarpine is one of the medications among salivary stimulants and has been suggested as the best available agent.[2] However, several side-effects such as sweating, hot flashes, nausea, and increased airway mucus secretion have also been reported with pilocarpine.[12]

Pilocarpine mouthwash has been proposed as an alternative to oral pilocarpine tablets to minimize the side-effects of systemic pilocarpine.[13,14] Besides, pilocarpine mouthwash has been proven to be safe even for the elderly.[13] Previous clinical trials on this subject used different medication regimens, resulting in different findings.[15,16] Therefore, this clinical trial aims to investigate the effect of pilocarpine 1% mouthwash on salivary flow rate in patients with radiation-induced xerostomia.

Patients and Materials

Study design

This study was a double-blind, randomized clinical trial in which blinding was performed for both therapists and patients. This study was carried out according to the CONSORT statement.[17]

Sample size

To determine the sample size, the study of Haddad et al.[3] was used, in which the average rate of salivary flow reduction in the two groups of pilocarpine and placebo was 40.32 ± 22.04 and 57.05 ± 21.53 ml, respectively. Thus, considering the error rate of the first type equal to 0.05 and the test power of 80%, the minimum number of 28 patients in each group was calculated. Finally, 90 patients were assessed for eligibility, and 66 patients (33 samples in each group) were included in the study (Figure 1).

All sequential patients diagnosed with head and neck carcinoma who underwent radiotherapy in the Radiation Oncology Department of Shahid Madani Hospital of Tabriz University of Medical Sciences in 2021-2022 were screened for the study.

The http://www.graphpad.com/quickcalcs/index.cfm website was used by FH to create a randomization list. In the next step, sequential patients enrolled in the study were randomly assigned to intervention and control groups by sealed and opaque envelopes with an allocation ratio of 1:1. The hospital staff assigning the

patients to study groups was not aware of the allocation sequence until the moment of assignment (allocation concealment).

Inclusion criteria

1. Patients who have completed radiotherapy for head and neck cancers.
2. Patients aged 18 to 60 years old.
3. Patients with complaints of xerostomia.

Exclusion criteria

1. Patients for whom pilocarpine is contraindicated (established allergy to pilocarpine, history of cardiovascular disease, glaucoma, asthma).
2. Patients with residual or recurrent disease.
3. Patients who have received concurrent chemotherapy.
4. Patients who have undergone any xerostomia treatment.
5. Patients with autoimmune diseases such as Sjögren's syndrome.
6. Smokers.

All patients in both groups underwent radiotherapy (5000 cGy) utilizing an Elekta Synergy system (Elekta AB, Stockholm, Sweden), using an oral shield to safeguard oral structures, particularly the salivary glands.

Preparation of mouthwashes

To prepare a 1% pilocarpine mouthwash, 0.5 ml of sterile 2% pilocarpine ocular eye drop (Glaupin 2%, Sina Darou, Iran) was combined with 9.5 ml of Irsha Kids Mouthwash (Shafa Pharmaceutical, Alborz, Iran) to achieve a final volume of 10 ml, as outlined in previous studies.[18] Irsha Kids Mouthwash (Shafa Pharmaceutical, Alborz, Iran) underwent dilution with water to match the taste and color profile of placebo mouthwashes. A pharmacologist used identical containers to encode the mouthwashes as sample A for the pilocarpine mouthwashes and sample B for the placebo mouthwashes.

A dental nurse, unacquainted with the coding, dispensed the samples. The clinician and patients were blinded to the specific mouthwash allocated to each patient. The nature of the intervention administered to individual patients remained undisclosed until data analysis. Patients were instructed to retain 30 drops of the mouthwash

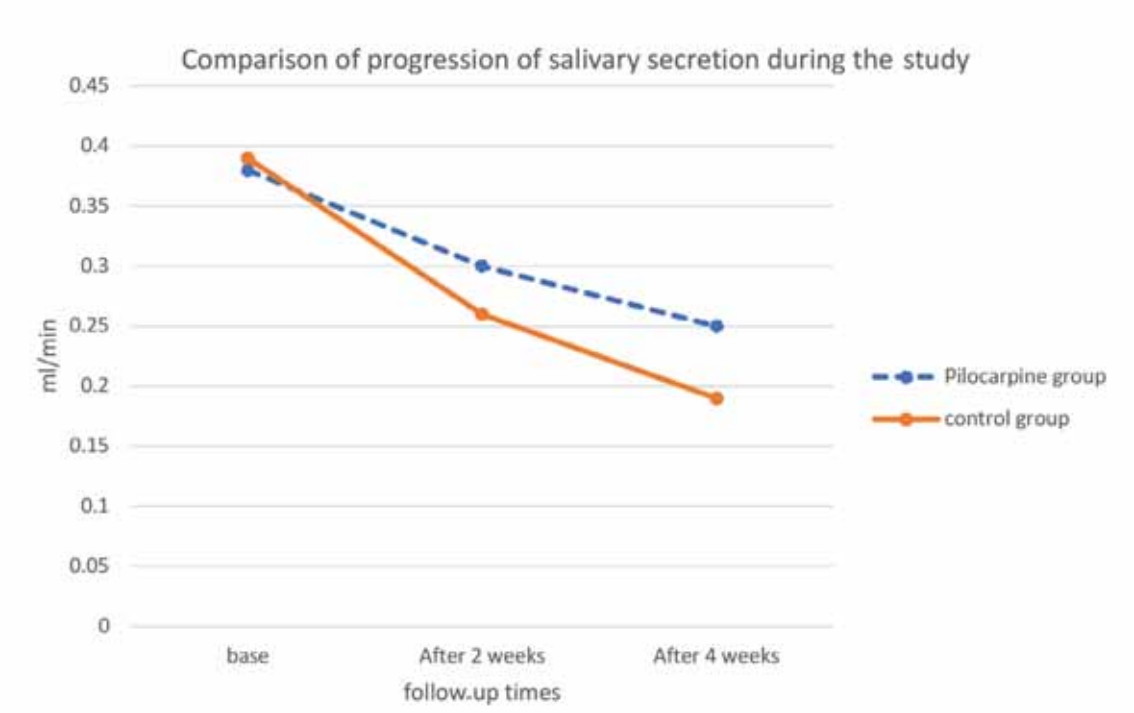

Figure 2. This figure presents a comparative analysis of salivary secretion between the pilocarpine mouthwash and the control groups at various time intervals following radiotherapy. The results reveal a noteworthy disparity in salivary flow rates, with the control group exhibiting a significantly lower rate than the pilocarpine mouthwash group during follow-up sessions.

Table 2. Mean salivary flow rate in pilocarpine and placebo mouthwash groups at different times after radiotherapy

Groups	Times	Mean ± SD (ml/min)	Standard error	Min	Max	95% confidence interval		*P*-value[a]
						Lower band	Upper band	
Intervention group (pilocarpine mouthwash)	Base	0.38 ± 0.16	0.02	0.18	0.60	0.32	0.43	< 0.001
	After 2 weeks	0.30 ± 0.11	0.01	0.10	0.48	0.26	0.33	
	After 4 weeks	0.25 ± 0.13	0.02	0.08	0.41	0.20	0.29	
Control group (placebo)	Base	0.39 ± 0.20	0.03	0.19	0.69	0.32	0.46	< 0.001
	After 2 weeks	0.26 ± 0.14	0.02	0.09	0.46	0.21	0.30	
	After 4 weeks	0.19 ± 0.11	0.01	0.06	0.34	0.15	0.22	

[a]*P*-value based on Repeated Measures ANOVA; Min: Minimum; Max: Maximum

four times daily, with each application lasting two minutes. They were instructed not to ingest the solution and to ensure complete expulsion by spitting out the entire volume. Any instances of discoloration led to the immediate disposal of the mouthwash.

During the initial appointment, a two-week supply of mouthwash was dispensed to the patients. They were instructed to return any remaining mouthwash at the subsequent two-week follow-up session. The weight of the mouthwash within each container was measured as a means of assessing patient compliance. New mouthwash supplies were furnished to the patients after the second week. Weekly reminder phone calls were conducted to reinforce compliance. Demographic data, including age, gender, and pertinent medical histories, such as cancer stage and site, received treatments, and treatment termination dates, were extracted from the patient's medical records.

Intervention

Two weeks prior to the first session of radiotherapy, a salivary sample was obtained and considered as a baseline, and the use of mouthwashes began the next day and continued for one month. Salivary sampling was repeated two and four weeks after the completion of radiotherapy.

Silaometry

The unstimulated saliva flow rate was measured in three stages using the spitting method for all patients.[19] Patients were asked to abstain from drinking or eating anything for 90 minutes before sampling. They were then asked to drain their saliva once or twice a minute for 5 minutes in a calibrated test tube.[20] The salivary flow rate was recorded in milliliters per minute.

Ethical considerations

The study was conducted following the Declaration of Helsinki and received approval from the ethics committee of Tabriz University of Medical Sciences (IR.TBZMED.REC.1400.499). It has been registered with the Iranian Registry of Clinical Trials under the identifier IRCT20210830052335N1. The study protocol can be accessed at https://en.irct.ir/trial/58396. Following a comprehensive explanation of the study to the patients, all eligible individuals were requested to complete and provide their signatures on the informed consent form.

Statistical analysis

The SPSS version 17 was used for statistical analysis. The Kolmogorov-Smirnov test was used to investigate the normality of the data distribution. Chi-square and independent t-tests were used to compare the variables between the groups. Analysis of variance with repeated measures and the Sidak post hoc test were used to evaluate salivary secretion over time. In all cases, $P < 0.05$ was considered statistically significant.

Results

For each group, the numbers of participants who were randomly assigned, received the allocated treatment, and were included in the analysis are depicted in figure 1. Recruitment commenced in October 2021, and the final follow-up of the last patient occurred in August 2022. The age range of the pilocarpine group was 40-

62 years, with a mean age of 53.32 ± 6.08 years. In the control group, the age range was 38-65, with a mean age of 51.48 ± 8.03. There were no significant differences in the ages of the study group participants ($P = 0.314$) (Table 1).

Regarding gender, 67.7% of participants in the pilocarpine mouthwash group and 61.3% in the control group were males. Gender distribution between the two study groups was analyzed using the chi-square test (Table 2). The results did not reveal a significant difference ($P = 0.596$). Laryngeal cancer was the predominant cancer type in both groups, with a prevalence of 45.2% in the pilocarpine mouthwash group and 38.7% in the control group. Similarly, comparing cancer types between the two study groups by the chi-square test did not show any significant differences ($P = 0.826$) (Table 2). Notably, most patients in both groups were in stage three of the disease. Additionally, the comparison of cancer stages between the two study groups, which was evaluated using the chi-square test (Table 2), did not reveal any significant differences ($P = 0.786$).

The comparison of salivary secretion in the pilocarpine mouthwash group at different time points after radiotherapy, conducted through repeated measures analysis of variance, demonstrated a significant difference ($P < 0.001$). The Sidak post hoc test results indicated that the salivary flow rate consistently decreased significantly at all time points ($P < 0.001$).

Similarly, the analysis of salivary secretion in the control group at different time points after radiotherapy using repeated measures analysis of variance showed a significant difference over time ($P = 0.005$). The Sidak post hoc test results revealed a consistent significant decrease in salivary secretion over time in this group ($P < 0.001$).

The comparison of basal salivary volume between the study groups, assessed by independent t-test, did not yield a significant difference ($P = 0.974$).

When comparing salivary secretion between the pilocarpine mouthwash group and the control group during various periods after radiotherapy, as shown in figure 2, a significant difference between the two groups was observed ($P < 0.001$). The Sidak post hoc test indicated that the salivary flow rate in the control group was significantly lower than that in the pilocarpine mouthwash group during follow-up sessions ($P < 0.001$) but not at baseline ($P = 0.076$).

Five patients in the pilocarpine mouthwash group reported experiencing palpitations, while two mentioned excessive sweating. However, these symptoms were mild, and the patients continued the trial.

Discussion

Comparison of salivary secretion in the pilocarpine mouthwash group at two and four-week follow-ups after radiotherapy showed that the salivary flow rate had consistently decreased significantly. The salivary flow rate in the control group was significantly lower than that of the pilocarpine mouthwash group at follow-up sessions. Despite many advances in cancer biology and radiation therapy in recent decades, salivary gland dysfunction remains a significant and lasting problem after radiotherapy of head and neck malignancies.[21, 22] The patients in the present study in both the pilocarpine and control mouthwash groups were in their fifth decade of life, and the majority (over 60%) were male. Previous studies have reported a higher prevalence of head and neck malignancies in men than in women.[23, 24] In the study of Haddad et al., 60% of the patients with this kind of cancer were male.[3] Moreover, numerous reports have indicated that the typical age for head and neck cancers is around 50 to 70 years old.[2, 25] In the present study, laryngeal cancer was the most common kind of cancer in patients. Several reports have reported that the most common head and neck cancer in Iran is laryngeal cancer.[26,27]

In the present study, 1% pilocarpine mouthwash was used 4 times daily for 2 minutes each time. The study by Song et al. stated that the minimum effective dose for increasing the level of unstimulated saliva by pilocarpine mouthwash is 1% after at least 1 minute of use.[28] The present study examined patients' salivation at three time intervals before starting radiotherapy, two and four weeks after the beginning of the radiotherapy.

Several studies have shown that salivary gland dysfunction after radiotherapy for head and neck malignancies usually begins within the first weeks after starting treatment.[20, 21, 29] Onset of serous acinar cell destruction can occur in a few days after radiotherapy.[30]

Decreased salivation in patients receiving radiotherapy is due to the destruction of serous acinar cells, with the development of acute inflammation.[31] The histological basis for decreased salivation after radiation therapy is not fully understood. Recent molecular studies have revealed that inflammatory cytokines, such as TNF-α, reduce the release of aquaporin 5 (a group of plasma membrane proteins responsible for transporting water molecules from the membrane), thereby reducing aqueous salivary secretions.[32] Stimulation of salivary gland function can help patients with some residual salivary gland parenchyma through sialogogue medications such as pilocarpine and cevimeline.[33] The use of systemic pilocarpine during radiation therapy has been suggested to reduce xerostomia[3, 34,35] and the use of pilocarpine for treating chronic hyposalivation has been thoroughly investigated.[36] pilocarpine is a parasympathomimetic drug that affects the muscarinic cholinergic receptors in the acinar cells of salivary glands, thereby improving salivary secretion.[2] Muscarinic acetylcholine receptors have five subtypes, M1–M5; pilocarpine's main therapeutic effects are mediated by M3 receptors, which activate the effector enzyme phospholipase C beta, which hydrolyses phospholipid PIP2, causing the production of the second messenger's inositol triphosphate and diacylglycerol and calcium and protein kinase. As a result, M3 cholinergic agonists can upregulate calcium and lead to smooth muscle contraction.[37] A systematic review by Riley et al., although linking pilocarpine to increased salivary secretion, suggested the need for further evidence.[38] A systematic review concluded that the administration of systemic pilocarpine has beneficial effects on salivary flow after radiotherapy.[39]

In the present study, the mean salivation in pilocarpine mouthwash patients was lower than average only in the last measurement (four weeks after radiotherapy). In contrast, in the control group, the mean salivation was lower than average two and four weeks after radiotherapy. Some studies investigate the effect of pilocarpine in topical form to reduce its adverse effects.[13, 40] However, few studies have studied the effects of topical pilocarpine in radiation-induced xerostomia. A clinical trial by Akhavan Karbasi et al. studied the preventive effects of pilocarpine and reported that pilocarpine mouthwash effectively prevents xerostomia.[16] Besides, it can prevent the reduction of saliva. Similarly, the present study's findings indicated that the salivary secretion in the control group decreased significantly over time more than in the pilocarpine mouthwash group. Taweechaisupapong et al. studied the efficacy of pilocarpine lozenge in patients with post-radiation xerostomia and showed that salivary production in pilocarpine treatment groups increased significantly.[14]

In the present study, Only 1% pilocarpine mouthwash was used, but a study by Motamed et al. showed that pilocarpine 2 and 1% mouthwash for 2 weeks increased salivary flow in patients with radiation-induced xerostomia, and the effect was dose-dependent. No side-effects were reported with higher dose mouthwash.[18]

The participants of this study had different types of head and neck cancer, and they were in different stages of the disease; therefore, it can be suggested that the results can be used for the reduction of the symptoms of radiation-induced xerostomia in all these situations.

The limitation of this study was that it assessed only the short-term effects of the pilocarpine mouthwash on radiation-induced xerostomia; therefore, in order to achieve more accurate results regarding the effect of pilocarpine mouthwash on saliva secretion in these patients, it is suggested to design a study with larger sample size and considering factors such as chemotherapy and long follow-ups. Another limitation of this study is that received doses of salivary glands in the participants were not estimated and matched between groups.

Conclusion

The salivary flow rate decreased over time in both groups. The reduction in salivary flow rate was notably more pronounced in the control group compared with the pilocarpine mouthwash group. After four weeks, the salivary flow rate was significantly elevated in the pilocarpine mouthwash group compared with the control group. In light of the findings from this current study, it is advisable to consider using 1% pilocarpine mouthwash as a therapeutic option for radiation-induced xerostomia.

Acknowledgment

The authors would like to thank the staff of Shahid Madani Hospital for their cooperation during this study.

Conflict of Interest

None declared.

References

1. Shaikh T, Handorf EA, Murphy CT, Mehra R, Ridge JA, Galloway TJ. The impact of radiation treatment time on survival in patients with head and neck cancer. *Int J Radiat Oncol Biol Phys.* 2016;96(5):967-75. doi:10.1016/j.ijrobp.2016.08.046.
2. Villa A, Connell CL, Abati S. Diagnosis and management of xerostomia and hyposalivation. *Ther Clin Risk Manag.* 2014;11:45-51. doi:10.2147/TCRM.S76282.
3. Haddad P, Karimi M. A randomized, double-blind, placebo-controlled trial of concomitant pilocarpine with head and neck irradiation for prevention of radiation-induced xerostomia. *Radiother Oncol.* 2002;64(1):29-32. doi:10.1016/s0167-8140(02)00104-4.
4. Wu VW, Leung KY. A review on the assessment of radiation induced salivary gland damage after radiotherapy. *Front Oncol.* 2019;9:1090. doi:10.3389/fonc.2019.01090.
5. Millsop JW, Wang EA, Fazel N. Etiology, evaluation, and management of xerostomia. *Clin Dermatol.* 2017;35(5):468-76. doi:10.1016/j.clindermatol.2017.06.010.
6. Molek M, Florenly F, Lister INE, Wahab TA, Lister C, Fioni F. Xerostomia and hyposalivation in association with oral candidiasis: a systematic review and meta-analysis. *Evid Based Dent.* 2022: In press. doi:10.1038/s41432-021-0210-2.
7. Enoki K, Matsuda KI, Ikebe K, Murai S, Yoshida M, Maeda Y, et al. Influence of xerostomia on oral health-related quality of life in the elderly: a 5-year longitudinal study. *Oral Surg Oral Med Oral Pathol Oral Radiol.* 2014;117(6):716-21. doi:10.1016/j.oooo.2014.03.001.
8. Feller G, Khammissa RAG, Nemutandani MS, Feller L. Biological consequences of cancer radiotherapy in the context of oral squamous cell carcinoma. *Head Face Med.* 2021;17(1):35. doi:10.1186/s13005-021-00286-y.
9. Marín C, Díaz-de-Valdés L, Conejeros C, Martínez R, Niklander S. Interventions for the treatment of xerostomia: A randomized controlled clinical trial. *J Clin Exp Dent.* 2021;13(2):e104-11. doi:10.4317/jced.57924.
10. Salum FG, Medella-Junior FD, Figueiredo MA, Cherubini K. Salivary hypofunction: An update on therapeutic strategies. *Gerodontology.* 2018;35(4):305-16. doi:10.1111/ger.12353.
11. Farag AM, Holliday C, Cimmino J, Roomian T, Papas A. Comparing the effectiveness and adverse effects of pilocarpine and cevimeline in patients with hyposalivation. *Oral Dis.* 2019;25(8):1937-44. doi:10.1111/odi.13192.
12. Davies AN, Thompson J. Parasympathomimetic drugs for the treatment of salivary gland dysfunction due to radiotherapy. *Cochrane Database Syst Rev.* 2015;2015(10):CD003782. doi:10.1002/14651858.CD003782.pub3.
13. Sarideechaigul W, Priprem A, Limsitthichaikoon S, Phothipakdee P, Chaijit R, Jorns TP, et al. Efficacy and safety of two artificial saliva-based polymers containing 0.1% pilocarpine for treatment of xerostomia: A randomized clinical pilot trial. *J Clin Exp Dent.* 2021;13(10):e994-1000. doi:10.4317/jced.58415.
14. Taweechai Supapong S, Pesee M, Aromdee C, Laopaiboon M, Khunkitti W. Efficacy of pilocarpine lozenge for post-radiation xerostomia in patients with head and neck cancer. *Aust Dent J.* 2006; 51(4): 333-7. doi:10.1111/j.1834-7819.2006.tb00453.x.
15. Pereira RMS, Bastos MDR, Ferreira MP, de Freitas O, de Macedo LD, de Oliveira HF, et al. Topical pilocarpine for xerostomia in patients with head and neck cancer treated with radiotherapy. *Oral Dis.* 2020;26:1209-18. doi:10.1111/odi.13343.
16. Akhavan Karbasi M, Zarghani H, Akhavan S, Donyadide N, Shamshiry P. Assessment of the preventive effect of pilocarpine on radiotherapy-induced xerostomia in patients with head and neck cancers. *Iran J Medical Phys.* 2015;12(4):235-41. doi:10.22038/ijmp.2016.6836.
17. Schulz KF, Altman DG, Moher D; CONSORT Group. CONSORT 2010 Statement: Updated guidelines for reporting parallel group randomised trials. *J Clin Epidemiol.* 2010;63(8):834-40. doi:10.1016/j.jclinepi.2010.02.005.
18. Motamed B, Alaee A, Azizi A, Jahandar H, Fard MJK,

Jafari A. Comparison of the 1 and 2% pilocarpine mouthwash in a xerostomic population: a randomized clinical trial. *BMC Oral Health.* 2022;22:548. doi:10.1186/s12903-022-02576-6.
19. Navazesh M, Christensen CM. A comparison of whole mouth resting and stimulated salivary measurement procedures. *J Dent Res.* 1982;61(10):1158-62. doi:10.1177/00220345820610100901.
20. Saleh J, Figueiredo MA, Cherubini K, Salum FG. Salivary hypofunction: an update on aetiology, diagnosis and therapeutics. *Arch Oral Biol.* 2015;60(2):242-55. doi:10.1016/j.archoralbio.2014.10.004.
21. Vissink A, van Luijk P, Langendijk JA, Coppes RP. Current ideas to reduce or salvage radiation damage to salivary glands. *Oral Dis.* 2015;21(1):e1-0. doi:10.1111/odi.12222.
22. Likhterov I, Ru M, Ganz C, Urken ML, Chai R, Okay D, et al. Objective and subjective hyposalivation after treatment for head and neck cancer: Long-term outcomes. *Laryngoscope.* 2018;128(12):2732-9. doi:10.1002/lary.27224.
23. Germano F, Melone P, Testi D, Arcuri L, Marmiroli L, Petrone A, et al. Oral complications of head and neck radiotherapy: prevalence and management. *Minerva Stomatol.* 2015;64(4):189-202.
24. Park JO, Nam IC, Kim CS, Park SJ, Lee DH, Kim HB, et al. Sex differences in the prevalence of head and neck cancers: a 10-year follow-up study of 10 million healthy people. *Cancers.* 2022;14(10):2521. doi:10.3390/cancers14102521.
25. Rettig EM, D'Souza G. Epidemiology of head and neck cancer. *Surg Oncol Clin N Am.* 2015;24(3):379-96. doi:10.1016/j.soc.2015.03.001.
26. Emadzadeh M, Shahidsales S, Mohammadian Bajgiran A, Salehi M, Massoudi T, Nikfarjam Z, et al. Head and neck cancers in north-east Iran: A 25 year survey. *Iran J Otorhinolaryngol.* 2017;29(92):137-45.
27. Taziki MH, Fazel A, Salamat F, Sedaghat SM, Ashaari M, Poustchi H, et al. Epidemiology of head and neck cancers in Northern Iran: A 10-year trend study from Golestan province. *Arch Iran Med.* 2018;21(9):406-11.
28. Song JI, Park JE, Kim HK, Kim KS. Dose and time-related effects of pilocarpine mouthwash on salivation. *J Oral Med Pain.* 2017;42(3):72-80.doi:10.14476/jomp.2017.42.3.72.
29. Barazzuol L, Coppes RP, van Luijk P. Prevention and treatment of radiotherapy-induced side effects. *Mol Oncol.* 2020;14(7):1538-54.doi:10.1002/1878-0261.12750.
30. Chitapanarux I, Iamaroon A. Salivary glands and dental complications after radiotherapy for nasopharyngeal carcinoma. *Ann Nasopharynx Canc.* 2020;4:7. doi: 10.21037/anpc-20-17.
31. Marmary Y, Adar R, Gaska S, Wygoda A, Maly A, Cohen J, et al. Radiation-induced loss of salivary gland function is driven by cellular senescence and prevented by il6 modulation cellular senescence in radiation-induced xerostomia. *Cancer Res.* 2016;76(5):1170-80. doi: 10.1158/0008-5472.CAN-15-1671.
32. Yao QT, Wu YH, Liu SH, Song XB, Xu H, Li J, et al. Pilocarpine improves submandibular gland dysfunction in irradiated rats by downregulating the tight junction protein claudin-4. *Oral Dis.* 2022;28(6):1528-38. doi:10.1111/odi.13870.
33. Mercadante V, Al Hamad A, Lodi G, Porter S, Fedele S. Interventions for the management of radiotherapy-induced xerostomia and hyposalivation: A systematic review and meta-analysis. *Oral oncol.* 2017;66:64-74. doi:10.1016/j.oraloncology.2016.12.031.
34. Cheng CQ, Xu H, Liu L, Wang RN, Liu YT, Li J, et al. Efficacy and safety of pilocarpine for radiation-induced xerostomia in patients with head and neck cancer: a systematic review and meta-analysis. *J Am Dent Assoc.* 2016;147(4):236-43. doi:10.1016/j.adaj.2015.09.014.
35. Yang WF, Liao GQ, Hakim SG, Ouyang DQ, Ringash J, Su YX. Is pilocarpine effective in preventing radiation-induced xerostomia? A systematic review and meta-analysis. *Int J Radiat Oncol Biol Phys.* 2016;94(3):503-11. doi:10.1016/j.ijrobp.2015.11.012.
36. Al Hamad A, Lodi G, Porter S, Fedele S, Mercadante V. Interventions for dry mouth and hyposalivation in Sjögren's syndrome: A systematic review and meta?analysis. *Oral Dis.* 2019;25(4):1027-47. doi:10.1111/odi.12952.
37. Kapourani A, Kontogiannopoulos KN, Barmpalexis P. A review on the role of pilocarpine on the management of xerostomia and the importance of the topical administration systems development. *Pharmaceuticals.* 2022;15(6):762. doi:10.3390/ph15060762.
38. Riley P, Glenny AM, Hua F, Worthington HV. Pharmacological interventions for preventing dry mouth and salivary gland dysfunction following radiotherapy. *Cochrane Database Syst Rev.* 2017;7(7):CD012744. doi:10.1002/14651858.CD012744.
39. Yang WF, Liao GQ, Hakim SG, Ouyang DQ, Ringash J, Su YX. Is pilocarpine effective in preventing radiation-induced xerostomia? A systematic review and meta-analysis. *Int J Radiat Oncol Biol Phys.* 2016;94(3):503-11. doi:10.1016/j.ijrobp.2015.11.012.
40. Katebi K, Hassanpour S, Eslami H, Salehnia F, Hosseinifard H. The effects of pilocarpine mouthwash on patients with xerostomia: a systematic review and meta-analysis. *J Dent (Shiraz).* 2023;24(Supplement-March-2023):76-83. doi:10.30476/DENTJODS.2022.94335.1778.

Original Article
Middle East Journal of Cancer; April 2024; 15(2): 117-127

The Role of Lovastatin in Curative Chemoradiotherapy for Patients with Head and Neck Cancer: A Randomized Trial

Azadeh Sharifian*♦, MD, Mahdi Aghili, MD**

**Radiation Oncology Research Center (RORC), Cancer Institute, Tehran University of Medical Sciences, Tehran, Iran*
***Department of Radiation Oncology, Cancer Institute, Tehran University of Medical Sciences, Tehran, Iran*

Please cite this article as: Sharifian A, Aghili M. The role of lovastatin in curative chemoradiotherapy for patients with head and neck cancer: a randomized trial. Middle East J Cancer. 2024;15(2):117-27. doi:10.30476/mejc.2023.97387.1911.

Abstract

Background: Evidence suggests that statins can improve survival outcomes and ameliorate treatment-related side-effects in certain malignancies. Statins exhibit various mechanisms of action, including apoptosis induction, proliferation inhibition, tumor radiosensitization, lipid production suppression, and anti-inflammatory effects. This trial aimed to assess the impact of lovastatin on patients with locally advanced head and neck squamous cell carcinoma (HNSCC) undergoing definitive chemoradiation.

Method: In this double-blinded randomized phase 2 clinical trial, 35 patients were randomly allocated to receive either 80 mg of lovastatin daily in conjunction with chemoradiotherapy (case group, n=18) or a placebo (control group). Primary outcomes included the response rate (RR) after three months, the occurrence of acute/late side-effects, median progression-free survival (PFS), and overall survival (OS).

Results: The complete RR was slightly higher in the statin group (83.3% vs. 64.7%), although it did not reach statistical significance (P = 0.592). Acute adverse events did not significantly differ between the two groups. Grade 3 dermatitis occurred more frequently in the placebo group (35.3% vs. 11.1%), while grade 3 mucositis was more common in the statin group (38.9% vs. 11.8%). The median OS was 22 months (confidence interval (CI) 95% = 6.3-37.6) in the statin group and 17 months (CI 95% = 4.9-29.1) in the control group (P = 0.50). Median PFS was 20 months (CI 95% = 15.8-24.1) in the statin group and 15 months (CI 95% = 8.2-21.7) in the control group (P = 0.609).

Conclusion: Combining lovastatin with chemoradiation augments the therapeutic effect in HNSCC. Larger-scale studies incorporating advanced radiotherapy techniques and baseline lipid profile assessments are necessary to investigate statins' efficacy in HNSCC further.

Keywords: Head and neck neoplasms, Squamous cell carcinoma, Statin, Chemoradiotherapy

♦Corresponding Author:
Azadeh Sharifian, MD
Radiation Oncology Research Center (RORC), Cancer Institute, Tehran University of Medical Sciences, Tehran, Iran
Tel: 021 61192567
Fax: 66948672
Email: Azadeh_sh90@yahoo.com

Received: April 19, 2023; Accepted: December 04, 2023

Introduction

Head and neck squamous cell carcinomas (HNSCCs) are among the most common cancers (4% of all cancers), and about 60% of HNSCCs are locally advanced at presentation.[1,2] The treatment choice for these cancers is surgical resection in resectable disease and adjuvant radiotherapy. Concurrent chemoradiotherapy (CRT) is recommended as a definitive treatment for unresectable locally advanced head and neck cancer (LAHNC). Chemotherapy administered concurrently as a radiosensitizer has improved survival in this group of patients; however, the prognosis of such patients is still poor.[1] Consequently, other agents with potential anticancer and radio-sensitizing effects might improve outcomes.[3]

Lipids are one of the basic structures of cell membranes and contribute to cell metabolism, including protein synthesis, cell signaling, energy storage, proliferation, differentiation, and apoptosis.[4, 5] Statins inhibit lipid metabolism by blocking the activity of 3-hydroxy-3-methyl-glutaryl-coenzyme A reductase (HMG-CoA), a key enzyme involved in the regulation of signaling proteins called guanosine diphosphate (GTPase) superfamily, which contribute to tumorigenesis, proliferation, and survival of tumor cells.[5-7] In vivo, studies have shown that statins have anti-proliferative and radiosensitizing effects,[3] and they increase sensitization to radiation by stopping the cell cycle in the late G1 phase.[6] In vivo, studies have demonstrated the apoptotic effects of lovastatin in HNSCC and cervical squamous cell carcinoma (SCC).[8, 9]

Several studies have demonstrated the potential oncologic benefits of statins for some cancers, such as colorectal, prostate, and breast cancers.[10] In a cohort study performed on HNSCC patients, those with hyperlipidemia who received statins showed improvement in overall survival (OS) and disease-specific survival (DSS), compared with the other two groups, including those without hyperlipidemia who used statins and those who neither had hyperlipidemia nor used statins.[11] Another retrospective study conducted on human papillomavirus (HPV)-negative HNSCC showed improvement in OS and DSS in patients who have used statin at least 1 month before and 4 months after diagnosis, compared with non-exposed statin patients.[12]

Most of the studies in the literature have been retrospective cohort trials. Additionally, the number of trials conducted on head and neck cancers in this regard is relatively limited. Consequently, a randomized clinical trial was undertaken to evaluate the effect of lovastatin on the response rate (RR) and complications in patients with locally advanced HNSCC who underwent radiotherapy.

Materials and Methods

Study design and target group

This double-blinded randomized clinical trial was conducted on patients with locally advanced HNSCC referred to the Cancer Institute of Tehran University of Medical Sciences, Tehran, Iran, between 2012 and 2013. The patients were undergoing either definitive CRT due to unresectable tumors or organ preservation.

Inclusion and exclusion criteria

Patients diagnosed with newly detected locally advanced HNSCC (T2-4, N0-3), as per the tumor staging criteria outlined in the American Joint Committee on Cancer (AJCC) 8th edition of 2010, originating from the larynx, base of the tongue, and hypopharynx, and confirmed through biopsy, were enrolled for definitive CRT. They were then randomly assigned into two groups using the permuted block technique (block size = 4). All patients underwent a comprehensive physical examination, and their medical histories were documented. Patients without distant metastasis and displaying average complete blood count (CBC), liver function tests (LFT), and renal function tests (RFT) results were eligible for inclusion in the study. Patients with metastasis or those requiring medications with potential interactions with lovastatin were excluded from the trial.

Treatment protocol

All patients received conventional radiation therapy with a dose of 2 Gy per fraction and three-dimensional conformal radiotherapy. The

Table 1. Comparison of patient groups: age, gender, tumor site, AJCC 8th edition staging, chemotherapy protocol, treatment duration

	Statin group (n=18)	Placebo group (n=17)	*P* value
Mean age	57.9	57.2	0.235
Gender			
Male	84.2%	88.9%	0.677
Female	15.8%	11.1%	
Primary tumor site			
Oral cavity	10.5%	11.1%	0.997
Larynx	84.2%	83.3%	
Hypopharynx	5.3%	5.6%	
Staging			
T4	31.6%	33.3%	0.137
T3	63.2%	66.7%	
T2	5.3%		
N0	26.3%	33.3%	0.137
N1	21.1%	38.9%	
N2	15.8%	22.2%	
N3	36.8%	5.6%	
Chemotherapy protocol			
3-week chemotherapy		16.7%	0.195
Weekly chemotherapy	100%	83.3%	0.195
Duration of treatment			
7 weeks	82%	66%	0.333
7-8 weeks	12%	28%	
More than 8 weeks	6%	6%	

AJCC: American Joint Committee on Cancer

total radiation dose administered to the gross target volume was 70 Gy, and 44-46 Gy was delivered to the subclinical target volume over 7 weeks, with treatment sessions held 5 days per week. Chemotherapy consisted of cisplatin at a dose of 35 mg/m^2, administered weekly or every 3 weeks (35 mg/m^2 on days 1-3) depending on patients' compliance. Additionally, the intervention group was prescribed 80 mg of lovastatin daily, divided into four doses, on days when patients underwent radiotherapy. In contrast, the control group received a placebo for the same duration.

Treatment evaluation

The primary outcome of this study involved evaluating RR through imaging after three months of treatment. Additionally, acute and late side-effects, median progression-free survival (PFS), and OS were assessed in both groups.

Acute reactions were monitored weekly through physical examinations, specifically evaluating mucositis using the World Health Organization (WHO) scoring system and assessing esophagitis and dermatitis based on the Common Terminology Criteria for Adverse Events (CTCAE) version 4.0 scoring system, all performed by the same physician. The highest grade observed during treatment was recorded as the patient's adverse events. Furthermore, routine tests, including CBC, blood urea nitrogen, and creatinine tests, were conducted weekly for all patients. LFT was only required, if patients reported unexplained muscular pain.

Response evaluation was carried out after three months of completing treatment using computed tomography (CT) scans or magnetic resonance imaging (MRI) in conjunction with physical examinations. This assessment involved comparing the pretreatment tumor volume, following the Response Evaluation Criteria in Solid Tumors (RECIST) criteria, to determine the RR in both patient groups.

During the follow-up period, which included history-taking and physical examinations, patients were seen every two months for the initial two years and, subsequently, every six months for five years. Any suspicious local recurrence or distant metastasis cases were confirmed through further diagnostic procedures such as CT scans, MRIs, or biopsies.

Statistical analysis

The formula for comparing the equality of two proportions was applied to determine the sample

Table 2. Treatment complications: Acute reactions (mucositis, esophagitis, dermatitis) graded according to CTCAE v4.0, hematologic complications (Weekly CBC) graded using the WHO system

Complications	Statin group (n=18)	Placebo group (n=17)	*P* value
Mucositis			
G1	11.1%	76.5%	0.176
G2	50%	11.8%	
G3	38.9%	11.8%	
Dermatitis			
G1	38.9%	17.65	0.163
G2	50.2%	47.1%	
G3	11.1%	35.3%	
Dysphagia			
G0	5%	18.1%	0.199
G1	55%	44.4%	
G2	28%	24.4%	
G3	12%	13.3%	
Anemia			
G0	56.3%	70.6%	0.135
G1	43.8%	17.6%	
G2	11.8%	11.8%	
Leukopenia			
G0	38.9%	47.1%	0.866
G1	50%	41.2%	
G2	11.1%	11.8%	
Thrombocytopenia			
G0	27.8%	17.6%	0.767
G1	44.4%	52.9%	
G2	17.8%	29.4%	

CTCAE: Common Terminology Criteria for Adverse Events; CBC: Complete blood count; G0: Grade 0; G1: Grade 1; G2: Grade 2; G3: Grade 3

size. The used significance level (alpha) was 0.05, and the desired statistical power was 80%.

Following prior research findings, the RR associated with definitive chemoradiation was estimated at approximately 65%. Our objective was to enhance this rate to 85% by administering statins. Consequently, our initial target sample size was 70 individuals for each experimental and control group. However, due to a slower-than-anticipated rate of subject enrollment, recruitment was halted after enlisting 35 participants, and an interim analysis was conducted.

The data collected underwent thorough analysis utilizing the Statistical Package for the Social Sciences (SPSS), specifically, Version 21 for Windows (SPSS Inc; Chicago, IL, USA). A $P < 0.05$ was regarded as indicative of statistical significance in all statistical tests conducted.

Kaplan-Meier survival analysis was utilized to estimate actuarial OS and PFS. OS was defined as the duration between the randomization point and the last follow-up or censoring event. Similarly, PFS was defined as the duration between the randomization point and the occurrence of recurrence, the last uneventful follow-up, death, or censoring. The Cox hazards test was also employed to identify factors predictive of OS and PFS.

Ethical considerations

This study was conducted conclusively with the World Medical Association Declaration of Helsinki and approved by the Ethics Committee of Tehran University of Medical Sciences (ethics code: 91/D/130/1291). The trial is registered on IRCT (IRCT 2014121920368N1). The goals of the study were explained to the participants. Then, the patients signed informed consent and were assured that their data would remain confidential to the research team.

Results

In this study, due to the prolonged rate of patient enrollment, 35 patients were randomized

Table 3. Radiologic response and survival rates: 2-year and 5-year events. Details: patient outcomes (no recurrence, locoregional recurrence, death, bone metastasis), 2-year and 5-year survival and PFS medians and percentages

	Statin group	Placebo group	*P* Value
Partial response	16.7%	35.3%	0.592
Complete response	83.3%	64.7%	
Median OS	22m (CI95%=6.3-37.6)	17m (CI95%=4.9-29.1)	0.5
Median PFS	20m (CI95%=15.8-24.1)	15m (CI95%=8.2-21.7)	0.609
Mean OS	30m (CI95%=20.9-40.3)	26m (CI95%=16.3-35.8)	0.5
Mean PFS	27.6m (CI95%=18.2-37)	22.7m (CI95%=13.1-32.7)	0.609
2-year events			0.87
No recurrence	33.3%	23.5%	
LTF	16.6%	23.5%	
Alive LRR	5.5%	5.8%	
Death met	11.1%	17.6%	
Death LRR	16.6%	17.6%	
Alive bone metastasis	11.1%	5.8%	
Death infection	5.5%	0.0%	
Death MI	0.0%	5.8%	
2y OS	49% (CI95%=26-72)	41% (CI95%=18-64)	
2y PFS	33% (CI95%=14-52)	24% (CI95%=5-43)	
5-year events			
Previously death	33.3%	35.2%	0.82
LFT	33.3%	29.4%	
Alive LRR	0.0%	5.8%	
No recurrence	11.1%	5.8%	
Death LRR	5.5%	5.8%	
Death due to metastasis	5.5%	17.6%	
Death stroke	5.5%	0.0%	
Death MI	5.5%	0.0%	
5y OS	25% (CI95%=4-46)	18% (CI95%=0-37)	
5y PFS	17% (CI95%=0-34)	18% (CI95%=0-37)	

LTF: Lost to follow-up; LRR: Locoregional recurrence; OS: Overall survival; PFS: Progression - free survival; CI: Confidence interval; MI: Myocardial infarction

into two groups: the intervention group (n=18) and the placebo group (n=17). Differences in patient characteristics, including age, gender, stage, treatment protocol, and therapy duration, were not statistically significant. A summary of these details is presented in table 1. Acute adverse events such as mucositis, acute dermatitis, and acute dysphagia were compared between the two groups, revealing no statistically significant differences. However, a higher incidence of high-grade (grade 3) dermatitis was observed in the placebo group (35.3% vs. 11.1%).

Conversely, a higher incidence of high-grade (grade 3) mucositis was noticed in the intervention group (38.9% vs. 11.8%). A summary of the relevant details is presented in table 2. Hematologic acute adverse events were assessed, indicating no significant differences in anemia, leukopenia, or thrombocytopenia when comparing the two groups. Details are provided in table 2. The RR between the two groups was described, with a complete response rate of 83.3% in the intervention group compared to 64.7% in the placebo group. However, this difference did not reach statistical significance ($P = 0.592$).

The median OS was 22 months (confidence interval (CI) 95% = 6.3-37.6) in the statin group and 17 months (CI 95% = 4.9-29.1) in the control group ($P = 0.50$). Likewise, the median PFS was 20 months (CI 95% = 15.8-24.1) in the statin group and 15 months (CI 95% = 8.2-21.7) in the control group ($P = 0.609$). The 5-year OS rates

were 25% (CI 95% = 4-46) in the statin group and 18% (CI 95% = 0-37) in the control group. Correspondingly, the 2-year OS rates were 49% (CI 95% = 26-72) in the statin group and 41% (CI 95% = 18-64) in the control group. The 5-year PFS rates were 17% (CI 95% = 0-34) in the statin group and 18% (CI 95% = 0-37) in the control group. Similarly, the 2-year PFS rates were 33% (CI 95% = 14-52) in the statin group and 24% (CI 95% = 5-43) in the control group. Details of the 2-year and 5-year events are summarized in table 3 and illustrated in figures 1, 2, and 3. Table 4 summarizes the late toxicity score rates concerning dysphagia, laryngeal mucositis, xerostomia, and superficial soft tissue fibrosis during the follow-up period. The median follow-up duration for the statin and control groups was 22 and 17 months, respectively.

Discussion

The study prescribed lovastatin at 80 mg daily, concurrent with definitive CRT in locally advanced HNSCC for the statin group comprising 18 patients. This was compared with a control group consisting of 17 patients. After five years of follow-up, it was observed that RR, median OS, and PFS were non-significantly better in the statin group. The acute and chronic adverse events did not show significant differences.

HNSCCs are among the most common cancers, and CRT is the treatment of choice in unresectable LAHNC.[1, 2] Lipids are one of the basic structures of cell membranes.[5] Recent studies have recognized lipid metabolism as a hallmark of malignancy.[4] Lipids contribute to cell signaling by a group of proteins that are claimed to be upregulated in different cancers that subsequently stimulate tumor growth.[6] Statins inhibit lipid metabolism by preventing HMG-CoA reductase that regulates the activity of signaling proteins called the GTPase superfamily that contributes to tumorigenesis, proliferation, and survival of tumor cells.[7, 3] Several lines of evidence suggest that statins impair the metastatic potential of tumor cells by inhibiting cell migration, attachment to the extracellular matrix, and invasion of the basement membrane. In addition, they have antiangiogenic effects.[13]

Inflammatory risk factors, such as obesity, diabetes mellitus, and smoking, are carcinogenic even without hyperlipidemia; therefore, inflammatory suppression reduces both cardiovascular and cancer mortalities.[14] Statins have anti-inflammatory effects that contribute to

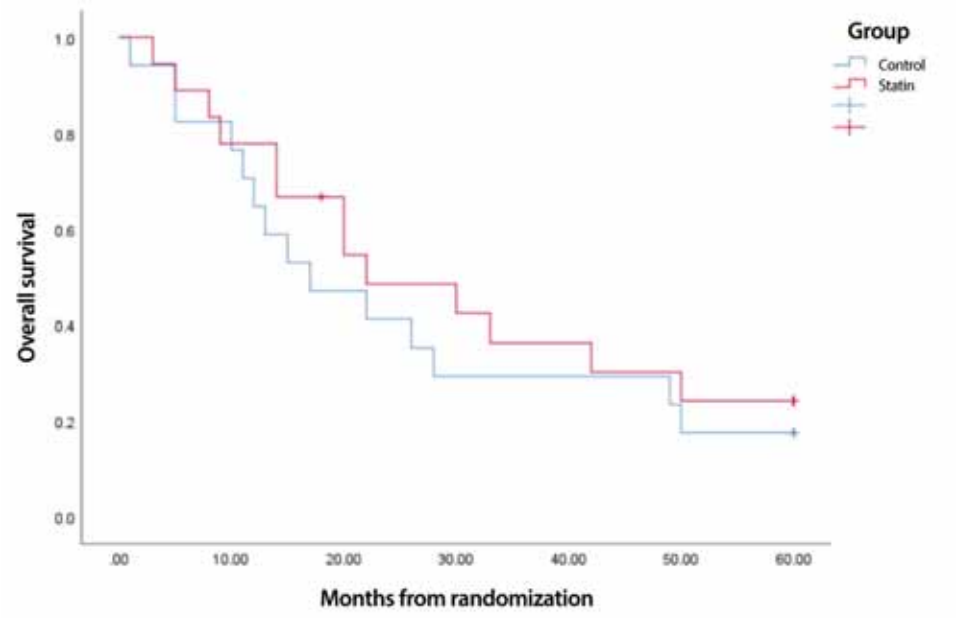

Figure 1. This figure illustrates the OS curve in the control group (blue line) and the statin group (red line). The median OS is 22 months (CI95%=6.3-37.6) in the statin group and 17 months (CI95%=4.9-29.1) in the control group ($P = 0.50$).
OS: Overall survival; CI: Confidence interval

their beneficial effects independent of lowering cholesterol.[15] In vivo studies have shown that statins have antiproliferative and radiosensitizing effects.[3] They increase sensitization to radiation by stopping the cell cycle in the late G1 phase.[6] Statins are relatively inexpensive and safe with predictable side-effects, with the most common at standard dosing reported as transient gastrointestinal upset and headaches.[8, 12]

Lovastatin apoptotic properties have been demonstrated among several tumors, such as monomyelocytic leukemia, rhabdomyosarcoma, medulloblastoma, astrocytoma, SCC of the head and neck, and cervical SCC.[8, 9] Studies have shown that cholesterol optimization should be considered in all patients with cancer due to a reduction in both cardiovascular and cancer-specific mortalities; therefore, it seems that statins can be prescribed in patients who have clinical indications.[12] A phase I clinical trial showed disease stabilization in HNSCCs with high-dose lovastatin.[8] In the present study, lovastatin was administered at 80 mg/day in divided doses on treatment days.

As most studies were retrospective and primarily performed on common-site malignancies, such as breast, colon, and prostate, the current study, an interventional investigation on head and neck cancers, is unique. Some meta-analyses showed that statins could improve OS and reduce all-cause mortality.[10, 16] Subgroup analysis showed that post-diagnosed statin users gained more benefits,[16, 17] especially in prostate subgroups.[18] However, the results regarding the association of statin therapy and prostate cancer are controversial.[19, 20, 21] Other studies on colorectal cancers showed that both pre-diagnosed and post-diagnosed statin users had significant OS benefits.[14, 22, 23] As a result, the best prescription sequence remains unknown.

In a retrospective study performed on 1,592 HNSCC patients, subjects whose lipid profiles were available a year before treatment and underwent at least one year of follow-up were included. Statin users were defined as those with at least three prescriptions filled a year before diagnosis and at least three filled since diagnosis, if the patient was still alive.[11] Patients with hyperlipidemia who received statins showed improvement in OS and DSS, compared with the other two groups, including those without hyperlipidemia who were under statin therapy

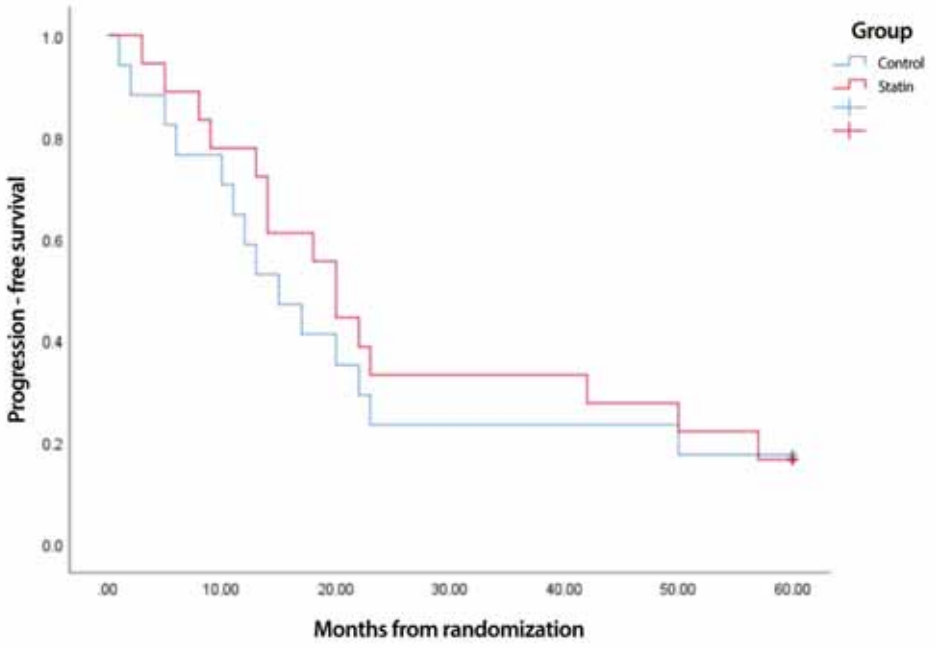

Figure 2. This figure depicts the PFS curve in the control group (blue line) and the statin group (red line). The median PFS is 20 months (CI95%=15.8-24.1) in the statin group and 15 months (CI95%=8.2-21.7) in the control group ($P = 0.609$).
PFD: Progression-free survival; CI: Confidence interval

Table 4. 2-year and 5-year late reactions: dysphagia, xerostomia, soft tissue fibrosis, laryngeal mucositis. (Grading based on CTCAE v4.0)

Adverse events	Statin group (n=18)	Placebo group (n=17)	
Dysphagia 2 years			
Not measurable	50%	58.8%	1
G1	33.3%	29.4%	
G2	16.6%	11.7%	
Dysphagia 5 years			0.999
Not mentioned	83.3%	88.2%	
G1	5.5%	5.8%	
G2	11.1%	5.8%	
Xerostomia 2 years			
Not mentioned	50%	58.8%	0.998
G1	27.7%	35.2%	
G2	22.2%	5.8%	
Xerostomia 5 years			0.999
Not mentioned	83.3%	88.2%	
G1	5.5%	5.8%	
G2	11.1%	5.8%	
Superficial soft tissue fibrosis 2 years			0.996
Not mentioned	50%	58.8%	
G1	0.0%	0.0%	
G2	50%	41.1%	
Superficial soft tissue fibrosis 5 years			0.999
Not mentioned	83.3%	88.2%	
G1	0.0%	0.0%	
G2	11.1%	5.8%	
G3	5.5%	5.8%	
Laryngeal mucositis 2 years			1
Not mentioned	44.4%	47%	
G1	22.2%	5.8%	
G2	27.7%	23.5%	
G3	5.5%	23.5%	
Laryngeal mucositis 2 years			1
Not mentioned	83.3%	88.2%	
G1	5.5%	5.8%	
G2	5.5%	5.8%	
G3	5.5%	0.0%	

G0: Grade 0; G1: Grade 1; G2: Grade 2; G3: Grade 3; CTCAE: Common Terminology Criteria for Adverse Events

and those who neither had hyperlipidemia nor used statins.[11] In the above-mentioned study, the patients were older than 66, and most underwent surgery and radiotherapy but not chemotherapy.[11] In the current study, there was no evaluation of lipid profile and whether the patients were statin users; however, this study is unique as it is a randomized clinical trial with homogeneous groups regarding the mean age and disease stage.

In another retrospective study conducted on 1,194 HPV-negative HNSCC patients, 572 patients (47.9%) received statins at the time of diagnosis with a minimum of 1 month before diagnosis and at least 4 months after that. Additionally, 622 (52.1%) patients served as controls without statin usage within a minimum of 1 year of their diagnosis date. The results demonstrated statistically significant benefits in the case group, compared with those of the control group, for both median OS and DSS. All participants were older than 65, and comorbidity was higher in the case group. It is interesting to note that the level

of DSS improvement was higher than that of OS; this finding might suggest that the benefit of statins is specifically achieved through targeting the patient's cancer, as opposed to generally improving his/her health status.[12]

The only prospective study for the role of statins in the combination of radiotherapy is the study of Razmjoo et al. that has been performed at Jundishapour University for using lovastatin in patients with advanced head and neck cancer and showed that lovastatin improved non-significant RR in combination with chemoradiation with cisplatin in this group of patients.[24] This study showed that lovastatin could improve objective RR without more acute adverse effects of treatment than the control group. However, the long-term outcomes of patients were not mentioned in the study conducted by Razmjoo et al. Although the study is similar to Razmjoo et al.'s, there are some advantages. This study evaluated the RR 12 weeks after treatment, which is more extended than the 8 weeks used in Razmjoo's study. Additionally, long-term follow-ups were conducted for 2 and 5 years to assess PFS, OS, and late adverse effects. This study confirms the previous research on the role of lovastatin in combination with CRT in head and neck cancer and the positive possibility of the role of statins in cancer treatment. Both studies suffer from the limitation of having an insufficient number of patients included in the study; therefore, to adequately answer the efficacy and proper role of statins in cancer treatment, prospective randomized studies with appropriate design (concurrent or long-term adjuvant use of statins) and a more significant number of patients with longer follow-up are needed. More advanced radiation techniques, such as intensity-modulated radiation therapy, would primarily affect the adverse events and should be used in future trials.

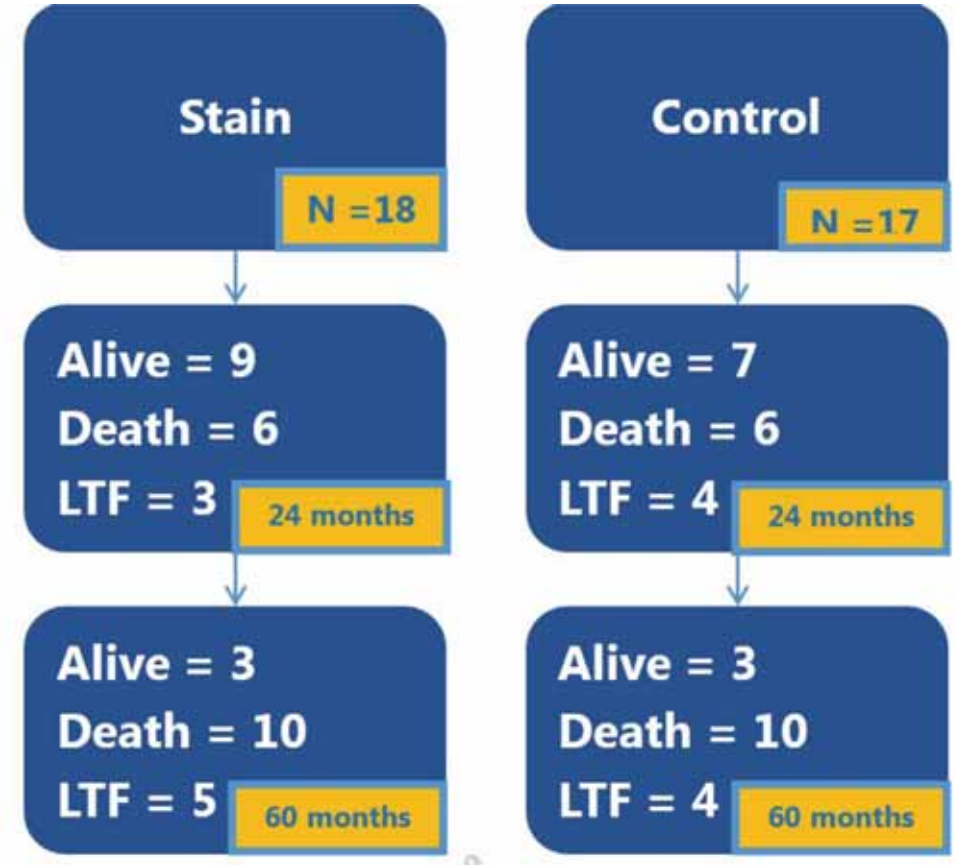

Figure 3. This flow diagram illustrates the statin and control groups' 2- and 5-year follow-ups.
LTF: Lost to follow-up

Conclusion

In the current investigation, statin therapy was administered concurrently with radiotherapy to harness its radiosensitizing properties. Nevertheless, the statin group exhibited marginally improved RR, PFS, and OS, alongside some observed side-effects, albeit without reaching statistical significance. This outcome may be attributed to the limited sample size, prompting us to conclude this study prematurely. However, it is essential to underscore the uniqueness of this study, which incorporated randomization and sustained long-term follow-up. Furthermore, patients may accrue lasting benefits from prolonged statin use.

Additionally, evaluating patients' lipid profiles and their potential implications for patient outcomes is strongly recommended. This study is relatively tiny participant pool can be attributed to the limited number of patients seeking treatment at our facility during the study period and suboptimal patient recruitment. Therefore, advocating for conducting randomized trials with more extensive participant cohorts is essential. Moreover, further research is warranted, encompassing randomized studies with larger patient cohorts undergoing definitive or adjuvant radiotherapy, employing cutting-edge techniques such as intensity-modulated radiotherapy.

Conflict of Interest

None declared.

References

1. Halperin EC, Brady LW, Wazer DE, Perez CA. Perez and Brady's: Principles and practice of radiation oncology. In: Edward C. Halperin, David E. Wazer, Carlos A. Perez, Luther W, editors. Locally advance squamous carcinoma of the head and neck. 7th ed. Philadelphia: Lippincott Williams & Wilkins; 2013.p.885.
2. DeVita VT, Lawrence TS, Rosenberg SA. DeVita, Hellman, and Rosenberg's cancer: Principles and practice of oncology. In: Vincent T. DeVita Jr., Theodore S. Lawrence, Steven A, editors. Cancer of head and neck. 11th ed. The United Stated: EBSCO eBooks; 2019.p. 542.
3. Knox JJ, Siu LL, Chen E, Dimitroulakos J, Kamel-Reid S, Moore MJ, et al. A Phase I trial of prolonged administration of lovastatin in patients with recurrent or metastatic squamous cell carcinoma of the head and neck or of the cervix. *Eur J Cancer.* 2005;41(4):523-30. doi: 10.1016/j.ejca.2004.12.013.
4. Apostolova SN, Toshkova RA, Momchilova AB, Tzoneva RD. Statins and Alkylphospholipids as new anticancer agents targeting lipid metabolism. *Anticancer Agents Med Chem.* 2016;16(12):1512-22. doi: 10.2174/1871520616666160624093955.
5. Altwairgi AK. Statins are potential anticancerous agents (review). *Oncol Rep.* 2015;33(3):1019-39. doi: 10.3892/or.2015.3741.
6. Di Bello E, Zwergel C, Mai A, Valente S. The innovative potential of statins in cancer: new targets for new therapies. *Front Chem.* 2020;8:516. doi: 10.3389/fchem.2020.00516.
7. Gazzerro P, Proto MC, Gangemi G, Malfitano AM, Ciaglia E, Pisanti S, et al. Pharmacological actions of statins: a critical appraisal in the management of cancer. *Pharmacol Rev.* 2012;64(1):102-46. doi: 10.1124/pr.111.004994.
8. Dimitroulakos J, Marhin WH, Tokunaga J, Irish J, Gullane P, Penn LZ, et al. Microarray and biochemical analysis of lovastatin-induced apoptosis of squamous cell carcinomas. *Neoplasia.* 2002;4(4):337-46. doi: 10.1038/sj.neo.7900247.
9. Gupta A, Stokes W, Eguchi M, Hararah M, Amini A, Mueller A, et al. Statin use associated with improved overall and cancer specific survival in patients with head and neck cancer. *Oral Oncol.* 2019;90:54-66. doi: 10.1016/j.oraloncology.2019.01.019.
10. Lebo NL, Griffiths R, Hall S, Dimitroulakos J, Johnson-Obaseki S. Effect of statin use on oncologic outcomes in head and neck squamous cell carcinoma. *Head Neck.* 2018;40(8):1697-706. doi: 10.1002/hed.25152.
11. Hindler K, Cleeland CS, Rivera E, Collard CD. The role of statins in cancer therapy. *Oncologist.* 2006;11(3):306-15. doi: 10.1634/theoncologist.11-3-306.
12. Davies JT, Delfino SF, Feinberg CE, Johnson MF, Nappi VL, Olinger JT, et al. Current and emerging uses of statins in clinical therapeutics: a review. *Lipid Insights.* 2016;9:13-29. doi: 10.4137/LPI.S37450.
13. Jeong GH, Lee KH, Kim JY, Eisenhut M, Kronbichler A, van der Vliet HJ, et al. Statin and cancer mortality and survival: an umbrella systematic review and meta-analysis. *J Clin Med.* 2020;9(2):326. doi: 10.3390/jcm9020326.
14. Katz MS, Minsky BD, Saltz LB, Riedel E, Chessin DB, Guillem JG. Association of statin use with a pathologic complete response to neoadjuvant chemoradiation for rectal cancer. *Int J Radiat Oncol Biol Phys.* 2005;62(5):1363-70. doi: 10.1016/j.ijrobp.2004.12.033.
15. Shen Y, Wang C, Ren Y, Ye J. A comprehensive look at the role of hyperlipidemia in promoting colorectal

cancer liver metastasis. *J Cancer.* 2018;9(16):2981-6. doi: 10.7150/jca.25640
16. Tan P, Wei S, Yang L, Tang Z, Cao D, Liu L, et al. The effect of statins on prostate cancer recurrence and mortality after definitive therapy: a systematic review and meta-analysis. *Sci Rep.* 2016;6:29106. doi: 10.1038/srep29106.
17. Ling Y, Yang L, Huang H, Hu X, Zhao C, Huang H, et al. Prognostic significance of statin use in colorectal cancer: a systematic review and meta-analysis. *Medicine (Baltimore).* 2015;94(25):e908. doi: 10.1097/MD.0000000000000908.
18. Chen Y, Li X, Zhang R, Xia Y, Shao Z, Mei Z. Effects of statin exposure and lung cancer survival: A meta-analysis of observational studies. *Pharmacol Res.* 2019;141:357-65. doi: 10.1016/j.phrs.2019.01.016.
19. Raval AD, Thakker D, Negi H, Vyas A, Kaur H, Salkini MW. Association between statins and clinical outcomes among men with prostate cancer: a systematic review and meta-analysis. *Prostate Cancer Prostatic Dis.* 2016;19(2):151-62. doi: 10.1038/pcan.2015.58. Erratum in: *Prostate Cancer Prostatic Dis.* 2016; 19(2):222.
20. Danzig MR, Kotamarti S, Ghandour RA, Rothberg MB, Dubow BP, Benson MC, et al. Synergism between metformin and statins in modifying the risk of biochemical recurrence following radical prostatectomy in men with diabetes. *Prostate Cancer Prostatic Dis.* 2015;18(1):63-8. doi: 10.1038/pcan.2014.47.
21. Li Y, Li Y, Lei X, Liu L, Zhang D, Tang S. Prognostic value of statin for cancer patients: A meta-analysis. *Zhong Nan Da Xue Xue Bao Yi Xue Ban.* 2015;40(7): 770-81. doi: 10.11817/j.issn.1672-7347.2015.07.012.
22. Allott EH, Howard LE, Cooperberg MR, Kane CJ, Aronson WJ, Terris MK, et al. Postoperative statin use and risk of biochemical recurrence following radical prostatectomy: results from the Shared Equal Access Regional Cancer Hospital (SEARCH) database. *BJU Int.* 2014;114(5):661-6. doi: 10.1111/bju.12720.
23. Cai H, Zhang G, Wang Z, Luo Z, Zhou X. Relationship between the use of statins and patient survival in colorectal cancer: a systematic review and meta-analysis. *PLoS One.* 2015;10(6):e0126944. doi: 10.1371/journal.pone.0126944.
24. Razmjoo S, Hoseyni M, Shahbazian H, Arvandi S, Ghadamgahi P. A phase III randomized clinical trial study of chemoradiation using lovastatin/cisplatin in patients with head and neck squamous cell carcinoma. *Middle East J Cancer.* 2022;13(1):120-7. doi: 10.30476/mejc.2021.87318.1407.

Original Article
Middle East Journal of Cancer; April 2024; 15(2): 128-135

Evaluation of the Interchangeability of Cone Beam Computed Tomography and Catalyst for Patient Positioning in Radiotherapy for Head and Neck Cancer Patients

Taha I. Hewala*, PhD, Mohamed A. Fahmy, MSc student, Sanaa A. El-Benhawy*♦, PhD, Hany M. Ammar**,***, PhD,**

**Radiation Sciences Department, Medical Research Institute, Alexandria University, Alexandria, Egypt*
***Department of Radiation Therapy, Children Cancer Hospital 57357, Cairo, Egypt*
****Clinical Oncology Department, Faculty of Medicine, University of Aswan, Aswan, Egypt*

Please cite this article as: Hewala TI, Fahmy MA, El-Benhawy SA, Ammar HM. Evaluation of the interchangeability of cone beam computed tomography and catalyst for patient positioning in radiotherapy for head and neck cancer patients. Middle East J Cancer. 2024;15(2):128-35. doi:10.30476/mejc.2023.97547.1866.

♦Corresponding Author:
Sanaa A. El-Benhawy, PhD
Radiation Sciences Department, Medical Research Institute, Alexandria University, Alexandria, Egypt
Tel: 03-4282373
Fax: 03-4285455
Email: dr_sanaa_ali13@yahoo.com

Abstract

Background: This study aims to evaluate the interchangeability between cone beam computed tomography (CBCT) and the optical surface scanning system (Catalyst) for daily positioning during radiation therapy in head and neck cancer patients.

Method: This study was designed as a prospective observational descriptive study divided into two parts. The first part involved a phantom study using the computerized imaging reference systems (CIRS) child atom phantom. It aimed to detect deviations in patient position across six degrees of freedom (lateral, longitudinal, vertical, rotation, roll, and pitch) using the optical light scanner and Catalyst and compare them with deviations detected by CBCT in the same treatment sessions. The second part included 252 sessions, during which 30 head and neck cancer patients were treated at Children Cancer Hospital 57357, Egypt, using both Catalyst and CBCT for setup treatment positioning.

Results: The differences between CBCT and Catalyst in all six degrees of deviation were not statistically significant (lateral ($P = 0.175$), longitudinal ($P = 0.296$), vertical ($P = 0.110$), rotation ($P = 0.936$), roll ($P = 0.527$), and pitch ($P = 0.270$)).

Conclusion: The optical light scanner system Catalyst is comparable to CBCT. Surface scanning (Catalyst) has proven reliable and feasible for daily patient positioning, with the advantage of avoiding daily exposure to additional radiation.

Keywords: Radiotherapy, Image-Guided, Cone-beam computed tomography, Catalyst, Head and neck neoplasms

Introduction

Image-guided radiation therapy (IGRT) uses various imaging modalities to improve the precision

Received: December 22, 2022; Accepted: October 15, 2023

and accuracy of radiation treatment delivery by correcting potential patient position setup errors. One of the key obstacles in the everyday clinical activities of radiation therapy is the reproducibility of patient setup and organ motion management.[1]

Ionizing radiation machines, such as linear accelerators (for X-ray or photon) or cyclotron/synchrotrons (for proton), are equipped with unique imaging technology (X-ray portal image, computed tomography (CT), 3D body surface mapping, magnetic resonance imaging (MRI), and ultrasound (US) that allow the therapist to image the tumor immediately before or even during the time radiation is delivered.[2,3] These images are compared to the reference images taken during the simulation.

Technological advancements, such as the advent of cone beam CT (CBCT), have greatly enhanced the precision of tumor dosage delivery and reduced uncertainty.[4,5,6] CBCT-based X-ray technology enables the visualization of internal anatomy with its ability for penetration. The increased frequency of CBCT imaging increases the quantity of radiation dose delivered to patients, increasing the possibility of secondary cancers.

Surface-based systems also allow for continuous, touch-free optical surface scanning of the patient's exterior surfaces, a useful tool for correcting patient position without exposing the patient to further radiation. Optical surface positioning technologies that have recently been created have been brought into clinical practice.[7,8,9]

The Catalyst high-definition optical surface scanner comprises a ceiling-mounted scanning unit and the c4D software. The scanners in the linear accelerator room allow for continuous surface detection. The instrument emits 405 nm (blue) visible light during the scan, and integrated charge-coupled device cameras collect re-projections. The comparison of the surface scan with an initially acquired reference scan is based on photogrammetry principles explained by the fundamental principle used in photogrammetry: triangulation. By taking photographs from at least two different locations, so-called 'lines of sight' can be developed from each camera to points on the object, carried out using a non-rigid iterative nearest point technique in 6 degrees of freedom (refers to the six mechanical degrees of freedom of movement of a rigid body in three-dimensional space for patient body lateral, longitudinal, vertical, rotation, roll and pitch).[10,11]

Additionally, the system includes integrated light-emitting diode (LED) projectors for projecting positional deviations onto the patient's surface to aid in patient positioning. For different deviations, different colored light (green: 528 nm, red: 624 nm) is used to visualize the reference position on the patient's surface.[12,13] Catalyst scanning system based on optically visible light without any additional radiation exposure for patient positioning with visual user assistance in identification of positioning accurately with inter-fractional movements control and automated respiratory gating.[14,15] The purpose of the present study is to evaluate the usage of Catalyst versus CBCT in image guided radiation sessions for head and neck cancer patients to decrease the total radiation exposure dose received during the treatment course.

Materials and Methods

This study was designed as a prospective observational descriptive research endeavor, encompassing 30 head and neck cancer patients who received treatment at the Children's Cancer Hospital 57357 in Egypt. The study was conducted from June 2020 to November 2020, following approval by the SMAC Committee at 57357 Hospital. All study participants' parents provided written informed consent. Before commencing the study, approval was obtained from the Research Ethics Committee of the Medical Research Institute (ethics code: IORG0008812) at Alexandria University, Egypt. Our investigation relied on specialized measurement equipment and irradiation facilities, including CT (Somatom, Siemens Healthcare, Germany), MRI (Megatom, Siemens Healthcare, Germany), Treatment Planning System (TPS) (Monaco, Elekta, Sweden), Thermoplastic Mask (Civco, US), Linear Accelerator (Elekta, Versa HD, Sweden), X-ray

Table 1. Comparison between CBCT and Catalyst according to lateral, longitudinal, and vertical degrees in the phantom study

Lateral	CBCT	Catalyst
-3 cm	2.96 cm	2.91 cm
-2 cm	2.03 cm	1.96 cm
-1 cm	0.94 cm	0.97 cm
+1 cm	-1.00 cm	-0.96 cm
+2 cm	-1.99 cm	-1.98 cm
+3 cm	-3.00 cm	-3.01 cm
Longitudinal		
-3 cm	2.97 cm	2.95 cm
-2 cm	2.04 cm	2.03 cm
-1 cm	1.01 cm	1.02 cm
+1 cm	-0.96 cm	-0.96 cm
+2 cm	-1.97 cm	-1.93 cm
+3 cm	-2.98 cm	-2.94 cm
Vertical		
-3 cm	3.01 cm	3.05 cm
-2 cm	2.08 cm	2.07 cm
-1 cm	1.05 cm	0.98 cm
+1 cm	-0.95 cm	-0.99 cm
+2 cm	-1.99 cm	-2.07 cm
+3 cm	-2.94 cm	-2.98 cm

CBCT: Cone-beam computed tomography

Volume Imaging (XVI CBCT) (Elekta, Sweden), and Optical Light Scanning System Catalyst (C-RAD, Uppsala, Sweden).

The CT simulation was performed on the initial day of the patients' presentation at the radiotherapy department. A suitable fixation thermoplastic mask with reference marks was meticulously delineated on it. Subsequently, the patients were immobilized in the supine position atop a solid, flat carbon fiber couch at the CT site. An appropriately sized headrest and thermoplastic mask were employed to ensure optimal patient comfort and stability. The headrest was positioned beneath the patient's head, while the mask was prepped in a water bath at a high temperature of 65°C to become flexible and conform to the patient's facial contours. It was then securely affixed to the couch. An index was created and attached to each mask, containing essential patient data and the most comfortable headrest size. These components, the headrest and mask, played a pivotal role in guaranteeing the reproducibility of patient fixation, thereby minimizing setup errors and facilitating initial target localization. Patients were consistently positioned throughout treatment using the same headrest, mask markers, and immobilization device.

In this study, a CT scanner can acquire multiple images or slices during a single rotation of the X-ray beam around the patient. This advanced CT technology enabled the generation of a three-dimensional (3D) image, which was subsequently integrated into the Monaco planning system for contouring and treatment planning purposes.

Phantom study

In the present study, a phantom was utilized to assess the level of agreement regarding the directions and quantity of deviations between the CBCTs and Catalyst scans. This was achieved by positioning the phantom on the treatment room table couch and utilizing fixed lasers and skin marks to align it with the isocenter.

CBCT imaging was employed to verify the accurate placement of the phantom. The reference surface was captured using the Catalyst system and camera settings, with tolerance adjustments made accordingly.

To ensure the Catalyst and CBCT systems aligned with the same deviation parameters and direction corrections, the treatment couch was manually displaced at intentionally induced 1, 2, and 3 cm deviations in positive and negative directions relative to the isocenter. The results of these deviations are presented in table 1.

Daily workflow

The initial step in our daily workflow involves positioning the patients using a green laser system pre-aligned in the treatment room. Also, reference marks on the mask, previously established during the CT simulation, are used. Following this, the C-RAD Catalyst system is opened, the patient is selected, and the patient's surface is scanned.

Any deviations in setup from the CT simulation (referred to as the reference surface) and the current patient setup in the treatment room surface are meticulously recorded using the C-RAD software. A single camera, securely fixed on the ceiling above the table couch end, aids in this process. Figure 1 provides a visual representation of the setup deviations detected by the Catalyst system.

The subsequent step entails conducting CBCT scan on the patient to estimate their positioning precisely. This involves registering the CBCT scan with the reference CT images and aligning them with the setup deviations recorded earlier (Figure 2).

To ensure the accuracy of our patient positioning, a thorough comparison of the setup errors is needed. The optical light scanner, Catalyst HD, detects the 6 degrees of deviation, including lateral, longitudinal, vertical, rotation, roll, and pitch errors. These deviations are then meticulously compared with the setup errors identified by CBCT, which serves as the gold standard for IGRT.

Statistical analyses

The current study involved a rigorous statistical analysis of data using IBM SPSS software package version 20 (Armonk, NY: IBM Corp). The Kolmogorov-Smirnov test was employed to assess the normal distribution of the data. Quantitative data were summarized using the range (minimum and maximum values), median, mean, and standard deviation.

As determined by the Catalyst technique, patient positioning was subjected to a statistical comparison with positioning data obtained through the CBCT technique, considered the gold standard in IGRT. The significance of the results obtained was assessed at a 5% significance level ($P < 0.05$).

Results

The mean ± standard deviation (SD) for deviations in the lateral, longitudinal, and vertical dimensions when comparing CBCT to Catalyst were as follows: -0.01 ± 2.14 cm versus -0.018 ± 2.12 cm, with a *P*-value of 0.662 for lateral; 0.023 ± 2.14 cm versus 0.021 ± 2.13 cm, with a *P*-value of 0.875 for longitudinal; and 0.043 ± 2.15 cm versus 0.01 ± 2.18 cm, with a *P*-value of 0.120 for vertical.

Statistical analysis of these results revealed non-significant differences between CBCT and

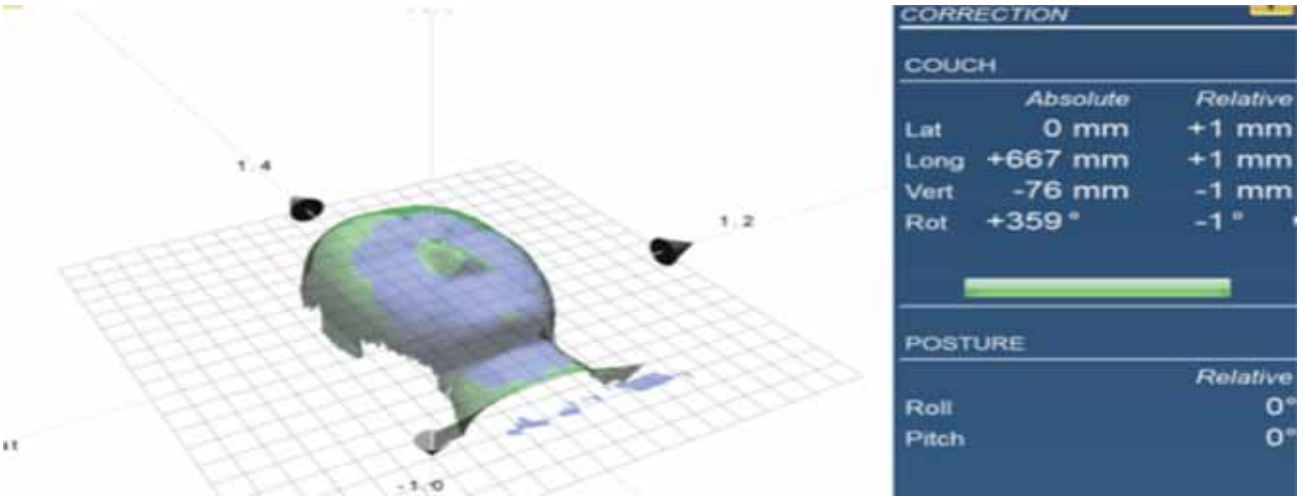

Figure 1. CBCT imaging the patient to estimate the patient's positioning. CBCT scan matching registration was done with the reference CT images, and the setup deviations were recorded.
CBCT: Cone-beam computed tomography; Lat: lateral; Long: longitudinal; Vert: vertical; Rot: Rotation; CT: Computed tomography

Table 2. Comparison between CBCT and Catalyst according to six different degrees in the clinical study.

Degree	CBCT	Catalyst	Z	P
Lateral				
Min. – Max.	-0.16 – 0.33 cm	-0.33 – 0.32 cm	1.355	0.175
Mean ± SD.	0.0 ± 0.096	0.03 ± 0.141		
Longitudinal				
Min. – Max.	-0.53 – 0.50 cm	-0.20 – 0.50 cm	1.046	0.296
Mean ± SD.	0.02 ± 0.25	0.06 ± 0.18		
Vertical				
Min. – Max.	-0.30 – 0.20 cm	-0.50 – 0.40 cm	1.600	0.110
Mean ± SD.	-0.12 ± 0.13	-0.16 ± 0.18		
Rotation				
Min. – Max.	-2.29° – 1.91°	-2.0 °– 1.17°	0.080	0.936
Mean ± SD.	-0.23° ± 0.82	-0.25° ± 0.79		
Roll				
Min. – Max.	-2.50 °– 1.50°	-2.0° – 2.67°	0.633	0.527
Mean ± SD.	-0.15° ± 1.10	0.13° ± 1.33		
Pitch				
Min. – Max.	-1.33° – 1.40°	-1.50° – 2.09°	1.103	0.270
Mean ± SD.	0.22° ± 0.66	0.47°± 0.91		

Z: Z-test describes the deviation from the mean in standard deviation units; *P*: *P* value for comparing CBCT and Catalyst; CBCT: Cone-beam computed tomography; Min: Minimum; Max: Maximum; SD: Standard deviation

Catalyst deviations in lateral, longitudinal, and vertical dimensions ($P > 0.05$).

Clinical study

30 patients, comprising 18 males and 12 females, underwent head and neck cancer treatment. The choice between a closed head mask or a head and neck mask depended on the specific tumor site for each patient. All patients received fractionated external beam radiotherapy, administered using the Elekta Versa HD linear accelerator, with CBCT and Catalyst employed for IGRT.

The following results reveal the deviations in patient positioning detected by CBCT and Catalyst during all scheduled radiation treatment sessions, totaling 252 sessions. These deviations were assessed for each of the six degrees individually. In this study, translation degrees (lateral, vertical, and longitudinal) were expressed in centimeters (cm), while the rotational degrees (rotation, roll, and pitch) were expressed in degrees (°).

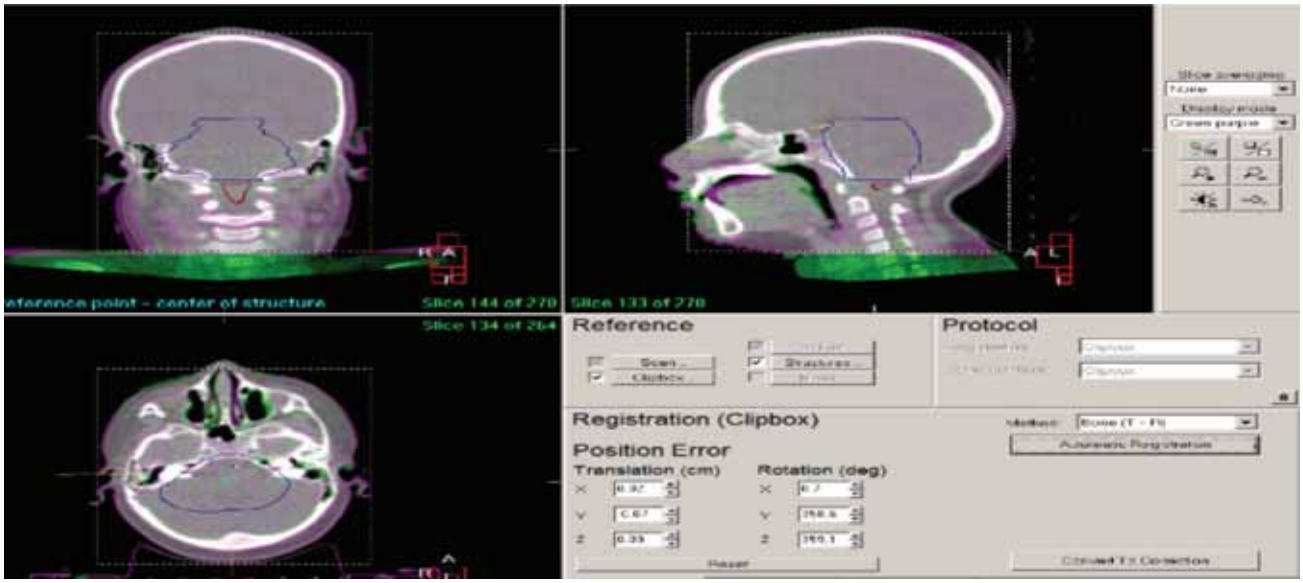

Figure 2. CBCT scan matching registration was done with the reference CT images, and the setup deviations were recorded.
CBCT: Cone-beam computed tomography; CT: Computed tomography

Comparison between CBCT and Catalyst based on various deviation parameters in a clinical study

Table 2 presents the six different deviation parameters detected by CBCT and Catalyst, while figure 3 illustrates Bland-Altman Plot graphs depicting the agreement between CBCT and Catalyst across these six parameters.

For lateral deviation, CBCT exhibited a range of (-0.16 to 0.33 cm) with a mean ± SD of (0.0 ± 0.096 cm), whereas Catalyst displayed a range of (-0.33 to 0.32 cm) with a mean ± SD of (0.03 ± 0.14 cm). Statistical analysis of these data demonstrated no significant difference between CBCT deviation parameters and Catalyst concerning lateral deviation ($P = 0.175$).

Regarding vertical deviation, CBCT had a range of (-0.30 to 0.20 cm) with a mean ± SD of (-0.12 ± 0.13 cm), while Catalyst showed a range of (-0.50 to 0.40 cm) with a mean ± SD of (-0.16 ± 0.18 cm). The statistical analysis indicated no significant difference between CBCT and Catalyst concerning vertical deviation ($P = 0.110$).

For rotation deviation, CBCT exhibited a range of (-2.29° to 1.91°) with a mean ± SD of (-0.23° ± 0.82°), while Catalyst displayed a range of (-2.0° to 1.17°) with a mean ± SD of (-0.25° ± 0.79°). The statistical analysis of rotation deviation demonstrated no significant difference between CBCT and Catalyst ($P = 0.936$).

In the case of roll deviation, CBCT had a range of (-2.50° to 1.50°) with a mean ± SD of (-0.15° ± 1.10°), while the Catalyst showed a range of (-2.0° to 2.67°) with a mean ± SD of (0.13° ± 1.33°). The statistical analysis of roll deviation revealed no significant difference between CBCT and Catalyst ($P = 0.527$).

Lastly, in terms of pitch deviation, CBCT exhibited a range of (-1.33° to 1.40°) with a mean ± SD of (0.22° ± 0.66°), while the Catalyst displayed a range of (-1.50° to 2.09°) with a mean ± SD of (0.47° ± 0.91°). The statistical analysis for these data indicated no significant difference between CBCT and Catalyst concerning pitch deviation ($P = 0.270$).

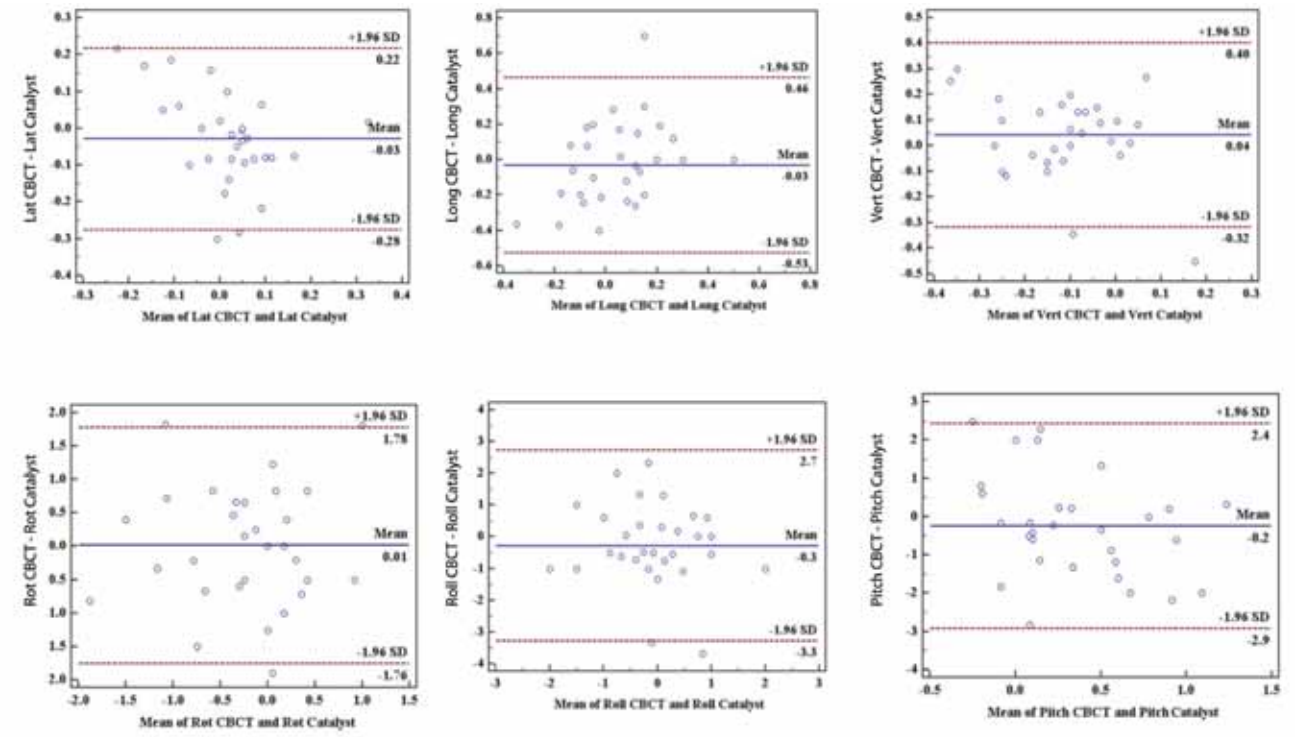

Figure 3. Bland Altman Plot graphs showing agreement between CBCT and catalyst according to six different degrees.
CBCT: Cone-beam computed tomography; Lat: lateral; Long: longitudinal; Vert: vertical; Rot: Rotation; SD: Standard deviation

Discussion

The differences between CBCT and Catalyst in all six degrees of deviation were not significant (lateral (P = 0.175), longitudinal (P = 0.296), vertical (P = 0.110), rotation (P = 0.936), roll (P = 0.527) and pitch (P = 0.270)).

The Catalyst is now utilized to position the patients in several radiation therapy hospitals and clinics. There is restricted proof of its absolute dependability and durability in daily practice.[16]

The current study evaluated and compared the six deviation parameters between CBCT and Catalyst. The statistical analysis of these data did not show significant differences between CBCT and Catalyst in the six deviation parameters (lateral, longitudinal, vertical, rotation, roll, and pitch).

In line with the present study findings, Stanley et al. (2017),[11] Concluded that the patient alignment using the Catalyst was significantly approaching the alignment carried out by the CBCT. Further, the Catalyst is a trustworthy alternative to traditional positioning using X-ray-based techniques via CT simulation markers on the fixation mask and lasers in the treatment room. They recommended using the optical light scanner Catalyst in daily patient positioning to decrease the total ionizing radiation dose for patients. In the current study, a systematic analysis compared Catalyst imaging to CBCT in the same treatment session to prevent intrafractional patient position uncertainty.

A similar more recent study published by Ma et al. (2018),[13] utilized Catalyst in breast cancer patients for patient positioning during radiation therapy and the deviations were compared with CBCT and found that CBCT and Catalyst did not show any significant difference for all 3 translation deviations where they did not attempt the 3 other rotational deviation. Moreover, Liu et al. (2020),[17] suggested that optical surface imaging can be applied to positioning breast cancer patients accurately without unnecessary imaging doses.

Carl et al. (2018)[12] found that Catalyst was a reliable and beneficial positioning system for patients in the daily workflow without further radiation exposure. This was in concordance with the present study. A previous report created by Wikström et al. (2014)[14] recommended that the optical light scanning system was an excellent supplement to the CBCT system for accurate setup when no CBCT is deemed necessary for pelvic targets. Furthermore, cropping near the PTV will lead to removing the critical data that may affect the calculation of deviations.

Bekke et al. (2018)[15] contradicts our results; his study concluded that the target position verification cannot be based solely upon surface-based configuration, internal anatomical verification of target position techniques such as kV (CBCT) and MV (Portal images) is essential and required. However, the present study recommendations included the advantage of using the CBCT twice a week (more or less) to ensure that the Catalyst system works well with the same accuracy as the CBCT.

Based on this study, it is recommended that:

- Using an optical light scanner system Catalyst for daily patient positioning instead of CBCT without further ionizing radiation exposure, especially in children patients as included in the current study.
- Upgrading the Catalyst system from one to three camera scanners with open masks for head and neck cancer patients is an excellent choice to enhance the patient's positioning and comfort of the patient.
- CBCT is used periodically to confirm the effectiveness of the optical light scanner system Catalyst in patient positioning.

Some limitations in the current study include the following: The tumor's location is not defined inside the head and neck clinical site and is not related to our results; more investigations are needed to explore the dependency of catalyst imaging on how far the tumor is to the patient surface. Another limitation was the limited number of recruitment patients in the current study.

Conclusion

There is no significant difference between CBCT and Catalyst in all six degrees of deviation in head and neck patient positioning (lateral,

longitudinal, vertical, rotation, roll, and pitch). The Catalyst's optical light scanner system is compatible with CBCT, so the Catalyst is reliable and feasible IGRT for daily patient positioning without additional radiation exposure. Further Investigations should include other clinical sites such as chest, abdomen, and pelvic tumors in future work.

Conflict of Interest

None declared.

References

1. Goyal S, Kataria T. Image guidance in radiation therapy: techniques and applications. *Radiol Res Pract.* 2014;2014:705604. doi: 10.1155/2014/705604.
2. Yan G, Mittauer K, Huang Y, Lu B, Liu C, Li JG. Prevention of gross setup errors in radiotherapy with an efficient automatic patient safety system. *J Appl Clin Med Phys.* 2013;14(6):4543. doi: 10.1120/jacmp.v14i6.4543.
3. Torre LA, Bray F, Siegel RL, Ferlay J, Lortet-Tieulent J, Jemal A. Global cancer statistics, 2012. *CA Cancer J Clin.* 2015;65(2):87-108. doi: 10.3322/caac.21262.
4. Schneider U, Hälg R, Besserer J. Concept for quantifying the dose from image guided radiotherapy. *Radiat Oncol.* 2015;10:188. doi: 10.1186/s13014-015-0492-7.
5. Dang A, Kupelian PA, Cao M, Agazaryan N, Kishan AU. Image-guided radiotherapy for prostate cancer. *Transl Androl Urol.* 2018;7(3):308-20. doi: 10.21037/tau.2017.12.37.
6. Walter F, Freislederer P, Belka C, Heinz C, Söhn M, Roeder F. Evaluation of daily patient positioning for radiotherapy with a commercial 3D surface-imaging system (Catalyst™). *Radiat Oncol.* 2016;11(1):154. doi: 10.1186/s13014-016-0728-1.
7. Mututantri-Bastiyange D, Chow J. Imaging dose of cone-beam computed tomography in nanoparticle-enhanced image-guided radiotherapy: A Monte Carlo phantom study. *AIMS Bioengineering.* 2020;7(1):1-11. doi: 10.3934/bioeng.2020001.
8. De Los Santos J, Popple R, Agazaryan N, Bayouth JE, Bissonnette JP, Bucci MK, et al. Image guided radiation therapy (IGRT) technologies for radiation therapy localization and delivery. *Int J Radiat Oncol Biol Phys.* 2013;87(1):33-45. doi: 10.1016/j.ijrobp.2013.02.021.
9. Katsanos K, Kitrou P, Spiliopoulos S, Maroulis I, Petsas T, Karnabatidis D. Comparative effectiveness of different transarterial embolization therapies alone or in combination with local ablative or adjuvant systemic treatments for unresectable hepatocellular carcinoma: A network meta-analysis of randomized controlled trials. *PLoS One.* 2017;12(9):e0184597. doi: 10.1371/journal.pone.0184597.
10. Wiersma RD, Tomarken SL, Grelewicz Z, Belcher AH, Kang H. Spatial and temporal performance of 3D optical surface imaging for real-time head position tracking. *Med Phys.* 2013;40(11):111712. doi: 10.1118/1.4823757.
11. Stanley DN, McConnell KA, Kirby N, Gutiérrez AN, Papanikolaou N, Rasmussen K. Comparison of initial patient setup accuracy between surface imaging and three point localization: A retrospective analysis. *J Appl Clin Med Phys.* 2017;18(6):58-61. doi: 10.1002/acm2.12183.
12. Carl G, Reitz D, Schönecker S, Pazos M, Freislederer P, Reiner M, et al. Optical surface scanning for patient positioning in radiation therapy: a prospective analysis of 1902 fractions. *Technol Cancer Res Treat.* 2018;17:1533033818806002. doi: 10.1177/1533033818806002.
13. Ma Z, Zhang W, Su Y, Liu P, Pan Y, Zhang G, et al. Optical surface management system for patient positioning in interfractional breast cancer radiotherapy. *Biomed Res Int.* 2018;2018:6415497. doi: 10.1155/2018/6415497.
14. Wikström K, Nilsson K, Isacsson U, Ahnesjö A. A comparison of patient position displacements from body surface laser scanning and cone beam CT bone registrations for radiotherapy of pelvic targets. *Acta Oncol.* 2014;53(2):268-77. doi: 10.3109/0284186X.2013.802836.
15. Bekke SN, Andersen CE, Mahmood F, Lindvold LR, McNair HA, Elstrøm UV, et al. Evaluation of optical surface scanning of breast cancer patients for improved radiotherapy. Denmark: Lyngby Denmark Technical University; 2018.p.175.
16. Al-Hallaq HA, Cerviño L, Gutierrez AN, Havnen-Smith A, Higgins SA, Kügele M, et al. AAPM task group report 302: Surface-guided radiotherapy. *Med Phys.* 2022;49(4):e82-e112. doi: 10.1002/mp.15532.
17. Liu M, Wei X, Ding Y, Cheng C, Yin W, Chen J, et al. Application of optical laser 3D surface imaging system (Sentinel) in breast cancer radiotherapy. *Sci Rep.* 2020;10(1):7550. doi: 10.1038/s41598-020-64496-1.

Original Article
Middle East Journal of Cancer; April 2024; 15(2): 136-144

The Value of Serum Nestin in Monitoring the Effects of Surgery and Chemotherapy in Female Breast Cancer Patients: A Comparison with Serum CA15.3

Taha I. Hewala♦*, PhD, Mohamed S. Kamel, PhD, Yasmin N. Elwany***, PhD, Noha A. Zekry*, MSc**

**Department of Radiation Sciences, Medical Research Institute, Alexandria University, Alexandria, Egypt*
***Department of Experimental and Clinical Surgery, Medical Research Institute, Alexandria University, Alexandria, Egypt*
****Department of Cancer Management and Research, Medical Research Institute, Alexandria University, Alexandria, Egypt*

Please cite this article as: Hewala TI, Kamel MS, Elwany YN, Zekry NA. The value of serum nestin in monitoring the effects of surgery and chemotherapy in female breast cancer patients: a comparison with serum CA15.3. Middle East J Cancer. 2024;15(2):136-44. doi:10.30476/mejc.2023.98136.1886.

Abstract

Background: Traditional tumor markers such as cancer antigen 15.3 (CA15.3) and carcinoembryonic antigen (CEA) exhibit limited clinical utility in breast cancer due to their lack of sensitivity and specificity, particularly for detecting low-volume tumors. Other serum markers, such as nestin, may offer more promise. This study aimed to assess the clinical significance of serum nestin and CA15.3 in breast cancer patients.

Method: This case-control study enrolled 80 normal control females and 80 females with breast cancer. Serum samples were collected from both control and breast cancer groups. The serum nestin and CA15.3 levels were measured in all samples using enzyme-linked immunosorbent assay (ELISA) kits.

Results: The serum levels of nestin and CA15.3 were found to be significantly elevated in the breast cancer patient group compared with the control group. Preoperative serum nestin levels exceeding 9.9 ng/ml demonstrated a substantial odds ratio of 27 (confidence interval: 4.57-159.67; $P = 0.0003$). In receiver operating characteristic curve analysis, serum nestin exhibited the highest significant area under the curve at 85.2% ($P < 0.001$), followed by serum CA15.3 at 70% ($P = 0.021$). Post-surgery serum nestin levels significantly decreased compared with pre-surgery levels ($P = 0.045$).

Conclusion: Serum nestin outperforms serum CA15.3 in diagnosing breast cancer patients. Elevated serum nestin levels may represent a significant risk factor for the development of breast cancer. Furthermore, serum nestin can monitor the effects of surgery, whereas none of the assessed biomarkers exhibit a significant role in monitoring the effects of chemotherapy on breast cancer patients.

♦Corresponding Author:
Taha I. Hewala, PhD
Department of Radiation Sciences, Medical Research Institute, Alexandria University, Alexandria, Egypt
Tel: +201273199504
Email: tahahewala@hotmail.com

Keywords: Chemotherapy, Adjuvant, Breast neoplasms, Diagnosis, Nestin

Received: February 23, 2023; Accepted: November 13, 2023

Introduction

Worldwide, breast cancer is the most common malignancy and the second most frequent reason for death in women.[1] Breast cancer accounts for 24% of all cancers occurring in women.[2]

Cancer antigen 15.3 (CA15.3) is a glycoprotein belonging to a family of proteins called mucins (MUC). Mucins are large glycoproteins classified into 7 families (MUC 1 - MUC7) based on their genetic and biomolecular properties. MUC-1 is found in nearly all epithelial cells, with its overexpression in colon, breast, ovarian, lung, and pancreatic cancers.[3]

The main disadvantage of CA15.3 is its lack of sensitivity and specificity for low-volume tumors. So, it is of no value in either screening or diagnosing early breast cancer. Other markers for breast cancer, like nestin, may look promising, but further studies are required to be carried out before their clinical utility becomes well established.[4,5]

Nestin is one of the intermediate filament proteins in class VI. It was initially detected in neural stem cells during development. Its expression has also been found in different tissues with various pathological conditions. Many cancers express nestin protein, which correlates with the clinical course of breast cancer.[6]

Under pathological conditions, nestin is expressed upon wounding and tissue injury when cells undergo hyper-proliferation.[7] Nestin overexpression has been reported in various tumor cells, including breast cancer.[8] Nestin is also expressed in cancer stem cells, which promote cancer resistance.[9]

The current study aimed to compare the roles of serum levels of nestin and CA15-3 in breast cancer patients concerning the differentiation of breast cancer patients from controls, monitoring the effects of surgery and chemotherapy on breast cancer patients, and correlating the serum levels of each biomarker with the clinicopathological data of breast cancer patients.

For the time being, this is the first study that was performed to measure the serum levels of nestin to figure out the clinical role that may be played by this cytoskeleton protein in female breast cancer patients who were treated by surgery followed by chemotherapy.

Subjects and Methods

Subjects

This case-control study involved 160 female participants segregated into two distinct groups. group I consisted of 80 healthy control females, while group II comprised 80 recently diagnosed breast cancer patients in clinical stages II and III. The individuals in group II were carefully matched with those in group I regarding age and menstrual status. The inclusion criteria for the patients in

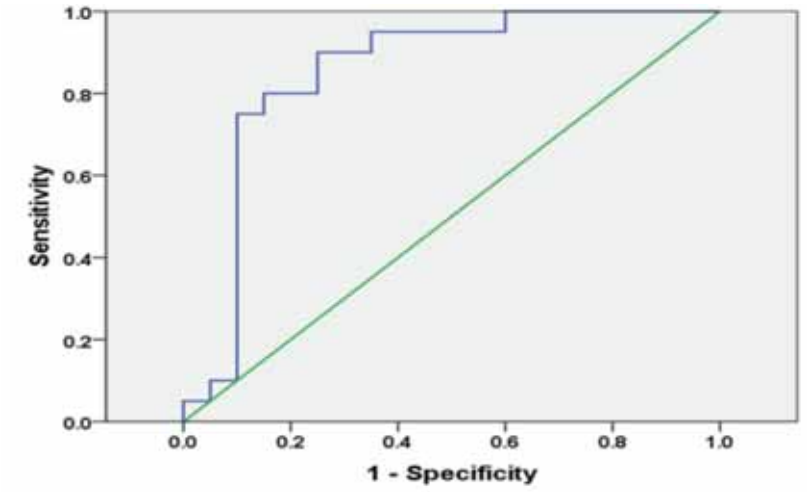

Figure 1. This figure shows the receiver operating characteristic curve for human serum nestin. The area under the curve was 85.2% ($P < 0.001$), with a sensitivity of 80% and specificity of 75% at a 9.90 ng/ml cut-off.

Table 1. The median (range) serum levels of nestin in the control group and the breast cancer patients group

Serum nestin levels (ng/ml)	Control group (n=80)	Breast cancer patients group (n=80)		
		Before surgery	After surgery (before chemotherapy)	After chemotherapy
Minimum	6.10	8.32	2.01	7.56
Maximum	13.68	15.06	12.69	11.06
Median	8.58	10.50	8.87	8.72
P- Values		***P1* = 0.000***	***P2* = 0.045***	***P3* = 0.307**

P1: Compared with control group; *P2:* Compared with the levels before surgery; *P3:* Compared with the levels after surgery (before chemotherapy); *: Statistically significant compared with the normal control group; Significance was considered at *P*-value < 0.05

group II were as follows: they had undergone breast conservative therapy, were node-positive, and exhibited a high-risk node-negative status.

Patients were selected among individuals admitted to the Experimental and Clinical Surgery Department and the Cancer Management and Research Department at Alexandria University, Egypt's Medical Research Institute (MRI). This data collection occurred from January 2021 to June 2022.

Methods

After approval from the ethical committee of the Medical Research Institute, Alexandria University, Egypt (ethics code: IORG0008812), signed informed consent was obtained from all subjects who agreed to participate in the current study. A complete history was recorded, and each patient underwent a thorough clinical examination, routine laboratory investigations, mammography of both breasts, radiological investigations including chest X-ray, ultrasonography of the abdomen and the liver, a computed tomography (CT) scan of the chest and abdomen, a bone scan when needed, and a needle biopsy of a breast mass to establish the pathological diagnosis of the patients.

The clinicopathologic data were obtained from patients' pathology reports. The collected data included tumor size, tumor pathological grade, axillary lymph node involvement, vascular invasion, estrogen receptor (ER) and progesterone receptor (PR) status, and human epidermal growth factor receptor 2 (HER-2) expression. For each patient, the clinical stage was determined by the oncologist according to the tumor-node-metastasis (TNM) classification system.[10]

All 80 breast cancer patients underwent modified radical mastectomy and then received adjuvant combination chemotherapy (5-fluorouracil, Adriamycin, and cyclophosphamide) for six cycles.[11] The patients were re-evaluated after three and six cycles of chemotherapy to estimate the clinical response.

Laboratory investigations

All laboratory assays were conducted at the Radiation Science Department, Medical Research Institute, Alexandria University, Egypt. Blood samples were collected once from the control group (group I) and three times from cancer patients (group II): prior to surgery, post-surgery (pre-chemotherapy), and post-chemotherapy. The blood samples were utilized to isolate sera for subsequent biochemical analyses. Serum levels of nestin and CA 15.3 were quantified in all study groups utilizing pre-packaged ELISA kits following the manufacturer's guidelines.

Determination of human serum nestin levels using ELISA kit

Assay procedure

The levels of human serum nestin were quantified employing a readily accessible ELISA kit, in strict accordance with the manufacturer's specified protocol (EIAAB-SCIENCE INC., China). Optical density at 450nm was assessed for each well using an ELISA reader. The concentration of human serum nestin within each serum sample was compared with a calibration curve.

Determination of human serum CA15-3 levels using an enzyme immunoassay kit

assay procedure

The levels of human serum CA15-3 were assessed by employing a commercially available EIA kit, specifically designed for immediate use, by the manufacturer's protocol (Bio-Inteco; UK). The optical density of each well was meticulously measured at 450 nm utilizing an ELISA reader.

A calibration curve accurately ascertained the concentration of human serum CA15.3 within each serum sample.

Histopathological examination

In group II, clinicopathological data were extracted from patients' data sheets. This dataset encompassed information about tumor size, tumor grade, ER status, PR status, HER-2 status, and the count of axillary lymph nodes involved. The attending oncologist assessed the clinical staging of each patient. These clinicopathological data were cross-referenced with pre-surgical serum levels of nestin and CA15-3.

Statistical analysis

Statistical analyses were conducted using the SPSS 21 software package. Quantitative data were characterized utilizing the median and range. The Mann-Whitney U-test was employed to examine disparities between the breast cancer patient group and the control group regarding serum levels of nestin and CA15.3. The Kruskal-Wallis test assessed differences in serum parameters before and after surgery and before and after chemotherapy. Spearman's test was employed to explore correlations between the examined serum biomarkers and breast cancer clinicopathological data. The diagnostic efficacy of various serum biomarkers was compared through receiver operating characteristic (ROC) curve analysis. Significance was established at a $P < 0.05$.

Results

Age distribution among normal control females and females with breast cancer

The median (range) age of breast cancer patients was 47 (30-59) years, while controls had an age distribution of 48 (31-61) years. Statistical analysis of this dataset revealed a non-significant difference between breast cancer patients and controls regarding age ($P = 0.551$).

Menopausal status distribution among normal control females and breast cancer patients

Among breast cancer patients, 32 (40%) were premenopausal females, and 48 (60%) were postmenopausal females. Similarly, among the normal healthy controls, there were 24 (30%) premenopausal females and 56 (70%) postmenopausal females. Statistical analysis of these results revealed a non-significant difference between the control group and the breast cancer patients' group regarding menopausal status ($P = 0.507$).

Serum levels of nestin in the normal control group and breast cancer patient group

Table 1 displays the serum levels of nestin in both the standard control group and the breast cancer patient group. Within the control group, the median (range) serum levels of nestin were 8.58 (6.10-13.68 ng/ml). In the breast cancer patients group, the median (range) serum levels of nestin were 10.50 (8.32-15.06 ng/ml) before surgery, 8.87 (2.01-12.69 ng/ml) after surgery

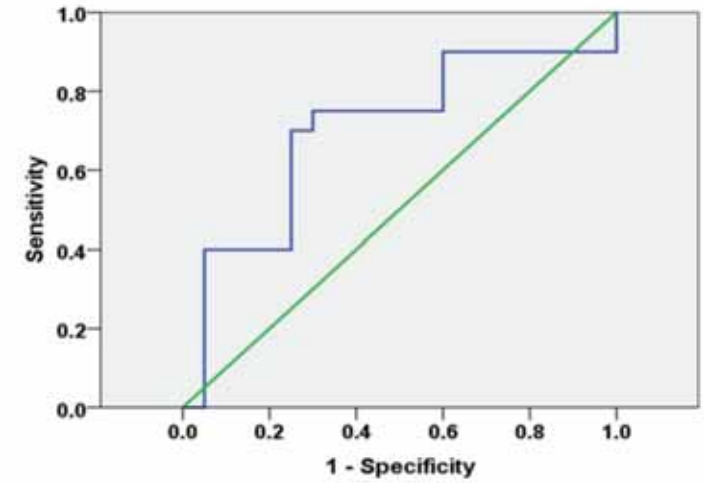

Figure 2. This figure shows the receiver operating characteristic curve for human serum CA15-3. The area under the curve was 70% ($P = 0.021$), with a sensitivity of 45% and specificity of 85% at a cut-off of 22.05 U/ml.

Table 2. Association of preoperative serum nestin levels with the risk of breast cancer incidence

Serum nestin (ng/ml)			Control group (n=80)	Breast cancer group (n=80)	Odds ratio	95% CI	*P*-value
Negative	≤	9.9®	72	18	27.00	4.57 – 159.67	0.0003 *
Positive	>	9.9	8	62			

n: Sample size; ®: Reference group; CI: Confidence interval; *: Significance was considered at *P*-value < 0.05

(before chemotherapy), and 8.72 (7.56-11.06 ng/ml) after chemotherapy. Statistical analysis revealed that the serum levels of nestin were significantly higher in the breast cancer patients' group compared with the standard control group ($P < 0.001$). There was also a significant decrease in nestin levels after surgery compared to before surgery ($P = 0.045$), with no significant differences before and after chemotherapy ($P > 0.05$).

Association of preoperative serum nestin levels with the risk of breast cancer incidence

Table 2 shows that 8/80 (10%) of controls exhibited elevated levels of serum nestin (> 9.9 ng/ml), while 72/80 (90%) of controls had decreased levels of serum nestin (≤ 9.9 ng/ml). In contrast, 62/80 (77%) of cases had elevated levels of preoperative serum nestin (> 9.9 ng/ml), while 18/80 (23%) had decreased levels of preoperative serum nestin (≤ 9.9 ng/ml). Statistical analysis revealed that females with preoperative nestin levels more significant than the cut-off value (9.9 ng/ml) had a significant odds ratio of 27 (95% confidence interval = 4.57-159.67; $P = 0.0003$) compared with those with preoperative nestin levels less than the cut-off value (9.9 ng/ml). This indicates that serum levels of nestin greater than 9.9 ng/ml may act as a risk factor for the development of breast carcinogenesis.

Serum levels of CA15.3 in the normal control group and breast cancer patient group

Table 3 displays the serum levels of CA15.3 in the standard control and breast cancer patient groups. In the control group, the median (range) serum levels of CA15.3 were 10.90 (9.11-20.30 U/ml). In the breast cancer patients group, the median (range) serum levels of CA15.3 were 19.2 (8-39 U/ml) before surgery, 14.67 (10-34.33 U/ml) after surgery (before chemotherapy), and 8.17 (2.67-36.33 U/ml) after chemotherapy. Statistical analysis revealed that the serum levels of CA15.3 were significantly higher in the breast cancer patients' group compared with the standard control group ($P = 0.021$), with no significant differences before and after surgery or before and after chemotherapy ($P > 0.05$).

Comparing the diagnostic values of preoperative serum nestin and CA15.3 in breast cancer patients using ROC curve analysis

Figures 1 and 2 illustrate the results of the ROC curve analysis, presenting the area under the curve (AUC), cut-off values, sensitivity, and specificity for comparing serum nestin and CA15-3 as diagnostic markers in breast cancer patients. The assessment of diagnostic performance relies on the AUC, where a higher AUC indicates a superior diagnostic test. Serum nestin exhibited a noteworthy AUC of 85.2% ($P < 0.001$), with a sensitivity of 80% and specificity of 75% at a 9.90 ng/ml cut-off value. Conversely, serum CA 15.3 demonstrated a significant AUC of 70% ($P = 0.021$), with a sensitivity of 45% and specificity of 85% at a cut-off value of 22.05 U/ml.

Correlation between the studied serum biomarkers and clinicopathological data in breast cancer patients prior to surgery

Based on the data derived from our current study, it is evident that none of the investigated serum biomarkers display a significant correlation with any of the clinicopathological parameters associated with breast cancer ($P > 0.05$).

Discussion

In the current study, nestin and CA15.3 serum levels were significantly higher in the breast cancer patient group than in the control group. Serum nestin is superior to serum CA15.3 in diagnosing breast cancer patients. Increased serum levels of nestin may be a significant risk factor for breast cancer development. Serum nestin was able to monitor the effects of surgery. None of the assayed biomarkers has a significant role in monitoring the effect of chemotherapy on breast

Table 3. The median (range) serum levels of CA15-3 in the control group and the breast cancer patients group

Serum CA15.3 levels (U/ml)	Control group (n=80)	Breast cancer patients group (n=80)		
		Before surgery	After surgery (before chemotherapy)	After chemotherapy
Minimum	9.11	8	10	2.67
Maximum	20.30	39	34.33	36.33
Median	10.90	19.2	14.67	8.17
***P*- Values**		***P*1 = 0.021***	***P*2 = 0.073**	***P*3 = 0.055**

*P*1: Compared with the control group; *P*2: Compared with the levels before surgery; *P*3: Compared with the levels after surgery (before chemotherapy). Significance was considered at a *P*-value < 0.05. *: Statistically significant compared with the standard control group

cancer patients.

Regarding the diagnostic role of serum levels of nestin, the statistical analysis of the current study showed that serum levels of nestin were significantly higher in the breast cancer patients group compared with the standard control group ($P < 0.001$). These results indicate that nestin may have a role in the development of breast cancer. To our knowledge, most studies on nestin in breast cancer analyzed its tissue expression immunohistochemically. Several studies reported significantly increased nestin expression in breast cancer tissues compared with normal breast tissues.[12]

The results of the current study confirmed those found by Sal et al.,[13] who reported that the preoperative serum nestin levels were significantly higher in patients with malignant ovarian tumors compared with patients with benign ovarian tumors. However, the results of the current study disagreed with the results obtained by Aglan et al.,[14] who found that patients with breast cancer had significantly lower levels of serum nestin compared with normal control subjects. It was reported that nestin has the potential to be used as a biomarker in daily clinical practice. Nestin may be a promising prognostic biomarker and a possible therapeutic target for tumor suppression in breast cancer.[8]

In the current study, the preoperative serum levels of nestin were found to be significantly higher in breast cancer patients compared with controls. At the same time, the results of the current study showed that the increased peroperative serum levels of nestin (> 9.9 ng/ml) might increase the risk of females getting breast carcinoma by a factor of 27 compared with females having lower concentrations of serum nestin (≤ 9.9 ng/ml). Because increased serum levels of nestin may increase the risk of breast cancer incidence, this result is strongly compatible with the increased serum levels of nestin in breast cancer patients compared with normal control subjects, which were the results that were found in the current study. To the best of our knowledge, the current study is the first to try to assess the role of serum nestin as a risk factor for the development of breast cancer. A correlation was found between nestin and aggressive growth, angiogenesis, metastasis, and poor prognosis in some tumors, but the roles of nestin in cancer cells have not been characterized.[15]

Regarding the correlation of preoperative serum levels of nestin with breast cancer clinicopathological data, the results of the current study showed a non-significant correlation between serum nestin and any of these clinicopathological data ($P > 0.05$). To the best of our knowledge, the current study is the first to try to assess the correlation of serum nestin with breast cancer clinicopathological data. On the other hand, the current results confirmed those reported by Sal et al.,[13] who found that preoperative serum levels of nestin were non-significantly correlated with the clinicopathological features of ovarian carcinoma.

Regarding the role of serum nestin levels in monitoring the effect of surgery on breast cancer, the current study showed that the serum levels of nestin after surgery were significantly decreased compared with their levels before surgery ($P = 0.045$). To the best of our knowledge, the current study is the first one to try to investigate the role of serum nestin in monitoring the effect of surgery on breast cancer patients.

Regarding the role of serum nestin levels in monitoring the effects of chemotherapy on breast

cancer, the current study showed that serum levels of nestin after chemotherapy were non-significantly decreased compared with their levels before chemotherapy ($P = 0.307$). To the best of our knowledge, the current study is the first to try to investigate the role of serum nestin in monitoring the effects of chemotherapy on breast cancer patients.

Regarding the diagnostic value of serum levels of CA15.3 in the differentiation between controls and breast cancer patients, the statistical analysis of the results of the current study showed that serum levels of CA15.3 were significantly higher in the breast cancer patient group compared with the standard control group ($P = 0.021$). This means that CA15.3 may have a role in the development of breast cancer. These results were in line with those reported by Mohammed et al.,[16] Moazzezy et al.,[17] Hewala et al.,[18] and Fejzič et al.,[19] who found that the serological levels of CA15.3 in breast cancer patients were significantly higher than the serum levels of normal controls.

Regarding the correlation of serum CA15.3 with breast cancer clinicopathological data, the current study's results showed no significant correlation between serum CA15.3 and breast cancer clinicopathological data.

Regarding the role of serum CA15.3 levels in monitoring the effect of surgery on breast cancer patients, the current study showed that serum levels of CA15.3 after surgery were non-significantly decreased compared with their serum levels before surgery ($P = 0.073$). This non-significant decrease in serum CA15.3 levels after surgery may be due to the longer half-life of CA15.3, as previously found by Ali et al.[20] In their study, they reported that since the half-life of CA15.3 is unknown, it remains controversial how to define the optimal interval for tumor marker follow-up.[20]

Regarding the role of serum CA15.3 levels in monitoring the effect of chemotherapy on breast cancer, the current study showed that serum levels of CA15.3 after chemotherapy were non-significantly decreased compared with their levels before chemotherapy ($P = 0.055$). This means that serum CA15.3 has no role in monitoring the response of breast cancer patients to chemotherapy. Although Yang et al.[21] reported that serum CA15.3 can play a role in monitoring therapy, the contradictory results obtained in the current study may be due to the small sample size included in the current study.

Regarding the comparison of the diagnostic values of serum nestin and CA15.3 in breast cancer using the ROC curve analysis, serum nestin showed a significant AUC (85.2%, $P < 0.001$) with sensitivity (80%) and specificity (75%) at a cut-off 9.90 ng/ml. Serum CA15.3 showed a significant AUC (70%, $P = 0.021$) with sensitivity (45%) and specificity (85%) at a cut-off of 22.05 U/ml. This means that serum nestin is more potent than serum CA15.3 in determining the difference between controls and breast cancer patients.

Aglan et al.[14] applied the ROC curve analysis to estimate the diagnostic value of serum nestin to differentiate breast cancer patients from controls. At a specific cut-off value of 39.9 pg/ml for serum nestin, they found that its diagnostic sensitivity was 84.8% and specificity was 65.1%, with a significant AUC of 81.2% ($P < 0.001$). These results are more or less compatible with the results of the current study.

No published study compared the diagnostic powers of serum nestin and CA15.3 in differentiating breast cancer patients from controls using ROC curve analysis. So, the current study may be the first designed to carry out this aim. The current study reported a significant role for nestin as a risk factor for the development of breast carcinoma. Nestin was also found to have a role in monitoring the effect of surgery on breast cancer. However, due to its relatively small sample size, the results of the current study regarding the roles of serum nestin and CA15.3 in monitoring the effect of chemotherapy need to be verified by performing further investigations, including a larger sample size of cases and controls.

Conclusion

The findings from the present study suggest that serum nestin may play a pivotal role in the pathogenesis of breast cancer and could serve as

a valuable diagnostic tool for identifying breast cancer patients. Serum nestin exhibits superior diagnostic efficacy in discriminating breast cancer patients from control subjects compared to serum CA15.3. Elevated serum nestin levels (> 9.9 ng/ml) are associated with a 27-fold increased risk of developing breast carcinoma in females, in contrast to individuals with lower serum nestin concentrations (9.9 ng/ml or below). Furthermore, serum nestin demonstrates utility in monitoring surgical outcomes, effectively distinguishing between breast cancer patients before and after surgery (P = 0.045). However, it is noteworthy that serum nestin does not exhibit a significant role in assessing the effects of chemotherapy in breast cancer patients. No statistically significant correlations were observed between preoperative serum nestin levels and various clinicopathological parameters associated with breast cancer.

On the other hand, CA15.3 also appears to be implicated in the onset of breast cancer and can be employed as a diagnostic marker for identifying breast cancer patients. Nonetheless, serum CA15.3 demonstrates comparatively lower diagnostic accuracy in distinguishing breast cancer patients from healthy controls when contrasted with serum nestin. Similarly, serum CA15.3 does not play a significant role in evaluating the impact of surgery or chemotherapy on breast cancer patients. No statistically significant associations were identified between preoperative serum CA15.3 levels and breast cancer clinicopathological parameters.

It is imperative to note that the current study's findings necessitate validation through subsequent investigations, which should ideally encompass a larger cohort of breast cancer patients and an appropriate control group for comprehensive assessment and confirmation of these observations.

Conflict of Interest

None declared.

References

1. Marconi R, Serafini A, Giovanetti A, Bartoleschi C, Pardini MC, Gianluca Bossi G, et al. Cytokine modulation in breast cancer patients undergoing radiotherapy: A revision of the most recent studies. *Int J Mol Sci*. 2019;20(2):382. doi: 10.3390/ijms20020382.
2. Svobodova S, Kucera R, Fiala O, Karlikova M, Narsanska A, Zedníková I, et al. CEA, CA 15-3, and TPS as prognostic factors in the follow-up monitoring of patients after radical surgery for breast cancer. *Anticancer Res*. 2018;38(1):465-9. doi: 10.21873/anticanres.12245.
3. Fu Y, Li H. Assessing clinical significance of serum CA15-3 and carcinoembryonic antigen (CEA) levels in breast cancer patients: a meta-analysis. *Med Sci Monit.* 2016;22:3154-62. doi:10.12659/msm.896563
4. Kabel AM. Tumor markers of breast cancer: New prospectives. *Journal of Oncological Sciences.* 2017;3:5-11. doi:10.1016/j.jons.2017.01.001.
5. Nowak A, Dziegiel P. Implications of nestin in breast cancer pathogenesis (Review). *Int J Oncol.* 2018; 53(2):477-87. doi: 10.3892/ijo.2018.4441.
6. Neradil J, Veselska R. Nestin as a marker of cancer stem cells. *Cancer Sci.* 2015;106(7):803-11. doi: 10.1111/cas.12691.
7. Sharma P, Alsharif S, Fallatah A, Chung BM. Intermediate filaments as effectors of cancer development and metastasis: a focus on keratins, vimentin, and nestin. *Cells.* 2019;8(5):497. doi: 10.3390/cells8050497.
8. Zhang X, Xing C, Guan W, Chen L, Guo K, Yu A, et al. Clinicopathological and prognostic significance of Nestin expression in patients with breast cancer: a systematic review and meta-analysis. *Cancer Cell Int.* 2020;20:169. doi: 10.1186/s12935-020-01252-5.
9. Meisen WH, Dubin S, Sizemore ST, Mathsyaraja H, Thies K, Lehman NL, et al. Changes in BAI1 and Nestin expression are prognostic indicators for survival and metastases in breast cancer and provide opportunities for dual targeted therapies. *Mol Cancer Ther.* 2015;14(1):307-14. doi: 10.1158/1535-7163.MCT-14-0659.
10. Paluch-Shimon S, Pagani O, Partridge AH, Bar-Meir E, Fallowfield L, Fenlon D, et al. Second international consensus guidelines for breast cancer in young women (BCY2). *Breast.* 2016;26:87-99. doi: 10.1016/j.breast.2015.12.010.
11. National Comprehensive Cancer Network (NCCN): NCCN Clinical practice Guidelines in Oncology (NCCN Guidelines). Breast Cancer. Version 5.2020. July 2020. NCCN guidelines for patients®. Available at: www.nccn.org/patients
12. De Lara S, Nyqvist J, Werner Rönnerman E, Helou K, Kenne Sarenmalm E, Einbeigi Z, et al. The prognostic relevance of FOXA1 and Nestin expression in breast cancer metastases: a retrospective study of 164 cases during a 10-year period (2004-2014). *BMC Cancer.* 2019;19(1):187. doi: 10.1186/s12885-019-5373-2.
13. Sal V, Kahramanoglu I, Bese T, Demirkiran F, Sofiyeva

N, Soyman Z, et al. Is serum level of Nestin useful in detecting epithelial ovarian cancer? *J Obstet Gynaecol Res.* 2017;43(2):371-7. doi: 10.1111/jog.13220.
14. Aglan SA, Elsammak M, Elsammak O, El-Bakoury EA, Elsheredy HG, Ahmed YS, et al. Evaluation of serum Nestin and HOTAIR rs12826786 C>T polymorphism as screening tools for breast cancer in Egyptian women. *J Med Biochem.* 2021;40(1):17-25. doi: 10.5937/jomb0-25295.
15. Matsuda Y, Hagio M, Ishiwata T. Nestin: a novel angiogenesis marker and possible target for tumor angiogenesis. *World J Gastroenterol.* 2013;19(1):42-8. doi:10.3748/wjg.v19.i1.42
16. Mohammed FZ, Gamal L , Mosa MF, Aref MI. Assessment of CA15-3 and CEA as potential markers for breast carcinoma prognosis in Egyptian females. *Alfarama Journal of Basic & Applied Sciences (AJBAS)*. 2021;2(1):44-50. doi:10.21608/AJBAS.2020.32631.1018.
17. Moazzezy N, Farahany TZ, Oloomi M, Bouzari S. Relationship between preoperative serum CA15-3 and CEA levels and clinicopathological parameters in breast cancer. *Asian Pac J Cancer Prev.* 2014;15(4):1685-8. doi: 10.7314/apjcp.2014.15.4.1685.
18. Hewala TI, Abd El-Monaim NA, Anwar M, Ebied SA. The clinical significance of serum soluble Fas and p53 protein in breast cancer patients: comparison with serum CA 15-3. *Pathol Oncol Res.* 2012;18(4):841-8. doi: 10.1007/s12253-012-9512-1.
19. Fejzić H, Mujagić S, Azabagić S, Burina M. Tumor marker CA 15-3 in breast cancer patients. *Acta Med Acad.* 2015;44(1):39-46. doi: 10.5644/ama2006-124.125.
20. Ali HQ, Mahdi NK, Al-Jowher MH. The value of CA15-3 in diagnosis, prognosis and treatment response in women with breast cancer. *J Pak Med Assoc.* 2013;63(9):1138-41.
21. Yang Y, Zhang H, Zhang M, Meng Q, Cai L, Zhang Q. Elevation of serum CEA and CA15-3 levels during antitumor therapy predicts poor therapeutic response in advanced breast cancer patients. *Oncol Lett.* 2017;14(6):7549-56. doi: 10.3892/ol.2017.7164.

Brief Report
Middle East Journal of Cancer; April 2024; 15(2): 145-152

Pancreatic Neuroendocrine Tumors: Spectrum of Clinical Presentation from a Tertiary Referral Center in Pakistan

Kalsoom Akhlaq*, MD, Hadi Khan, MD, Zafar Ali***, MD, Muslim Atiq*♦, MD, Shahzad Riyaz*, MD, Umar Yousaf Raja****, MD, Amen Kiani**, MD**

**Department of Gastroenterology, Shifa International Hospital, Islamabad, Pakistan*
***Department of Surgery, Shifa International Hospital, Islamabad, Pakistan*
****Department of Pathology, Shifa International Hospital, Islamabad, Pakistan*
*****Department of Endocrinology, Shifa International Hospital, Islamabad, Pakistan*

Please cite this article as: Akhlaq K, Khan H, Ali Z, Atiq M, Riyaz S, Raja UY, et al. Pancreatic neuroendocrine tumors: spectrum of clinical presentation from a tertiary referral center in Pakistan. Middle East J Cancer. 2024; 15(2):145-52. doi:10.30476/mejc.2023.98055.1883.

Abstract

Background: Pancreatic neuroendocrine tumors (P-NETs) constitute a subset of pancreatic mass lesions characterized by diverse clinical presentations. Despite their inherent malignant potential, the timely identification and treatment of these tumors are critical for achieving favorable clinical outcomes. This study aims to shed light on the heterogeneous tumor biology of P-NETs and the management strategies employed at a tertiary care center in Pakistan.

Method: A retrospective study encompassing all patients with a biopsy-confirmed diagnosis of P-NETs at Shifa International Hospital between January 1st, 2016, and June 30th, 2021, was conducted. Meticulous data extraction from pathology records and thorough searches of medical records were performed to gather relevant demographic and clinical information.

Results: A total of 24 patients were retrieved from our database, with 13 (54%) female patients. The mean age was 49.5 ± 16.3 years. Eight out of the 24 patients presented with abdominal pain. Most patients (14 out of 24) had lesions in the pancreatic head region. In three cases, lesions exhibited multicentricity. The mean lesion size measured 4.4 ± 2.3 cm. Three of the 24 patients displayed distant liver metastasis at the presentation time. 19 out of the 24 patients underwent surgical resections, while endoscopic ultrasound (EUS)-guided biopsy was performed in 4 out of 24 cases. EUS-guided tissue biopsy yielded accurate diagnoses in all four cases.

Conclusion: Most P-NETs are non-functional, and there is an almost equal distribution between male and female patients. Solitary lesions predominate, and metastasis is uncommon at initial presentation. EUS-guided fine needle biopsy stands out as a dependable diagnostic modality for P-NETs.

Keywords: Neuroendocrine tumors, Pancreas, Clinical presentation, Management, Diagnosis

♦Corresponding Author:
Muslim Atiq, MD, MPH
Departments of Gastroenterology, Shifa International Hospital, Islamabad, Pakistan
Tel: +92-51-8463000
Email: atiqsm@gmail.com

Received: February 16, 2023; Accepted: October 30, 2023

Introduction

Pancreatic neuroendocrine tumors (P-NETs) originating from the diffuse neuroendocrine cells are pretty uncommon and include a heterogeneous group of tumors of the pancreas. P-NETs comprise only 1 to 2% of all pancreatic malignancies, but their incidence has gradually increased over the past few decades.[1] Most P-NETs are indolent, but they do have malignant potential. The biological behavior of an individual P-NET is unpredictable. However, tumor grade, lymph node or liver metastasis, and tumor size help assess prognosis and clinical outcome.[2] P-NETs can be functional (i.e., associated with clinical symptoms about hypersecretion of a specific hormone), non-functional, sporadic, or associated with familial syndromes; indolent in the long-term; or aggressive and life-threatening. Genetic disorders associated with P-NETs include multiple endocrine neoplasia type 1, von Hippel-Lindau syndrome, and neurofibromatosis type 1.[3] P-NETs are typically hypervascular on imaging and undergo enhancement on arterial and venous phase images.[4]

Computed tomography (CT) scan has been reported to have significant prognostic value about pathological tumor grade as well as pancreatic duct involvement. Significant CT features that correlated with higher pathological grade include larger tumor size, non-hyperattenuation, presence of distant metastases, CT ratio, ill-defined tumor margins, lower sphericity, heterogeneous enhancing, lower attenuation values, vessel involvement, cystic degeneration, bile duct dilatation, and vascular invasion.[4] Nuclear imaging with octreotide is helpful in the diagnosis of occult tumors not detected by anatomical imaging.[5] Endoscopic ultrasound (EUS) is usually performed in conjunction with other imaging modalities, as it helps confirm the size and characteristics of these lesions and obtain tissue diagnosis simultaneously.[6] EUS is the mainstay modality for diagnosing P-NETs with high diagnostic accuracy.[6]

According to the World Health Organization (WHO) classification scheme, the diagnosis of this group of tumors is based on the tumor's histopathology and the assessment of proliferation fraction. However, the former can be challenging due to the lack of well-defined histologic criteria and that the established criteria of >20 mitoses/10 high-power fields or Ki67>20% may not sufficiently distinguish well-differentiated P-NETs from poorly-differentiated NETs.[7] Over the last few decades, significant progress has been made in diagnosing, understanding the pathophysiology, and managing P-NETs. There is a lack of data on P-NETs from South Asia. Therefore, our experience with P-NETs is presented regarding the demographic features, characteristic findings on laboratory and imaging studies, and histopathology.

Materials and Methods

Study population

A retrospective descriptive study was conducted at Shifa Tameer-e-Millat University in Islamabad, Pakistan. Patients undergoing evaluation at Shifa International Hospital for the diagnosis of P-NET from January 1st, 2016, to June 30th, 2021, were included in the study. Patients were identified through pathology records retrieved from the institutional database. Medical records were scrutinized for demographic, clinical, and diagnostic variables. The clinical data under

Figure 1. CT: This image illustrates a large, lobulated, well-circumscribed mass originating from the body of the pancreas, measuring 8.4 × 9 × 5.6 cm.
CT: Computed tomography

review encompassed age, gender, and symptoms presented at admission. Laboratory data included assessments of elevated hormone levels such as gastrin, insulin, vasoactive intestinal polypeptide (VIP), glucagon, chromogranin, and neuron-specific enolase. These parameters facilitated the distinction between functional and non-functional P-NETs. The diagnostic evaluation encompassed CT scan findings, with the pathological features of the tumor being also incorporated into the data collection process. Medical records were examined to determine if patients had undergone EUS-guided biopsy. The management plan and survival rate of patients were meticulously scrutinized and evaluated throughout the study. All statistical analyses were executed using Statistical Package for the Social Sciences (SPSS) version 29. The Institutional Review Board (IRB) of the Human Research and Ethics Committee (EC) approved this study, with the ethical code number IRB #061-21. This study adheres to the principles of the Declaration of Helsinki.

CT scan findings

The meticulous assessment was conducted on the CT features, encompassing the following aspects: tumor site and size, peripancreatic vascular involvement, and upstream pancreatic duct dilatation.

EUS- fine needle aspiration (EUS-FNA) examination

Seasoned gastroenterologists conducted all procedures following the acquisition of informed consent from the patient. A 22-gauge fine needle biopsy was employed for the examination, with patients routinely administered a singular dose of intravenous antibiotics concurrent with the procedure.

Results

A total of 24 patients were retrieved from our database. 13 patients (54%) were females. The mean age of the patients was 49.5 ± 16.3 years. The most prevalent clinical presentation was abdominal pain, observed in 8 out of 24 patients (33.0%) (Table 1). 5 (20.8%) patients presented with hypoglycemia, and 3 (12%) reported weight loss. The mean size of the lesion was 4.4 ± 2.3 cm (Figure 1). 14 out of the 24 (58.3%) patients had lesions involving the head region (Figure 2). In three cases, lesions were multicentric. 19 out of 24 (79.2%) patients underwent surgical resections. 3 out of 24 patients had liver metastasis at the time of presentation. 2 of these 3 patients had lesions in the tail of the pancreas. EUS was performed in four cases, and a correct diagnosis of PNET was established in all four cases (Figure 3).

Histological diagnosis was based on morphology and immunohistochemistry (IHC). Synaptophysin staining was conducted in 23 out of 24 cases, with positive results in 22 out of 23 cases. The diagnosis relied on morphology in 2 cases. The Ki-67 index was reported in 23 cases, with ten histological specimens graded as G1, nine as G2, and five as G3 (Figures 4 and 5). The most frequently performed surgery was a Whipple's procedure, conducted in 10 out of 19 cases (52.6%). The final histological diagnosis indicated a well-differentiated tumor in 20 out of 24 (83.3%) patients. At the time of study analysis, 22 out of 24 (91.66%) patients were still alive.

Discussion

Our study reports 24 cases of P-NETs from a tertiary care center in Pakistan. An almost equal incidence of P-NETs was observed in both genders, with a slightly increased incidence in

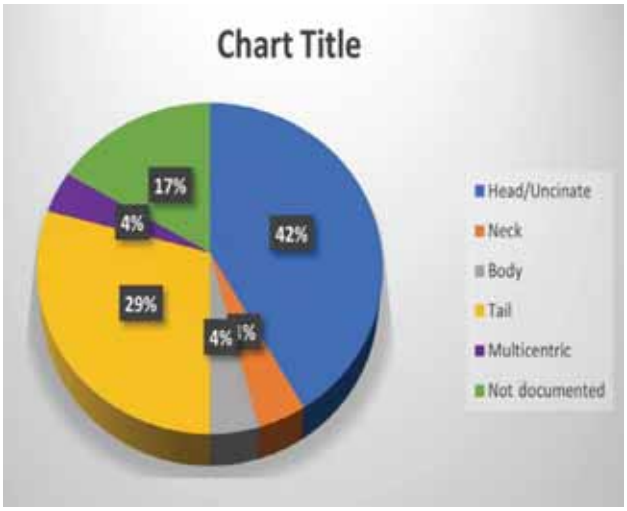

Figure 2. This figure shows the distribution of P-NETs with regards to location.
P-NET: Pancreatic neuroendocrine tumors

Table 1. Clinical presentation of patients with P-NETs

	No.	% (age)
Abdominal pain	8	33.3
Hypoglycemia	5	20.8
Weight loss	3	12.5
Jaundice	2	8.3
Incidental	1	4.2
Missing*	5	20.8

* Includes cases referred from outside facility; No.: Number

females.

Our study reports a significantly higher proportion of non-functional tumors. A similar trend has been observed in recent studies.[5] Patients in our report who were diagnosed with insulinoma had hypoglycemia on clinical presentation. On imaging, most patients presented with solitary lesions, and the head of the pancreas was the predominant location of the tumor. In three cases, patients had multicentric lesions, and one of these had distant metastasis to the liver. The mean size of the lesion was 4.4 +/- 2.3 cm, and it was noticed that lesions greater than 3 cm were associated with distant metastasis.

Our study reported positivity for synaptophysin in most patients on immunohistochemical analysis (figure 4B). This is consistent with literature reporting positivity for synaptophysin and other immunohistochemical markers, such as chromogranin A, which greatly aid the diagnosis.[8-10] Chromogranin A provides insight into tumor burden, assists with treatment, and predicts prognosis with sensitivity, specificity, and accuracy of 66%, 95%, and 71%, respectively.[8-10] P-NET diagnosis is based on a combination of pathology, imaging, and serum tumor markers. Other serum markers, such as neuron-specific enolase (NSE), pancreatic polypeptide (PP), pancreastatin, and subunits of human chorionic gonadotropin, can also aid in diagnosis. For functional P-NETs, patients often present with hormone-specific symptoms. Five patients (20.8%) in our study were diagnosed with insulinoma and presented with the clinical presentation of hypoglycemia. Our findings are consistent with the previous studies.[1]

Our study utilized CT as the primary imaging modality for tumor localization and vascular

Figure 3. This figure shows the endoscopic ultrasound: fine needle biopsy of a hypoechoic mass involving the body of pancreas.

involvement, following established imaging guidelines for P-NETs.[11,12] EUS-FNAC has a high sensitivity for grading malignancy in patients with small P-NETs, was performed in four cases, and correctly diagnosed P-NETs, demonstrating strong concordance between cytology and histopathological analysis.[4] This is evident in the study by Eusebi et al., which included 91 patients undergoing 102 EUS procedures.[10] The diagnostic sensitivity for EUS-FNA, EUS-FNB, and the combination of both methods was 88.4%, 94.3%, and 100%, respectively.[10] Recent advances in P-NET imaging have significantly impacted management strategies. The use of Somatostatin receptor imaging (SRI) with radiolabeled SS analogs (SSA), such as 111 In-pentetreotide (Octreoscan) or 68Ga-DOTA-SSA PET/CT, has become popular in detecting P-NETs and monitoring recurrence, as these tumors have a high expression of somatostatin receptors (SSTRs).[13] 68Ga PET tracers have been reported to have higher diagnostic accuracy than traditional imaging modalities.[13] Our study primarily relied on CT and EUS as the primary diagnostic modalities; PET scans were not performed on any of the patients.

In our study, most patients had G1/G2 tumors, and the Ki-67 index was available for almost all cases. The histopathological analysis revealed well-differentiated P-NET in 83.3% of the patients, with an overall favorable prognosis. During the follow-up period, 91.6% of the patients remained alive and healthy. Our findings are consistent with another study done in Pakistan by Ali et al., which showed 5-year overall survival (OS) rates of 88%, 57%, and 0% for low, intermediate, and high-grade P-NETs and 94%, 79%, and 43% for complete, incomplete, and unresectable disease, respectively.[14] Although P-NETs have a generally good prognosis after resection, about 21%-42% of patients have recurrence.[15] Post-surgical prognostic factors for recurrence and mortality include tumor grade, stage, invasion, extent, and molecular markers.[16] Furthermore, it has been

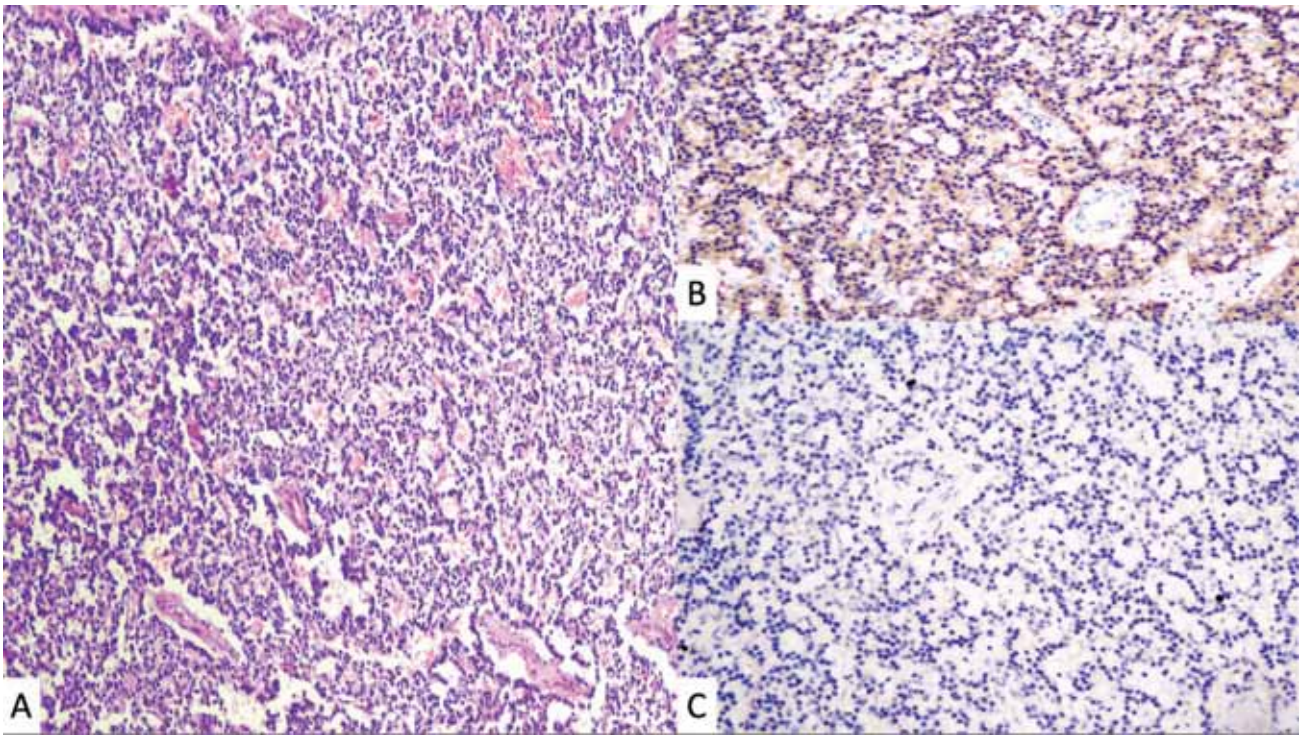

Figure 4. Histological features of P-NETs - grade 1: This figure delineates the histological characteristics of grade 1 well-differentiated neuroendocrine tumors (WD-NETs) of the pancreas. Panel A displays a photomicrograph revealing small, round, monotonous cells with coarse, salt-and-pepper nuclear chromatin and minimal atypia, organized in nests and trabeculae (H&E, ×200). Panel B exhibits synaptophysin immunohistochemical staining, demonstrating cytoplasmic positivity within the tumor cells (IHC, ×200). Panel C portrays Ki67 immunohistochemistry, showcasing rare positive cells (<1%) (IHC, ×200).

WD-NET: Well-differentiated neuroendocrine tumor; IHC: Immunohistochemistry; P-NET: Pancreatic neuroendocrine tumor

reported that larger tumor size, high Ki-67 index, grade, and stage predict shorter OS, progression-free survival (PFS), and recurrence-free survival.[17] In our study, 22 out of the 24 patients were alive and free from recurrence during the follow-up period.

Although P-NETs are said to have low-grade malignant potential, about 40%–80% of patients are metastatic at presentation, usually involving the liver (40%–93%).[18] This was also true for our study, as three patients had liver metastasis on presentation, and 2 out of these 3 patients had lesions involving the tail of the pancreas. Most of the patients in our study underwent curative surgical resection (79.2%). Pancreaticoduodenectomy (Whipple procedure) was the most common surgery (52.6%). This aligns with the existing literature, where surgical resection is the definitive treatment for achieving a cure.[19] There is an ongoing debate regarding managing non-functional lesions <2 cm in size, with no clear consensus between resection and surveillance. However, for patients with more significant than 2 cm P-NETs, invasive tumors, or radiographically positive lymph nodes indicating locally advanced disease, surgical resection is recommended as the primary treatment modality.[19] After surgery, imaging is recommended once every 3 to 12 months for the first year and then every 6 to 12 months after that, according to guidelines from the National Comprehensive Cancer Network (NCCN) and the North American Neuroendocrine Cancer Tumor Society (NANETS). In our cohort, the average tumor size was 4.4 +/- 2.3, leading to most patients undergoing resection. As a result, the overall prognosis was favorable, with 91.7% of patients remaining alive and in good health during the follow-up period.

Our study addresses the scarcity of data on P-NET incidence in Pakistan and contributes as one of the few reports from this region. It offers valuable insights into the complex tumor biology and management strategies for P-NETs. However, several limitations deserve attention. First, the retrospective nature of the study should be noted. Secondly, patients from external facilities lacked sufficient follow-up information. Lastly, the study's small sample size should be considered when

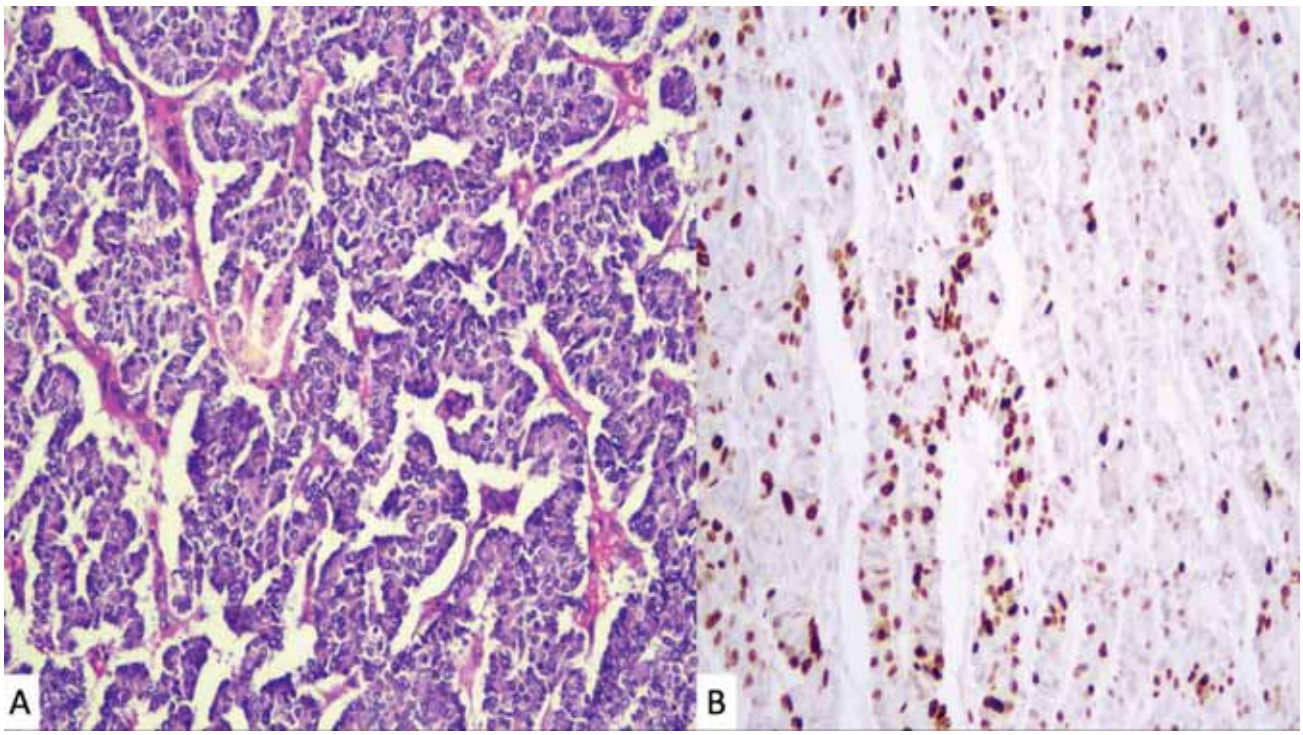

Figure 5. Histological features of P-NETs - grade 3: This figure illustrates the histological attributes of grade 3 well-differentiated neuroendocrine tumors (WD-NETs) of the pancreas. Panel A presents a photomicrograph displaying the trabecular arrangement of tumor cells (H&E, ×200). Panel B reveals Ki67 immunohistochemistry, indicating an elevated proliferative index (>20%) (IHC, ×200).
WD-NET: Well-differentiated neuroendocrine tumor; IHC: Immunohistochemistry

interpreting the results.

Conclusion

Most P-NETs are non-functional and solitary, exhibiting a similar distribution among both sexes. Targeted biopsies and IHC techniques can be employed to facilitate diagnosis. Surgical resections are a viable option for the majority of patients.

Conflict of Interest

None declared.

References

1. Ro C, Chai W, Yu VE, Yu R. Pancreatic neuroendocrine tumors: biology, diagnosis, and treatment. *Chin J Cancer.* 2013;32(6):312–24. doi: 10.5732/cjc.012.10295.
2. Gaujoux S, Menegaux F. Going above and beyond the pancreatic neuroendocrine tumor classification. *JCO Oncol Pract.* 2020;16(11):731-2. doi:10.1200/OP.20.00809.
3. Stevenson M, Lines KE, Thakker RV. Molecular genetic studies of pancreatic neuroendocrine tumors: New therapeutic approaches. *Endocrinol Metab Clin North Am.* 2018;47(3):525-48. doi: 10.1016/j.ecl.2018.04.007.
4. Lee L, Ito T, Jensen RT. Imaging of pancreatic neuroendocrine tumors: recent advances, current status, and controversies. *Expert Rev Anticancer Ther.* 2018;18(9):837-60. doi: 10.1080/14737140.2018.1496822
5. Sadowski SM, Neychev V, Millo C, Shih J, Nilubol N, Herscovitch P, et al. Prospective study of 68Ga-DOTATATE positron emission tomography/computed tomography for detecting gastro-entero-pancreatic neuroendocrine tumors and unknown primary sites. *J Clin Oncol.* 2016;34(6):588-96. doi: 10.1200/JCO.2015.64.0987.
6. Di Leo M, Poliani L, Rahal D, Auriemma F, Anderloni A, Ridolfi C, et al. Pancreatic neuroendocrine tumours: the role of endoscopic ultrasound biopsy in diagnosis and grading based on the WHO 2017 classification. *Dig Dis.* 2019;37(4):325-33. doi: 10.1159/000499172.
7. Tang LH, Basturk O, Sue JJ, Klimstra DS. A practical approach to the classification of WHO grade 3 (G3) well-differentiated neuroendocrine tumor (WD-NET) and poorly differentiated neuroendocrine carcinoma (PD-NEC) of the pancreas. *Am J Surg Pathol.* 2016;40(9):1192-202. doi: 10.1097/PAS.0000000000000662.
8. Han X, Zhang C, Tang M, Xu X, Liu L, Ji Y, et al. The value of serum chromogranin A as a predictor of tumor burden, therapeutic response, and nomogram-based survival in well-moderate nonfunctional pancreatic neuroendocrine tumors with liver metastases. *Eur J Gastroenterol Hepatol.* 2015;27(5):527-35. doi: 10.1097/MEG.0000000000000332.
9. Pulvirenti A, Rao D, Mcintyre CA, Gonen M, Tang LH, Klimstra DS, et al. Limited role of Chromogranin A as clinical biomarker *for pancreatic neuroendocrine tumors. HPB (Oxford).* 2019;21(5):612-8. doi: 10.1016/j.hpb.2018.09.016.
10. Thoeni RF, Mueller-Lisse UG, Chan R, Do NK, Shyn PB. Detection of small, functional islet cell tumors in the pancreas: selection of MR imaging sequences for optimal sensitivity. *Radiology.* 2000;214(2):483-90. doi: 10.1148/radiology.214.2.r00fe32483.
11. Choi TW, Kim JH, Yu MH, Park SJ, Han JK. Pancreatic neuroendocrine tumor: prediction of the tumor grade using CT findings and computerized texture analysis. *Acta Radiol.* 2018;59(4):383-92. doi: 10.1177/0284185117725367.
12. Falconi M, Eriksson B, Kaltsas G, Bartsch DK, Capdevila J, Caplin M, et al. ENETS consensus guidelines update for the management of patients with functional pancreatic neuroendocrine tumors and non-functional pancreatic neuroendocrine tumors. *Neuroendocrinology.* 2016;103(2):153-71. doi: 10.1159/000443171.
13. Graham MM, Gu X, Ginader T, Breheny P, Sunderland JJ. 68Ga-DOTATOC imaging of neuroendocrine tumors: a systematic review and metaanalysis. *J Nucl Med.* 2017;58(9):1452-8. doi: 10.2967/jnumed.117.191197.
14. Chouliaras K, Newman NA, Shukla M, Swett KR, Levine EA, Sham J, et al. Analysis of recurrence after the resection of pancreatic neuroendocrine tumors. *J Surg Oncol.* 2018;118(3):416-21. doi: 10.1002/jso.25146.
15. Lee L, Ito T, Jensen RT. Prognostic and predictive factors on overall survival and surgical outcomes in pancreatic neuroendocrine tumors: recent advances and controversies. *Expert Rev Anticancer Ther.* 2019;19(12):1029-50. doi: 10.1080/14737140.2019.1693893.
16. Ali J, Rahat A, Shah MH, Sajjad M, Malik I, Ikram SI, et al. The clinicopathologic characteristics and outcomes of gastroentero-pancreatic neuroendocrine tumors - experience from a tertiary cancer center. *Gulf J Oncolog.* 2022;1(40):7-14
17. Krogh S, Grønbæk H, Knudsen AR, Kissmeyer-Nielsen P, Hummelshøj NE, Dam G. Predicting progression, recurrence, and survival in pancreatic neuroendocrine tumors: a single center analysis of 174 patients. *Front Endocrinol (Lausanne).* 2022;13:925632. doi: 10.3389/fendo.2022.925632.
18. Dasari A, Shen C, Halperin D, Zhao B, Zhou S, Xu Y, et al. Trends in the incidence, prevalence, and

survival outcomes in patients with neuroendocrine tumors in the United States. *JAMA Oncol.* 2017;3(10):1335-42. doi: 10.1001/jamaoncol.2017.0589.

Case Report
Middle East Journal of Cancer; April 2024; 15(2): 153-160

Papillary Tumor of the Pineal Region with Leptomeningeal Seeding: A Case Report and Literature Review

Kazem Anvari*, MD, Parisa Rabiei*, MD, Hamidreza Hashemian, MD, Mohammad Farajirad***, MD, Soudeh Arastouei*, MD, Zohreh Pishevar Feizabad*♦, MD**

*Cancer Research Center, Mashhad University of Medical Sciences, Mashhad, Iran
**Department of Medical Microbiology and Pathology, Razavi Cancer Research Center, Razavi Hospital, Imam Reza International University, Mashhad, Iran
***Department of Neurosurgery, Ghaem Hospital, Mashhad University of Medical Sciences, Mashhad, Iran

Please cite this article as: Anvari K, Rabiei P, Hashemian H, Farajirad M, Arastouei S, Pishevar Feizabad Z. Papillary tumor of the pineal region with leptomeningeal seeding: a case report and literature review. Middle East J Cancer. 2024;15(2):153-160. doi:10.30476/mejc.2023.98435.1897.

Abstract

Papillary tumor of the pineal region (PTPR) is an infrequent neoplasm arising from the ependymal cells of the sub-commissural organ. This tumor entity was incorporated into the World Health Organization (WHO) classification of central nervous system tumors in 2007. Given the propensity for local recurrence observed in PTPR cases and the documented instances of leptomeningeal seeding in previous case reports, it presents a substantial risk of significant morbidity. Due to its rarity, there is no established standard for its management. Surgical intervention constitutes the primary treatment modality, while the role of adjuvant radiotherapy remains ambiguous. In this case report, we present the clinical course of a 46-year-old male diagnosed with PTPR who underwent surgical resection followed by adjuvant radiotherapy. 14 months post-initial treatment, the patient manifested intracranial and spinal metastases in the form of leptomeningeal dissemination. Subsequently, systemic chemotherapy utilizing vincristine and carboplatin was initiated, and the patient exhibited no evidence of disease progression over the last six months.

Keywords: Pineal gland, Papillary tumor, Leptomeningeal seeding, Brain neoplasms, Case report

♦Corresponding Author:
Zohreh Pishevar Feizabad, MD
Cancer Research Center, Mashhad University of Medical Sciences, Mashhad, Iran
Tel: +98 51-38426082
Fax: +98 51-38428622
Email: zohreh.pishevar@gmail.com

Introduction

Papillary tumor of the pineal region (PTPR) is a rare pineal parenchymal lesion, compromising less than 1% of all intracranial tumors.[1] It was first introduced by Jouvet in 2003,[2] and has been included in the classification of central nervous system tumors since 2007.[1] Pineal region tumors are of four general categories: Pineal parenchymal tumors, germ cell tumors, pineal metastasis, and other rare tumors, including meningioma,

Received: March 26, 2023; Accepted: November 25, 2023

lymphoma, and glial tumors.[2]

PTPR originates from the subcommissural organ's ependymal cells, showing papillary formations and an epithelial growth pattern.[2] It has a high propensity to recur locally. Due to its rare occurrence, its management is not standardized. A large study on patients' characteristics, optimal treatment, and survival is lacking, and most patients are presented as case reports or case series.[4-14]

Herein, we present a case of PTPR, who was treated with surgery and adjuvant radiotherapy and experienced recurrence 14 months later.

Case Presentation

A 46-year-old man experiencing a two-week history of nausea, vomiting, severe headache, dizziness, loss of balance, and somnolence was referred to the Department of Neurological Surgery at Mashhad University of Medical Sciences. Brain magnetic resonance imaging (MRI) revealed a 41 mm enhancing mass at the posterior part of the third ventricle, resulting in non-communicating hydrocephalus of the lateral ventricles (Figure 1).

To alleviate intracranial pressure (ICP), a ventriculoperitoneal shunt was placed, and subsequently, a subtotal mass resection was performed during the craniotomy. Pathological assessment of the 1.5 × 1 × 0.5 cm resected specimen revealed a neoplastic lesion with a diffuse proliferation of atypical cells characterized by round hyperchromatic nuclei, moderate nuclear atypia, clear to acidophilic cytoplasm, and some mitotic activity. These findings were consistent with a pineal parenchymal tumor with intermediate differentiation (Figure 2).

The patient received adjuvant radiotherapy, which commenced two weeks postoperatively, delivering a total dose of 5940 cGy in 33 fractions using a three-dimensional (3D) conformal technique. Pre- and postoperative MRI images were fused and registered on computed tomography simulation images to delineate the treatment volumes. The tumor bed and residual mass were defined as the gross tumor volume (GTV), with a 3D margin of 1.5 cm added to create the clinical tumor volume (CTV) (Figure 3). Due to limited evidence regarding the chemoresistance of the tumor and a lack of data on the role of systemic treatment in recurrence or cases of diffuse involvement, the patient was counseled, and he opted for surveillance with neurological examinations and brain MRIs every 4 to 6 months.

During follow-up, the patient remained clinically stable, with stable disease observed on MRI scans, consistent with the RANO criteria, for 14 months post-radiotherapy. Four months after his last follow-up, he presented to the emergency room with tonic-clonic seizures. On MRI, the mass in the pineal region remained

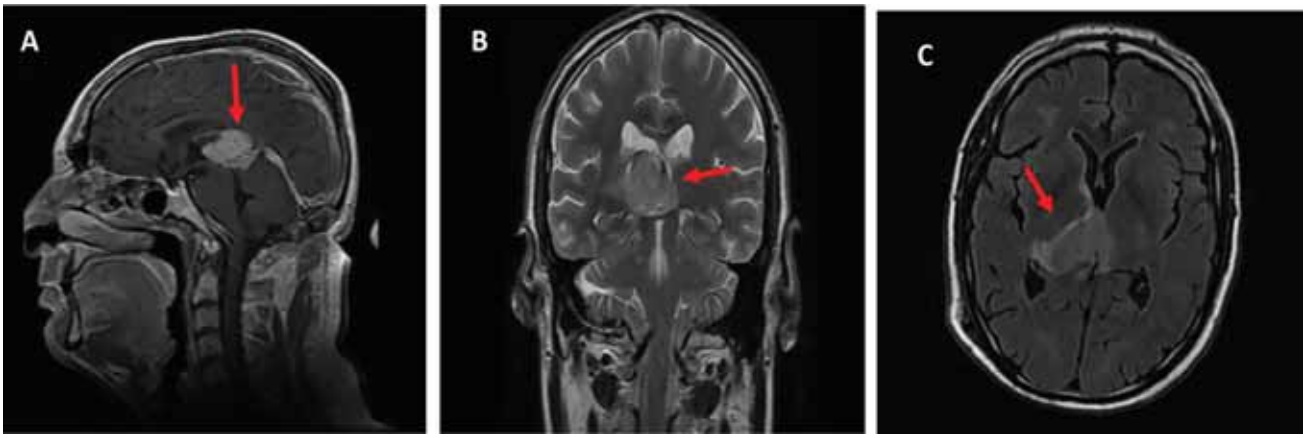

Figure 1. This figure depicts a well-defined enhancing mass situated at the posterior aspect of the third ventricle (indicated by the red arrow).1A showcases a Gd-T1w sequence, revealing a uniformly enhancing lesion above the tentorium. 1B and 1C feature T2-weighted and FLAIR sequences, respectively, illustrating midline invasion by the abovementioned lesion. Additionally, the lesion displayed heightened signal intensity without notable peritumoral edema.
Gd-T1w: Gadolinium-enhanced T1-weighted; FLAIR: Fluid attenuated inversion recovery

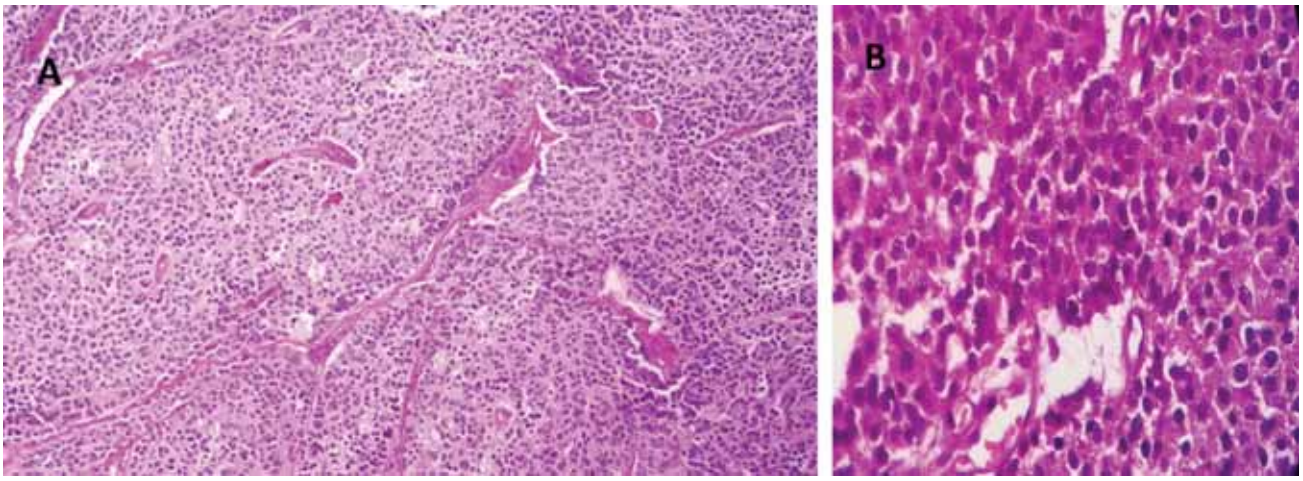

Figure 2. This figure shows, A) Papillary tumors originating from the pineal region exhibit discernible papillary features (H&E, 20× magnification), and B) Areas characterized by higher cellular density (H&E, 400× magnification).

stable, with a slight decrease in size; however, a new lesion, approximately 20 mm in size, had appeared in the right parasagittal region of the posterior parietooccipital lobe, radiologically mimicking meningioma characteristics (Figure 4). Considering the short interval since his last imaging, the clinical presentation of such a large meningioma seemed unlikely.

The new mass was surgically resected, and microscopic examination revealed a lobular proliferative disorder characterized by cell clusters with distinct boundaries, round to oval nuclei with salt-and-pepper chromatin, abundant vessels with a pseudorosette appearance around the vessels, and a clear pseudopapillary appearance. Additionally, there was cerebral parenchymal reaction and expansion in the meninges, along with a few scattered mitoses (Figure 5). Immunohistochemistry of this new lesion showed positivity for synaptophysin and negativity for glial fibrillary acidic protein (GFAP) and epithelial membrane antigen (EMA), with a Ki67 positivity rate of 30% (Figure 6).

The morphologic and immunophenotypic characteristics suggested the diagnosis of grade 4 pineoblastoma. A pathological review of formalin-fixed slides from both the old and new lesions was conducted to justify the change in pathology, revealing the exact diagnosis of the pineal parenchymal tumor with intermediate differentiation (PTPR) for both lesions. The parasagittal lesion was diagnosed as a metastasis of the primary PTPR, further substantiated by a complete spinal MRI revealing multiple spinal tumoral seedings

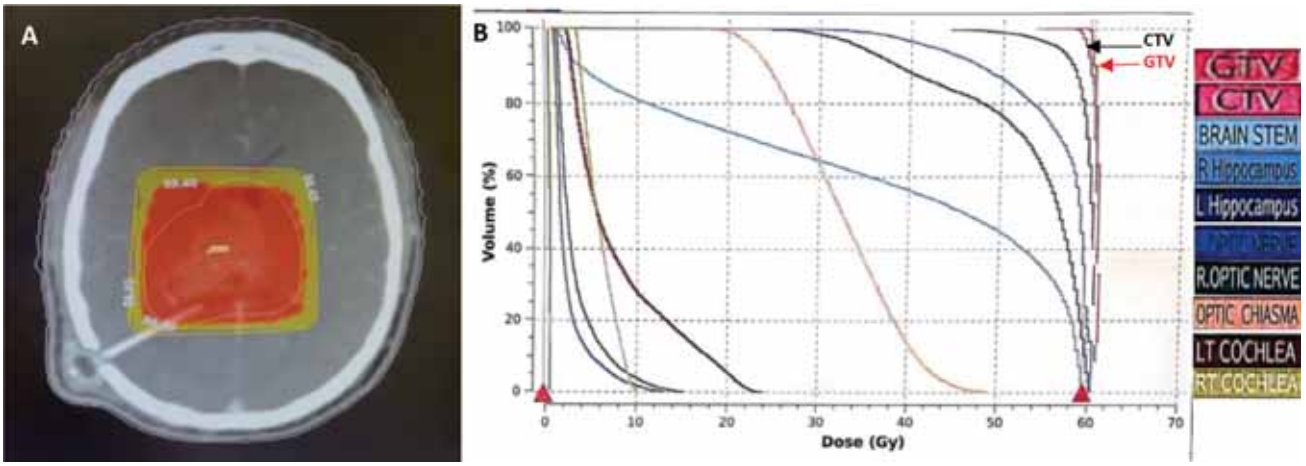

Figure 3. This figure provides insight into A) The transverse plane of treatment planning, highlighting the 95% isodose line in yellow and the 100% isodose line in red. B) The accompanying dose volume histogram depicts the at-risk targets and organs.

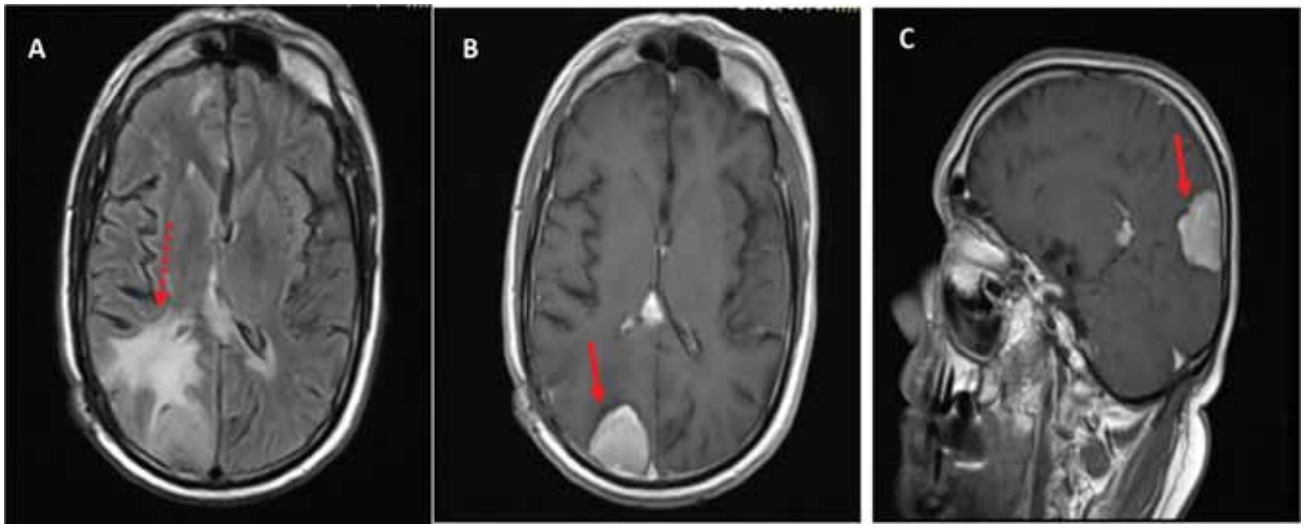

Figure 4. This figure encompasses A) A FLAIR sequence on the transverse plane, revealing the lesion and peritumoral edema (indicated by the round red arrow). 4B and 4C present the transverse and sagittal planes of the Gd-T1w sequence, showcasing a new 20mm enhancing lesion within the right parasagittal region of the posterior parieto-occipital lobe (highlighted by the red arrow), in addition to nodular enhancement within the previous tumor bed, suggestive of residual tumor.
FLAIR: Fluid attenuated inversion recovery; Gd-T1w: Gadolinium-enhanced T1-weighted

in the cervical and thoracic spine (Figure 7).

For the palliative treatment of this diffuse recurrence of PTPR, the patient was initiated on systemic chemotherapy, consisting of vincristine at a dose of 1.5 mg/m^2 (with a maximum dose of 2 mg) on days 1 and 8, along with carboplatin at an area under the curve of 2 on days 1, 8, and 15, every 28 days. The patient remains symptom-free after six months of follow-up, with no signs of disease progression observed on recent brain MRI images.

Ethical approval

The Ethics Committee of Mashhad University of Medical Sciences approved the publication of the present case report (code: IR.MUMS.REC. 1402.059).

Discussion

Papillary tumors of the pineal region are sporadic, constituting less than 1% of all adult central nervous system tumors.[1] Its peak incidence is in the third decade of life.[2] The reported cases ranged in age from 5 to 66 years. In some reports, both genders are affected equally, with a slight dominance for males.[3] Our patient was a male in his fifth decade of life, in the age range reported

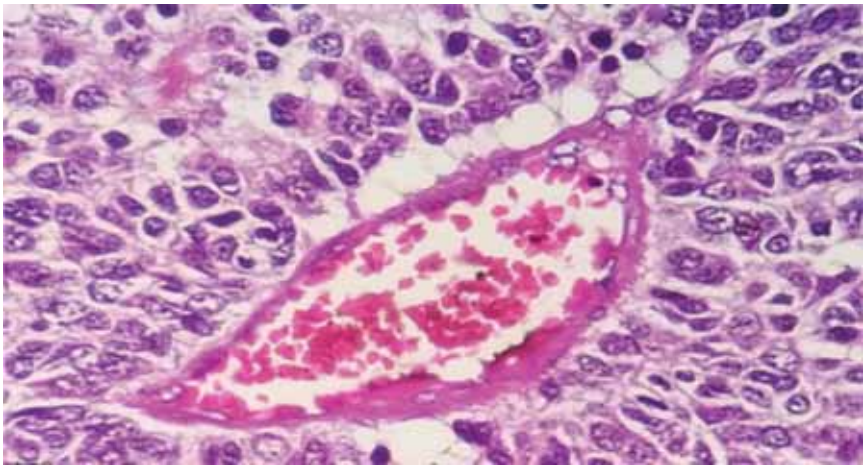

Figure 5. This figure shows a papillary tumor originating from the pineal region is typified by an epithelial appearance, displaying papillary features often manifest as ependymal-like actual rosette formations (H&E, 400× magnification).

in previous reports.

Preliminary symptoms leading to a diagnosis of our patient were headache, nausea, and vomiting, all caused by raised ICP. Due to the anatomical location of pineal tumors, they can cause hydrocephalus, thus increasing ICP. So, the patient may present with symptoms of increased ICP, such as nausea, vomiting, and headache. Visual disturbances and ataxia are also standard presenting features.[4] The evidence of increased ICP in our patient was presented on his brain MRI. Disseminated disease at the presentation is not a frequent finding. However, it may happen during disease. Our patient had no distant involvement when he was diagnosed. However, at the time of recurrence, there were leptomeningeal metastases. In a report of 17 patients with PPTIDs by Jo Nam et al. (2020), dissemination in the neuroaxis at the time of initial diagnosis was evident in only 3 patients.[13]

A mass-like lesion in the pineal region with subsequent obstructive effects on cerebrospinal fluid flow has a list of differential diagnoses. On imaging, there is no characteristic feature to distinguish PTPR from other lesions of the pineal parenchymal category. A well-defined mass with approximately heterogeneous enhancement, with or without cystic or calcification component that sometimes is a high signal in non-contrast T1-weighted sequences, makes diagnosing PTRP more likely.[1] In Our patient, middle and parasagital masses were iso signal on T1-weighted sequences, which enhanced homogenously on post-contrast images. Masses were iso- to hyper-signal on T2-

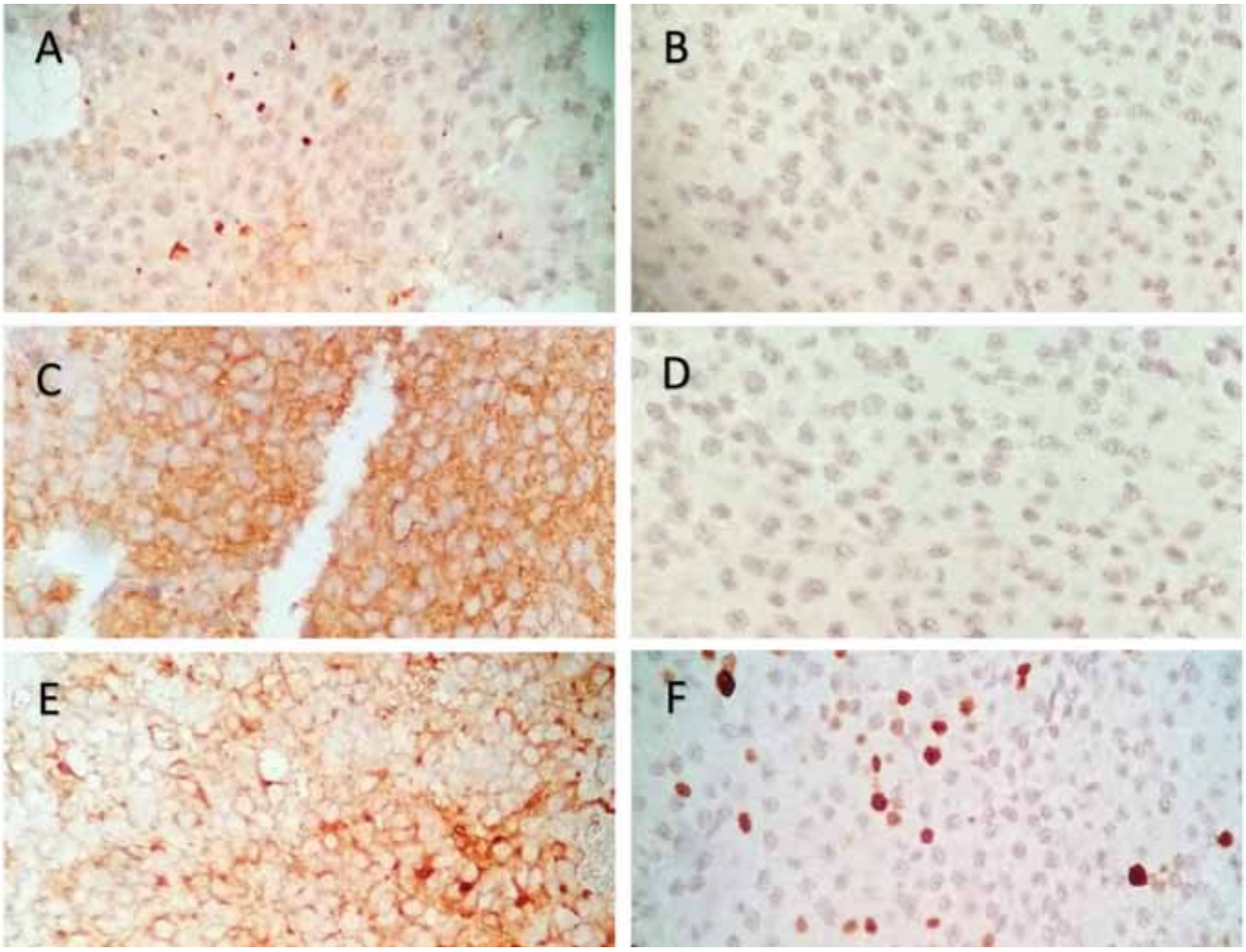

Figure 6. Immunohistochemical staining results are A) Negative immunoreactivity of tumoral cells for EMA. B) Negative immunoreactivity of tumoral cells for GFAP. C) Positive immunoreactivity of tumoral cells for synaptophysin. D) Negative immunoreactivity of tumoral cells for S100 protein. E) Positive immunoreactivity for chromogranin. F) Positive Ki 67 staining was observed in 30% of nuclei.
EMA: Epithelial membrane antigen; GFAP: Glial fibrillary acidic protein

weighted and FLAIR sequences, with substantial surrounding edema, and showed restriction on the diffusion-weighted sequence.

A papillary tumor in the pineal region brings to mind one of the differential diagnoses of papillary pineal parenchymal tumors, papillary ependymoma, choroid plexus papilloma, papillary meningioma, and papillary pineocytoma.[5] Special cells of the posterior third ventricle near the pineal gland, which are believed to be responsible for PTPR, simultaneously show ependymal and neuroendocrine features. Immunohistochemistry staining helps to differentiate PTPR from other papillary tumors of the pineal region. Cytokeratins, S100, Vimentin, and neuron-specific enolase are positive in this disease. EMA could also be positive. GFAP is generally negative.[1] In contrast to other pineal parenchymal neoplasm, there is a lack of retinal S-antigen and neurofilament protein expression in PTPR.[2] In our case, GFAP negativity distinguished PTPR from papillary ependymoma, while CD56 expression and absence of cytoplasmic stanniocalcin-1 and transthyretin helped differentiate it from choroid plexus tumors. Considering that EMA is also positive in meningiomas and S100 can also be positive in 33% of them,[6] meningiomas became the most important differential diagnosis of this patient's second dural-based lesion, radiologically and pathologically.

Surgery is the mainstay of treatment. While adjuvant radiotherapy has been employed, its role remains unclear.[3] Most commonly, it is employed in high-grade tumors or the state of recurrence.[3] A systematic review by Yamaki et al. found surgical resection, whether total or partial, to affect survival while reporting adjuvant treatments

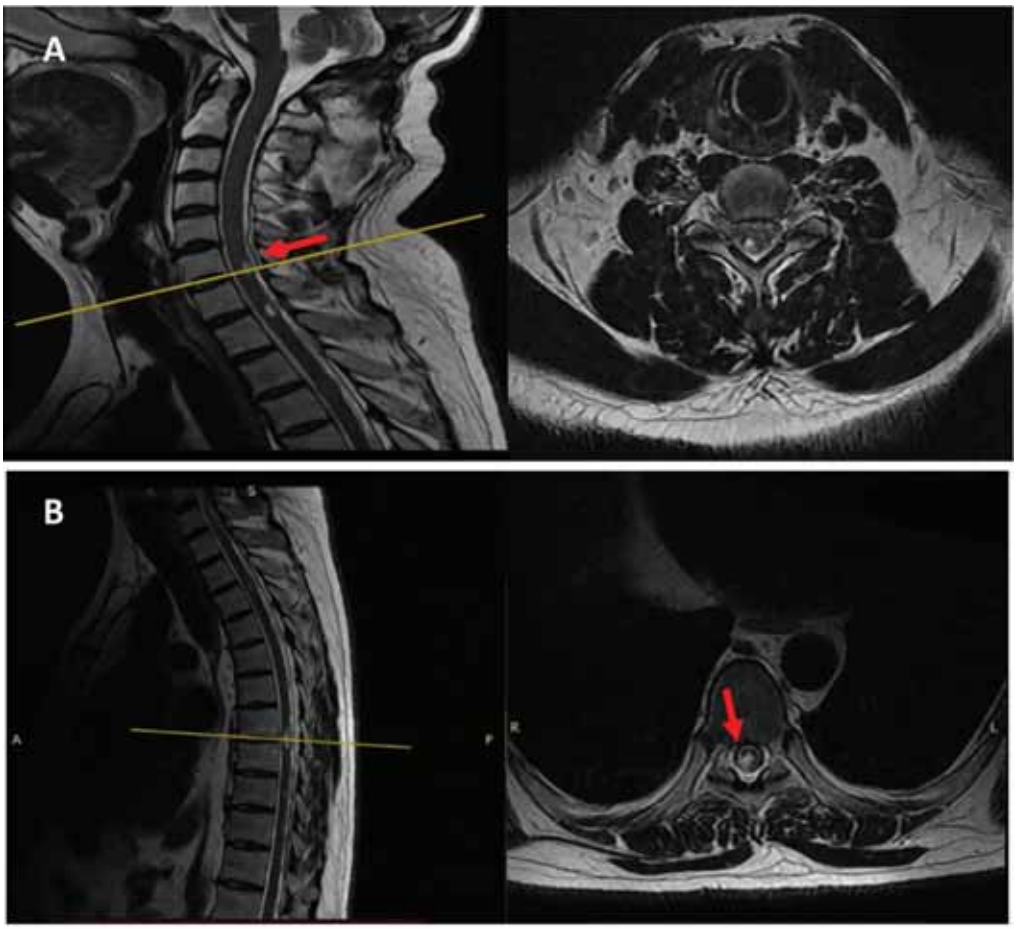

Figure 7. Images of the cervical and thoracic spine are presented, showcasing multiple tumoral implants within the spinal region (indicated by the red arrow).

to have no bearing on survival.[4] However, a 50-54 Gy dose of radiotherapy could be used as adjuvant treatment in incompletely resected and recurrent disease.[3]

Reports have described frequent local recurrence in this entity.[1,4] Leptomeningeal seeding of PTPR has previously been described.[2,8] As Jouvet et al. described this entity in 2003, they reported 6 cases with 4 local recurrences and one spinal dissemination. All patients were treated by surgery, with adjuvant radiotherapy mostly done following incomplete resection.[2] Similar to our case, a reported patient experienced recurrence with a mass in the foramen magnum following complete resection of the pineal tumor, with several cerebral foci of metastasis.[7]

Recurrent disease has mostly been treated with radiation therapy.[8] Systemic therapy has also been used: a patient remained stable on temozolomide for 9 years,[8] while bevacizumab resulted in progression-free survival of 13 months.[9] In a case of extensive leptomeningeal recurrence, everolimus resulted in the lesions' regression and disease control for at least two years.[10]

Using vincristine and platinum combinations, a 3-year-old child with grade III PTPR was disease-free for 3 years following adjuvant radiotherapy and chemotherapy containing vincristine, cisplatin, cyclophosphamide, and etoposide,[11] while a 6-year-old boy remained disease-free for four years following adjuvant radiotherapy and chemotherapy with cisplatin, lomustine, and vincristin.[12] In our case, a decision was made to put the patient on combination chemotherapy based on carboplatin and vincristine.

Conclusion

In conclusion, PTPR represents a rare and recently characterized entity characterized by a pronounced tendency for local recurrence and the potential for meningeal seeding. Despite undergoing surgical intervention and receiving adjuvant radiotherapy, our patient experienced a recurrence marked by extensive leptomeningeal involvement. Given the limited availability of data, especially concerning treatment modalities, accumulating additional case reports detailing treatment protocols and their respective outcomes and incorporating them into a comprehensive meta-analysis will delineate the optimal therapeutic approach for this condition.

Informed Consent

A written informed consent form was obtained from the patient prior to the publication of the present study.

Acknowledgment

We want to thank the patient for her consent to data publication.

Conflict of Interest

None declared.

Reference

1. Aggarwal S, Agarwal P, Sahu R. Papillary tumor of pineal region with an unusual clinical presentation: Case report and review of the literature. *Asian J Neurosurg*. 2016;11(01):119-22. doi:10.4103/1793-5482.172592.
2. Fèvre Montange M, Vasiljevic A, Champier J, Jouvet A. Papillary tumor of the pineal region: Histopathological characterization and review of the literature. *Neurochirurgie*. 2015;61(2-3):138-42. doi:10.1016/j.neuchi.2013.04.011.
3. Lombardi G, Poliani PL, Manara R, Berhouma M, Minniti G, Tabouret E, et al. Diagnosis and treatment of pineal region tumors in adults: A EURACAN overview. *Cancers (Basel)*. 2022;14(15):3646. doi: 10.3390/cancers14153646.
4. Yamaki VN, Solla DJF, Ribeiro RR, Da Silva SA, Teixeira MJ, Figueiredo EG. Papillary tumor of the pineal region: systematic review and analysis of prognostic factors. *Neurosurgery*. 2019;85(3):E420-E429. doi: 10.1093/neuros/nyz062.
5. Kuchelmeister K, Hügens-Penzel M, Jödicke A, Schachenmayr W. Papillary tumour of the pineal region: Histodiagnostic considerations: Scientific correspondence. *Neuropathol Appl Neurobiol*. 2006;32(2):203-8. doi:10.1111/j.1365-2990.2006.00741.x
6. Mathkour M, Hanna J, Ibrahim N, Scullen T, Kilgore MD, Werner C, et al. Papillary tumor of the pineal region in pediatric populations: An additional case and systematic review of a rare tumor entity. *Clin Neurol Neurosurg*. 2021;201:106404. doi: 10.1016/j.clineuro.2020.106404.

7. Boulagnon-Rombi C, Fleury C, Fichel C, Lefour S, Bressenot AM, Gauchotte G. Immunohistochemical approach to the differential diagnosis of meningiomas and their mimics. *J Neuropathol Exp Neurol.* 2017;76(4), 289-98. doi:10.1093/jnen/nlx008.
8. Nowicka E, Bobek-Billewicz B, Szymaš J, Tarnawski R. Late dissemination via cerebrospinal fluid of papillary tumor of the pineal region: A case report and literature review. *Folia Neuropathol.* 2016;54(1):72-9. doi:10.5114/fn.2016.58918.
9. Boßelmann CM, Gepfner-Tuma I, Schittenhelm J, Brendle C, Honegger J, Tabatabai G. Papillary tumor of the pineal region: a single-center experience. *Neurooncol Pract.* 2020;7(4):384-90. doi: 10.1093/nop/npaa014.
10. Cohen AL, Salzman K, Palmer C, Jensen R, Colman H. Bevacizumab is effective for recurrent papillary tumor of the pineal region: First report. *Case Rep Oncol.* 2013;6(2). 434-40. doi:10.1159/000354753.
11. Assi HI, Kakati RT, Berro J, Saikali I, Youssef B, Hourany R, et al. PTEN R130Q papillary tumor of the pineal region (PTPR) with chromosome 10 loss successfully treated with everolimus: a case report. *Curr Oncol.* 2021;28(2):1274-9. doi: 10.3390/curroncol28020121.
12. Fauchon F, Hasselblatt M, Jouvet A, Champier J, Popovic M, Kirollos R, et al. Role of surgery, radiotherapy and chemotherapy in papillary tumors of the pineal region: a multicenter study. *J Neurooncol.* 2013;112(2):223-31. doi: 10.1007/s11060-013-1050-5.
13. Nam JY, Gilbert A, Cachia D, Mandel J, Fuller GN, Penas-Prado M, et al. Pineal parenchymal tumor of intermediate differentiation: a single-institution experience. *Neurooncol Pract.* 2020;7(6):613-9. doi: 10.1093/nop/npaa024.

Calendar of Events

EACR Cancer Multiomics & Computational Biology
April 30, 2024 - May 02, 2024
Bergamo, Italy
Website: https://eacr.org/conference/cancermultiomics2024?utm_source=CS&utm_medium=web&utm_campaign=CMCB24

ESMO Breast Cancer 2024
May 15, 2024 - May 17, 2024
Berlin, Germany
Website: https://www.esmo.org/meeting-calendar/esmo-breast-cancer-2024

International Conference on Cancer and Oncology Research
May 30, 2024 - May 31, 2024
Rome, Italy
Website: https://spectusconferences.com/cancer-oncology-conference/

EACR2024 — EACR Congress 2024: Innovative Cancer Science
June 10, 2024 - June 13, 2024
Rotterdam, Netherlands
Website: https://2024.eacr.org/

DEGRO 2024 — 30th Congress of the German Society for Radiation Oncology
June 13, 2024 - June 15, 2024
Kassel, Germany
Website: https://www.degro-kongress.org/

ESMO Gynaecological Cancers Congress 2024
June 20, 2024 - June 24, 2024
Florence, Italy
Website: https://www.esmo.org/meeting-calendar/esmo-gynaecological-cancers-congress-2024

ESMO Gastrointestinal Cancers Congress 2024
June 26, 2024- June 29, 2024
Munich, Germany
Website: https://www.esmo.org/meeting-calendar/esmo-gastrointestinal-cancers-congress-2024

ICPM10 & IWPCT9 — 10th International Conference on Plasma medicine and 9th International Workshop on plasma for cancer treatment
September 08, 2024- September 13, 2024
Portoroŝ, Slovenia
Website: http://icpm10.ijs.si/

Molecular Analysis for Precision Oncology Congress 2024
October 16, 2024- October 18, 2024
London, United Kingdom
Website: https://www.esmo.org/meeting-calendar/molecular-analysis-for-precision-oncology-congress-2024

Oncology Research 2024 — 4th European Congress on Cancer and Oncology Research
October 28, 2024- October 29, 2024
Rome, Italy
Website: https://crgconferences.com/oncology